# The University of Queensland

**Bachelor of Engineering Thesis**

Engineering Optimization Showcase

Student Name: Jeisson Sebastian Quincha Muñoz

Course Code: MECH4500

Supervisor: Dr Michael Heitzmann

Submission Date: 27 October 2017

A thesis submitted in partial fulfilment of the requirements of the

Bachelor of Engineering Degree in Mechanical Engineering

**UQ Engineering**

**Faculty of Engineering, Architecture and Information Technology**

# Abstract

Optimization plays an essential role in modern Engineering. Current Finite Element and CAD Software implement advanced optimization techniques and algorithms so that efficient and cost-effective solutions to complex engineering problems can be encountered. The popular Finite Element software ANSYS 18 is the baseline optimization package considered for this study. A series of increasing difficulty cases relevant to the fields of Mechanical and Aerospace Engineering are selected and subsequently optimized in order to test the performance and capabilities of modern optimization software. Additionally, a tutorial-style methodology is developed with step by step definitions and guidelines of the optimization process for each of the study cases considered.

## Acknowledgements

My most sincere gratitude to my supervisor, Dr Michael Heitzmann for his continuous guidance and support throughout this project. I would also like to thank my family and girlfriend for their endless encouragement, and last but not least, to all my friends and colleagues who shared their support in one way or another.

# Table of Contents

# List of Tables

# List of Figures

*Note: Due to the large number of figures, only key figures have been included.*

# 1 Introduction

The ever-increasing pressure to effectively minimize production costs to endure global competition has driven scientists and engineers to continuously look for more rigorous decision-making approaches, such as optimization. Techniques to design and manufacture products and systems both economically and efficiently are comprehensive with modern optimization methods yet under active research.

Finite-element (FE) based design optimization is currently a well-established methodology for engineering design. Continuous advances in software and computer performance have made the overall design process more versatile with hundreds of hours typically invested in an engineering design cut down to a few, depending on the type of analysis. With rapidly evolving computer technology, there is an incessant expansion of engineering problems that can be solved using optimization techniques.

Optimization approaches, coupled with modern computer-aided design (CAD) software, are applied to substantially enhance the process of conceptual study, and detailed design of engineering systems. While there is countless optimization methods and algorithms currently available and under research, only a few methods are selected and implemented in FE and CAD software.

The current study focuses on the demonstration of optimization capabilities of modern finite element software with a few engineering-related cases of increasing complexity. The baseline Finite Element software selected for the analysis is ANSYS® 18. Additionally, the selected information delivery method is a tutorial-style methodology that offers an in-depth description of the essential steps followed for performing each of the optimization analyses.

The present study offers a more illustrative and descriptive approach towards engineering optimization than analysis depicted in previous literature.

## 1.1 Scope and Objectives

The main objectives that this report intends to achieve are detailed below.

- Find a total of four suitable study cases comprising analyses relevant to the fields of Mechanical and Aerospace engineering.
- Effectively test and demonstrate optimization capabilities of modern FEA software though the selected study cases.
- Create a tutorial-style methodology for each of the considered study cases which effectively demonstrates the optimization process from the initial model generation to the results acquisition.

The scope of this study is detailed in Table 1.

*Table 1: Scope of the study*

| In Scope | Out of Scope |
|---|---|
| ○ Finite element optimization performed in FE software ANSYS® 18.<br>○ Topological and Parametric optimization modules are explored.<br>○ Mechanical and Aerospace Engineering related optimization cases are considered.<br>○ Post-processing is applied to optimized results.<br>○ Tutorial-style description of optimization process. | ○ Optimization using a different FE or CAD Software.<br>○ Other optimization methods or algorithms not specified.<br>○ Optimization cases relevant to other fields or subjects.<br>○ Manufacturing analyses, mass production and other post processing methods.<br>○ Description of CAD generation process. |

Additionally, a number of assumptions are considered for this study including:

- The reader has a sound knowledge or has been previously exposed to Finite Element Analysis (FEA) software and specifically ANSYS® version 18.
- The reader is familiar with basic Mechanical and/or Aerospace engineering topics, concepts and applications as well as essential optimization principles.

# 2 Literature Review

Previous literature asserts that optimization techniques have reached a substantial degree of maturity in recent years, and are being implemented in an ever-increasing spectrum of industries. A thorough past literature analysis has been carried out in order to comprehend the extent of this project and thus, better understand the topic and potential advantages of the outcomes. The review focuses on engineering optimization from the early concepts to modern techniques and methods employed globally. In addition, the analysis focuses on optimization in the selected baseline software Ansys® 18 and what milestones have been currently reached regarding the capability and potential of the algorithms implemented.

## 2.1 History and Evolution of Optimization

Optimization has always been present in nature. Physical systems tend to seek a state of minimum energy. Molecules in a chemical system react with each other until the global potential energy is minimized. Optimization is an essential tool functional in nature as well as in everyday life. (Jorge Nocedal, 1999)

It is frequently argued that the first optimization problem known to history was solved by a Phoenician queen called Dido, who allegedly landed on the coast of North Africa in 814 BC. (Wilhelm Forst, 2009) The story suggests that upon arriving to the new land, she asked the ruler for as much land as could be enclosed with the skin of a bull, to which the ruler ingenuously acceded. Nevertheless, Dido figured that if she cut the skin into many thin strips, she could maximise the enclosed area around a harbour bay of what later became the city of Carthage. In modern times, this first optimization problem is referred to as maximising the enclosed area with a closed curve of fixed length.

Another example from antiquity is said to be Zenodorus (200-140 BC) a Greek mathematician who effectively proved that of all polygons with $n$ vertices and identical perimeter, the greatest area was that of the regular polygon or the polygon with equilateral triangles.

Furthermore, a noteworthy optimization problem, before the invention of *Calculus,* was solved by a famous mathematician known as Heron of Alexandria nearing the end of the first century. He proved that beams of light travel between two points through the path with the shortest length. A law which was later adjusted by Pierre de Fermat in 1657 asserting that light beams travel across media in minimum time.

Subsequently, optimization techniques were adapting and evolving in order to solve problems that were becoming more and more complex. Table 22 illustrates the history, developments, and evolution of optimization from the antiquity to modern times. (Kitti, 2016)

*Table 2: Optimization Evolution*

| *Period* | *Date* | *Events* |
|---|---|---|
| ***Antiquity*** | 300 bc | Euclid considers minimum distance between a point and a line. |
| | 100 bc | Heron postulates that beams of light always take the shortest path. |
| ***17th Century*** | 1636 | Fermat shows that light travels between two points in minimal time. |
| | 1687 | Newton studies the body of minimal resistance. |
| ***18th Century*** | 1712 | J.S. Konig shows that the shape of a honeycomb is optimal for the application. |
| | 1754 | Lagrange formulates the problem of minimal surfaces. |
| ***19th Century*** | 1806 | Legendre presents the least squares method for optimization. |
| | 1847 | A. L. Cauchy presents the gradient method. |
| | 1857 | J. W. Gibbs shows that chemical equilibrium is an energy minimum. |
| ***20th Century*** | 1917 | H. Hancock publishes the first book on optimization. |
| | 1917 | D. W. Thompson applies optimization to analyse the forms of living organisms. |
| | 1947 | G. Dantzig presents the simplex method for solving Linear Programming problems. |
| | 1951 | H. Markowitz presents his theory based on quadratic optimization. |
| | 1954 | Optimal control theory begins to develop, and the space race gives additional boost to the optimization field. |
| | 1957 | R. Bellman presents the optimality principle. |
| | 1980’s | Polynomial algorithms for optimization problems are developed. |
| | 1990’s | Computers become more efficient and algorithms for global optimization are developed (heuristic). |
| ***21st Century*** | | Modern algorithms are developed, and optimization software rapidly gains popularity. |

## 2.2 Types of optimization

Optimization studies are presented in a number of types and can be classified in several ways. A general description of optimization problems and classification of the most common problems are described below.

### 2.2.1 Statement of an Optimization Problem

A typical optimization problem can be described as the minimization or maximization of a function $f(x)$ which is subject to variable constraints and can be written as follows.

$$Find\ \boldsymbol{X} = \begin{Bmatrix} x_1 \\ x_2 \\ \vdots \\ x_n \end{Bmatrix} which\ minimizes\ f(\boldsymbol{X})$$

Subject to the constraints:

$$g_j(\boldsymbol{X}) \leq 0, \qquad j = 1,2, \dots, m$$

$$l_j(\boldsymbol{X}) = 0, \qquad j = 1,2, \dots, p$$

Where:

- $\boldsymbol{X}$ is an *n*-dimensional vector known as the *design vector* which represents a set of variables present in the design process.
- $f(\boldsymbol{X})$ is defined as the *objective function.* The objective function is a criterion used for effectively comparing and selecting an acceptable design from different alternatives that an optimization process may generate. The objective function type depends on the nature of the problem.
- $g_j(\boldsymbol{X})\ and\ l_j(\boldsymbol{X})$ are the *inequality* and *equality constraints* respectively. These design constraints are restrictions that need to be satisfied in order to obtain an acceptable design. Constraints that represent physical limitations on a design, such as manufacturability, availability, etc. are known as *geometric constraints*. Constraints that limit the performance of a system are termed *functional* constraints.

In an illustrative manner, the optimization problem is depicted in Figure 1.

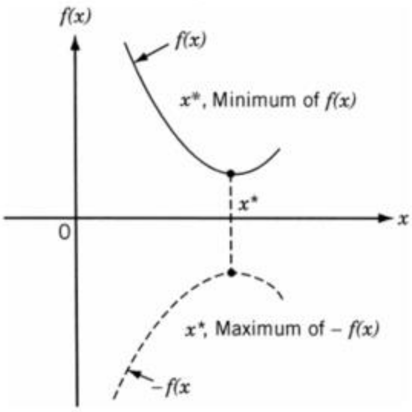


*Figure 1: Optimization diagram*

### 2.2.2 Classification of optimization problems

Optimization problems can be classified based on different characteristics. Such characteristics may involve the presence of constraints, number of type of objective function, physical or virtual structure of the problem, nature of equations or variable, separability of objective functions, permissible values of design variables, deterministic nature of the variables, and other (Chiandussi et al, 2011) A few classification examples are described next.

- ***Classification based on the existence of constraints.*** Models can be classified as *constrained* or *unconstrained,* which depends on the existence of constraints in the problem.
- ***Classification based on the nature of the design variables***. Problems can be classified into two categories:
  - *Parametric Optimization.* Focuses on assigning suitable values to a set of design parameters which minimize an objective function subject to a series of constraints.
  - *Dynamic Optimization.* In this type of optimization, the objective is to obtain a set of parameters in order to minimize an objective function under a number of constraints.
- ***Classification based on the physical structure of the problem.*** Optimization problems can be classified as *optimal* and *non-optimal* control analyses. An optimal control problem (OC) is a mathematical programming analysis that involves a series of stages which evolve from the preceding stage in a sequential manner. The objective is to obtain a set of control variables that minimize the objective function over the existing stages under certain constraints.

- ***Classification based on the nature of involved equations.*** The problems can be classified as linear, nonlinear, geometric, and quadratic programming analyses.
  - *Linear Programming.* If the constraints and the objective function of the problem are linear functions of the design variables, the problem is known as a *linear programming (LP)* problem.
  - *Nonlinear Programming.* If one or more of either the objective or constraint functions are nonlinear, the problem becomes a *nonlinear programming analysis.* This is one of the most common types of optimization problems.
  - *Geometric Programming.* A geometric programming problem is a type of analysis where the constraints and objective function/s are expressed as posynomials in $\boldsymbol{X}$. A posynomial function can be defined as the sum of power terms involving the function variables.
  - *Quadratic Programming*. A nonlinear type of problem with an objective function of the quadratic form and linear constraints.
- ***Classification based on permissible values of the design variables.*** If some or all of the design variables are limited to work only with integer or discrete values, the problem becomes an *integer programming problem.* Conversely, if the design variables have any real value as an input, the optimization problem is known as a *real-valued programming* analysis.
- ***Classification based on the deterministic nature of the variables.*** The problems can be defined as deterministic and stochastic programming analyses.
  - *Deterministic Programming.* A problem where a particular input computed with an objective function, will always produce the same output. In other words, its output is predetermined by the objective functions and the inputs.
  - *Stochastic Programming.* Refers to optimization problems where some or all the parameters and/or design variables are probabilistic (non-deterministic).
- ***Classification based on the separability of the functions.*** Problems can be defined as separable or non-separable optimization analyses based on whether the objective function of the problem is separable or not.
- ***Classification based on the number of objective functions.*** Depending on the number of objective functions considered, models can be defined as single or multi-objective problems.

Multi-objective and Parametric Optimization types involve most modern engineering problems and will be the main focus of this study.

### 2.2.3 Optimization methods

There is not a sole optimization technique available for efficiently solving all engineering problems. Therefore, a series of optimization techniques have been developed for solving different types of optimization cases. There is an increasing number of available optimization methods ranging from century old mathematical models to modern algorithms still under research. Optimization techniques can be classified as mathematical programming or traditional techniques that involve the application of iterative methods and modern algorithms that are currently being developed and improved.

Table 3 illustrates the most common optimization techniques available.

*Table 3: Classification of Optimization methods*

| Classification | Optimization Technique |
|---|---|
| **Iterative Methods (Traditional)** | Newton's method and variations |
| | Lagrangian method |
| | Least-squares method |
| | Coordinate descent method |
| | Conjugate gradient method |
| | Steepest descent method |
| | Ellipsoid method |
| | Interpolation and extrapolation |
| **Algorithms (Modern)** | Simplex method |
| | Memetic algorithm |
| | Evolutionary algorithms |
| | Dynamic relaxation |
| | Genetic algorithms |
| | Particle swarm optimization |
| | Bee colony optimization |
| | Simulated annealing algorithm |
| | Stochastic algorithms |
| | Hill climbing algorithm |
| | Probabilistic algorithms |

## 2.3 Optimization and Ansys®

FE based design optimization is currently a well-recognized and influential practice for engineering design. The application of this technique involves several stages such as geometric modelling, mesh generation, finite element method implementation, numerical optimization techniques and a number of post-processing stages (A. Vaidya, 2005). Software enhancements have made the overall design process more versatile and reliable. Ansys® 18 as the selected finite element software for this study, is one of the leading multi-objective optimization software in engineering. Its improved user interface offers effective user-machine communication where the engineering intent, data relationships and the state of the analysis can be effortlessly understood.

Ansys®18 implements two fundamental types of optimization that will be demonstrated in this study. The first, as previously discussed, is a Parametric Optimization feature, which is contained within its own module termed DesignXplorer™. Topological Optimization is the second technique implemented. Topological optimization is a form of shape improvement which is often referred to as layout optimization. This method is part of a global study module within Ansys®.

A standard optimization procedure in Ansys® is described in Figure 2: Optimization Process (Yun, 2004)

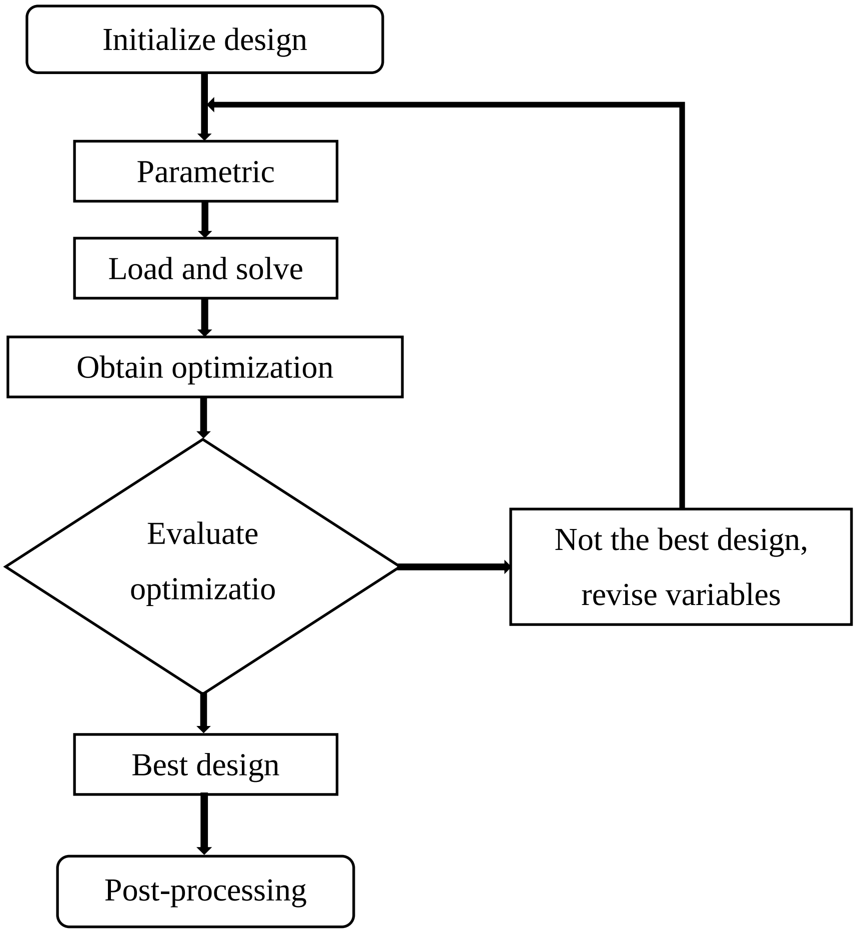


*Figure 2: Optimization Process (Yun, 2004)*

### 2.3.1 Background

Ansys® started as a finite element software in 1970. The initial versions involved a command-based interface referred to as APDL (Ansys Parametric Design Language) which was the principal language used to communicate with the solver. The scripting language was used to build parametric models and automate common tasks. However, version 12 of the software drastically changed the interface by implementing a platform where projects are represented graphically as connected systems in a flowchart-like diagram known as Ansys Workbench™.

The Ansys Workbench platform automatically forms connections between different types of studies and simulations. A desired study can be selected from an analyses menu and the study properties such as geometry, mesh, setup, solution, and results can be easily accessed or edited directly from the platform without the need of a script as in APDL.

Optimization was first implemented in an early version of Ansys APDL where a complete code needed to be developed which specified the system characteristics such as loads, dimensions, geometry, constraints, and other initial parameters. Once the model was outlined, the design variables and objective functions were defined along with the preferred optimization methods and techniques. The code was then run, and the outcomes highly depended on the convergence of the analysis. (Javidinejad, 2012)

With the release and enhancement of Ansys Workbench™ in version 12, users were allowed to create new, faster processes and efficiently interact with external tools such as CAD models. This improvement significantly increased the demand of finite element and optimization software in the engineering industry. (Thieffry, 2010)

The new Ansys® interface included a sole module for parametric optimization termed DesignXplorer™ together with a topology optimization module with faster implementation within Workbench.

### 2.3.2 Optimization modules

As previously mentioned, Ansys® 18 implements two different optimization types. A parametric optimization analysis can be carried out from the DesignXplorer™ module and a Topological optimization study, also accessible from the Workbench platform.

#### 2.3.2.1 DesignXplorer™ Module

The main purpose of the DesignXplorer™ module is to effectively identify the relationship between the design variables and the desired performance of a model. Based on the output, the analyst can modify and influence the design, so the required outcomes are obtained. DesignXplorer™ provides enough tools to perform parametric optimization cases with a reasonable number of parameters in a single or Multiphysics analysis.  In other words, DesignXplorer is a powerful approach to explore, understand, and optimize an engineering challenge.

Once run, the DesignXplorer™ module comprises a series of steps to obtain an optimized model. As soon as the model is generated, and the parameters or design variables are set, a what if study can be carried out. The *What if* study feature of the module automatically runs through a list of specified design points. Then, a sensitivity or parameter correlation analysis identifies input parameters that do not have a major impact on the outcomes of the simulation and can be implemented where a large number of parameters would hinder the successful continuation of a study . A Design of Experiments (DoE) phase specifies the type and range of each parameter and design points are automatically chosen to effectively explore the parametric design space. Subsequently, a response surface model can be implemented to rapidly provide approximated values for the output parameters without having to perform a complete simulation. After this step, the optimization phase takes place where objectives, constraints and input parameters are defined. If a response surface was implemented, thousands of configurations are then explored in a few seconds depending on the type of study. If a direct solver is preferred without a response surface, convergence algorithms are followed. Finally, a design robustness analysis can be carried out after the optimization phase to understand the system's performance and trade-off variables involved.

The DesignXplorer™ module is one of the most advanced optimization tools available and is widely used in the engineering industry as well as on a variety of research fields.

#### 2.3.2.2 Topology Optimization Module

The main objective of topological optimization is to find the best possible use of materials for a model that is subject to a single or multiple load distributions. In other words, the maximum stiffness design is sought, so the minimum efficient material use is achieved.

The topology optimization technology implemented in Ansys® Mechanical, provides the necessary tools to design lightweight and efficient components for a wide range of applications. Ansys® 18 includes a direct topological optimization module in the Workbench interface which greatly simplifies the steps required to carry out an analysis. The standard procedure for topology optimization involves defining the model and creating a mesh, specifying optimized and non-optimized regions, defining load cases and the optimization parameters (objective function/s and constraints). The study is then run, and the results can be reviewed and post-processed.

Figure 3 illustrates the standard process carried out in a topology optimization analysis.

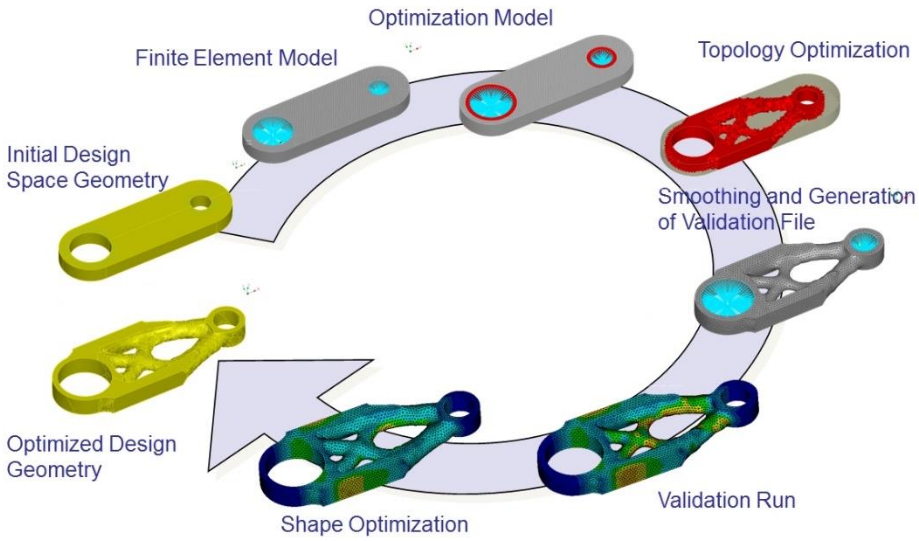


*Figure 3: Topology Optimization process (image from ansys.com)*

### 2.3.3 Optimization Methods implemented

Ansys® implements a variety of optimization techniques involving complex numerical optimization methods as well as modern optimization algorithms. The optimization method applied depends on the type of problem and defined parameters. Additionally, a desired optimization technique can be specified, or external optimization tools can be integrated which is a field with ongoing research and advances. Parametric and topological optimization solvers in Ansys® 18 use a variety of techniques and specific algorithms depending on the model and output requirements.

#### 2.3.3.1 Parametric Optimization Techniques

Once the model constraints and requirements are defined and the simulation's responses are characterized, DesignXplorer™ provides the following types of optimization algorithms:

• ***Shifted Hammersley Sampling.*** An optimization method used for sampling generation in the analysis. The Shifted Hammersley algorithm is a quasi-random number creator generally used for Quasi-Monte Carlo analyses (numerical integration simulations) where the algorithm provides low-discrepancy sequences (samples)

• ***Multi-Objective Genetic Algorithm (MOGA).*** The MOGA is a development of the NSGA-II (Non-dominated Sorted Genetic Algorithm) which is a type of Evolutionary algorithm. The main purpose of the algorithm is to augment the adaptive fit of a population of potential solutions to a Pareto front constrained by a set of specified objective functions. The technique implements an evolutionary procedure with selection, genetic crossover, and mutation operators. (Brownlee, 2011)

The typical steps involved in a MOGA analysis include the incorporation of an initial population from the defined parameters. Then, MOGA creates a new population via Crossover and Mutation and the design points in the new population are updated. Consequently, a convergence validation is carried out, if the optimization converged, the analysis is ended, and the results are generated. However, if the study did not converge, a stopping criteria validation is conducted. Depending on whether the maximum number of iterations set was reached, the analysis can be finished without iteration or the algorithm is run again generating a new population if the maximum number of iterations set was not reached. Figure 4 illustrates the workflow of the MOGA optimization method.

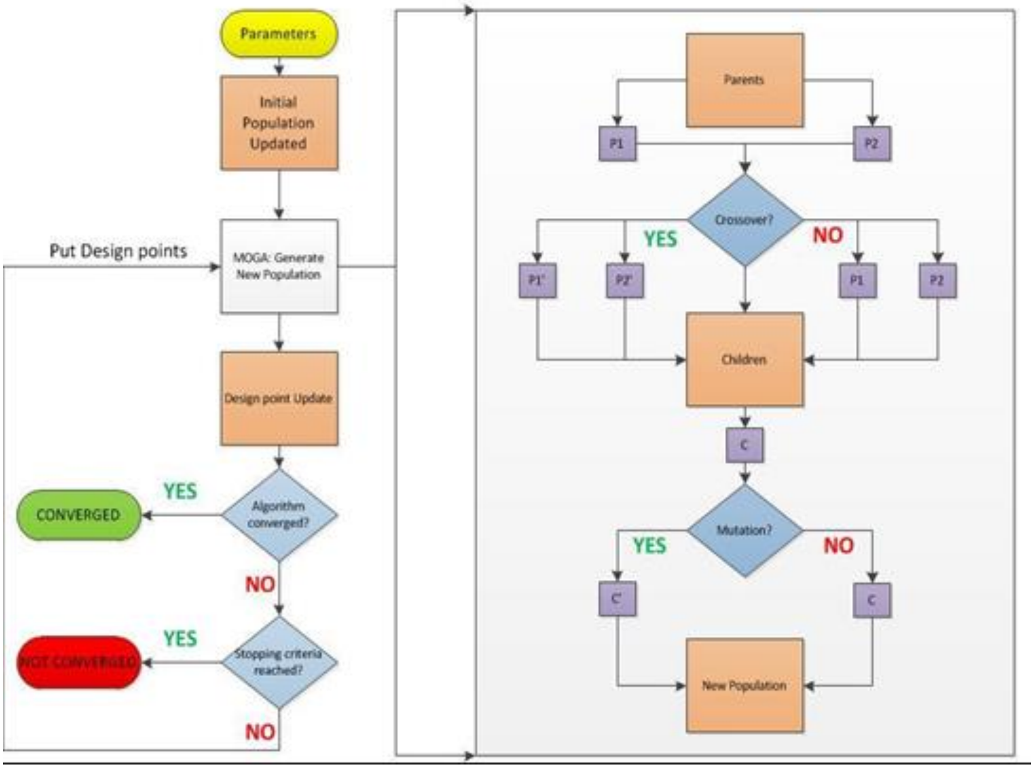


*Figure 4: MOGA Method Workflow*

• ***Nonlinear Programming by Quadratic Lagrangian.*** The NLPQL method is a numerical optimization algorithm. This technique is specially developed to solve constrained non-linear programming models. In principle, the method generates a sequence of subproblems obtained from a quadratic approximation of the Lagrangian function and linearization of constraints. Consequently, the information is updated by an iterative Newton's method and finally stabilized by a line search. The method assumes the problem size is relatively small-scale and the accuracy largely depends on numerical gradients obtained.

• ***Adaptive Single and Multi-Objective Optimization.*** ASO is a mathematical optimization technique that implements the MOGA optimization algorithm supporting single or multiple objectives, multiple constraints, and limited to continuous parameters.

In addition to the optimization algorithms embedded on DesignXplorer™, the implementation of external optimizers within the DesignXplorer™ module is also possible. Available optimization extensions can be installed, integrating the features of the external optimizer into the design workflow.

#### 2.3.3.2 Topology Optimization Techniques

Topological optimization, as previously explained, is a type of shape optimization which main objective is to encounter the best material use for a model so that a specified objective function (natural frequency, stiffness, etc.) is maximized or minimized subject to defined constraints (volume, mass reduction, etc.) Unlike Parametric optimization, topological optimization does not require an explicit definition of independent variables (parameters) to be optimized. The user defines the structural problem (materials, loads, etc.) and the objective function which is intended to be minimized or maximized.

In a general optimization problem statement, each finite element $(i)$generated in the meshing phase, is assigned a design variable $(\eta_i)$ which is an internal, pseudo-density of the model. The pseudo-density ranges from 0 to 1, where $\eta_i = 0$ represents material to be removed and $\eta_i = 0$ represents material to be kept. The topological optimization method can be also stated as follows:

$$minimize/maximize\ f(\eta_i)$$

Subject to:

$$0 < \eta_i \leq 1 \qquad (i = 1,2,3, \dots, N)$$

$$\underline{g_j} < g_j \leq \overline{g_j} \qquad (j = 1,2,3, \dots, M)$$

Where:

$M = number\ of\ finite\ elements$
$M = number\ of\ constraints$
$g_j = computed\ constraint\ value$
$\underline{g_j}\ and\ \overline{g_j} = lower\ and\ upper\ constraint\ bounds$

Once the model is set, numerical optimization techniques are implemented. The principal methods applied by Ansys® 18 are a sub-problem approximation technique and a first order optimization analysis.

The subproblem approximation method can be described as an advanced zero-order technique that requires the values of the dependent variables (objective function and state variables) without the need of the derivatives of such values. A least-squares fitting replaces the variables and the problem is converted into an unconstrained study using ‘so called’ penalty functions, which are functions that introduce an artificial constraint penalty to convert the problem from constrained to unconstrained. Minimization is then performed on the approximated function (sub-problem) until convergence is achieved.

On the other hand, the first order optimization method computes the derivative of the objective function and optimization parameters. Consequently, a series of steepest descent and conjugate direction studies are performed until convergence is reached.

### 2.3.4 Current Applications

Computational optimization, in its widest sense, is applied to solve an ever-increasing number of engineering problems. Some distinctive applications from various engineering disciplines that implement numerical optimization and optimization algorithms through software indicate the wide scope of the subject. (Rao, 2009)

- Optimization of aerospace assemblies for minimized weight.
- Trajectory optimization analyses for space vehicles.
- Structural design for bridges, towers, dams, etc. for minimized cost.
- Minimum-weight design of structures complying with predicted operating loads.
- Optimum design and analysis of gears, machine tools, and other mechanical components.
- Optimum design of electrical networks and systems.
- Design of optimum pipeline networks for industries or town planning.
- Efficient design of material handling gear, such as conveyors, trucks, and cranes, for minimum cost and enhanced operation.
- Optimization of engines, turbines, and heat transfer equipment for maximum efficiency and effective loading.
- Optimum design of electrical machinery such as motors, generators, and transformers.
- Efficient selection of machining conditions in metal-cutting processes for minimized associated costs.
- Optimal production planning, controlling, and scheduling.
- Analysis of statistical data from experimental outcomes to obtain the most accurate representation of the physical phenomenon.
- Optimum design and operation of chemical processing technology and plants.
- Effective maintenance and replacement planning of damaged equipment to reduce operating costs.

- Effectively regulating the waiting, idle times and queueing in production lines to reduce associated costs and workload.
- Optimum design of control systems.

An increasing number of applications outside the engineering field have started to incorporate optimization methods aiming to reduce inputs (money, time, workload) while maximizing profits.

### 2.3.5 Present and future improvements

Current effort has been dedicated to improving major aspects of existing engineering optimization software. Among the most significant advances made, the following can be mentioned (ANSYS, Design Exploration User's Guide, 2013)

- One of the major advancements involves significantly faster processing times as computer processors become increasingly efficient. Consequently, complex simulation and optimization models directly benefit from developments in computer processors.
- New and more efficient optimization techniques and algorithms are being developed and implemented into optimization software. This is due to the increase in finite element and optimization software demand that drives researchers and software developers to rapidly enhance or re-design optimization software algorithms. Modern adaptive algorithms are the focus of recent research studies because of their optimization potential.
- An increasing range of applications make optimization methods more versatile and reliable as new sorts of studies are implemented within optimization packages.
- More advanced post processing options are being developed that will generate robust optimized designs ready for manufacture. In topological optimization, current post processing methods offer assistance by smoothing the optimized surfaces and adding symmetry features.
- Another important improvement in optimization software is the simpler and more dynamic user interface, offering better adaptability and analysis of results.
- Significant memory management improvements have been developed and become advantageous as Multiphysics and multi-variable optimization studies can be completed in less running time and take up significantly less disk space than originally.
- More CAD and FEA software are implementing optimization (topological and parametric) algorithms as part of their former package.

In the near future, optimization software is set to become a major tool in engineering design and play an essential role in the engineering industry with more advanced optimization techniques and better performance that will provide vastly reliable, time effective and inexpensive solutions to major problems and challenges.

## 2.4 Other Optimization software

While there is plenty of commercial numerical (mathematical) optimization software available, a few CAD or FEA programs implement optimization as part of an engineering analysis. Mathematical optimization software offers simple solutions to user-defines functions, constraints, and variables in a theoretical manner, and in a modern programming language. In other words, an optimization procedure is carried out for an explicit mathematical function, generally for data analysis purposes (Chang, 2015) Popular software in this category include:

- ALGLIB
- GNU modules
- NMath
- OptaPlanner
- Python (SciPy Module)

All the previously mentioned software packages offer numerical optimization techniques for a set of functions, constraints, and variables defined by the user. On the other hand, optimization capabilities implemented as a separate module in commercial CAD or FEA software to the same extent of Ansys® have significantly evolved in recent years. Other CAD and FEA software that implement optimization modules employ similar optimization techniques and algorithms as Ansys® with the main differences being the user interface and the problem formulation procedures. Table 4 describes popular commercial packages.

*Table 4: CAD and FE Optimization Software*

| CAD Software | FEA Software |
|---|---|
| ○ Catia™<br>○ Autodesk Inventor (default CAD software for this study)<br>○ Pro/Engineer<br>○ SolidWorks® | ○ Abaqus®<br>○ FEMTools<br>○ Genesis<br>○ Odessy<br>○ PareTO<br>○ TopOpt |

# 3 Methodology

## 3.1 Overview of study cases

The case selection process involved a comprehensive literature review to obtain a clearer idea of what optimization methods and cases have been considered in previous studies as well as which optimization software and algorithms are implemented. The selected cases involve a wide range of Mechanical and Aerospace related areas such as structural and fracture mechanics, materials science (standard and composites), computational fluid dynamics (CFD) heat transfer, and others. Such studies, along with appropriate optimization methods, are the baseline criterion for testing the optimization capabilities of the modern Finite Element software ANSYS® and its current potential for solving complex engineering problems.

### 3.1.1 Optimization Cases

The cases considered comprise a standard *Car Wheel*, an indoors *Jib Crane*, a medium size *Rocket Nozzle* and a composite *Wind Turbine Blade*. The optimization method and parameters to be optimized depend on each individual case and its operational requirements.

<u>*Car Wheel:*</u> The default Car model defined for the analysis is a Mitsubishi Lancer Evolution X. The initial wheel geometry proposed is a plain solid model without spokes or material removed from the frontal section. The main intent of the optimization process is to find the optimal frontal shape which utilizes the minimum amount of material while meeting loading requirements and safety considerations regarding the yield strength limits of the material. A topological optimization analysis was deemed suitable for this study case as the minimization of material use in the frontal face of the model is one of the desired outcomes.

<u>*Jib Crane:*</u> An indoors standard-size Jib Crane is the second medium level complexity case selected to be optimized. Typical loading and fail-safe design conditions were implemented for more realistic and valuable results. The Jib or arm of the crane model is the main component considered for the optimization process. The initial geometry comprised a solid rectangular sized steel beam on which a topological optimization analysis is performed. An approximate truss-like model, similar to modern cranes, can be expected from the optimization results.

<u>*Rocket Nozzle:*</u> A medium size Rocket Nozzle is selected as the third optimization case. The initial geometry comprises a bell-shaped nozzle with arbitrary dimensions. A CFD study is carried out in order to observe the flow properties and behaviour throughout the converging and diverging sections of the nozzle. The main objective of the optimization analysis is to

obtain supersonic flow conditions and a perfect (or close to perfect) expansion of the flow exiting the nozzle. It is important to note that the analysis was intended to be of a 3D type. However, due to the significantly higher computational time required and limitations of the acquired license, a two-dimensional model is considered for the study.

*Wind Turbine Blade:* The optimization of a composite wind turbine blade is implemented as the last optimization case. This analysis aims to optimize the structural compliance of the blade by obtaining an optimum number of composite layers in each section of the blade with set orientations. Furthermore, given an initial set of loads and moments induced by a simulated wind force, the pitch angle of the turbine blade is also optimized through a CFD optimization process.

The selected cases, along with their respective related fields, analyses performed, and optimization techniques implemented, are detailed in Table 5.

*Table 5: Optimization Cases*

| **Case** | **Related fields** | **Analyses performed** | **Optimization Methods** |
|---|---|---|---|
| **Car Wheel** | ○ Structures and Dynamics<br>○ Materials science<br>○ Automotive mechanics | ○ Static Structural<br>○ Performance analysis | Topological |
| **Jib Crane** | ○ Structural mechanics<br>○ Materials science<br>○ Fracture mechanics | ○ Static Structural<br>○ Performance analysis | Topological and Parametric |
| **Rocket Nozzle** | ○ Structures and Dynamics<br>○ Computational fluid dynamics<br>○ Heat transfer/ thermodynamics | ○ Static Structural<br>○ CFD<br>○ Performance | Parametric |
| **Wind Turbine** | ○ Structures and Dynamics<br>○ Computational fluid dynamics<br>○ Composite materials | ○ Static Structural<br>○ CFD<br>○ Composite failure | Parametric |

## 3.2 Tutorial

The tutorial methodology aims to deliver the content in a more descriptive and illustrative manner. The optimization process for each of the previously mentioned cases is described in a step by step basis with relevant images to support the progress.

For most study cases, the tutorial begins with the FE analyses followed by the optimization phase assuming that the initial geometry has been already created or imported from a CAD software. Additionally, this tutorial assumes the reader has a sound knowledge of the Finite Element method and has been previously introduced to FEA and optimization software such as ANSYS®

### 3.2.1 Optimization Case 1 – Car Wheel

PROBLEM DESCRIPTION

Car wheels are an essential component of the vehicle as they transmit the torque generated by the engine making the automobile move by effectively acting against static and sliding friction. The mass and shape of a wheel are critical parameters for the overall performance and life of the vehicle. A mass greater than the optimal will generate extra centrifugal forces and larger deformations. Deformations, consequently, create uneven surfaces that damage tyres overtime and generate unwanted vibrations and instability issues. Therefore, an optimal mass and shape of a wheel offers a wide range of advantages including efficient force distribution and improved fatigue life of the wheel and tyre.

The default Car model defined for the analysis is a Mitsubishi Lancer Evolution X illustrated in Figure 5. The initial wheel geometry illustrated in Figure 6, is a plain solid wheel model created in Autodesk Inventor without any spokes or material removed from the frontal section. A topological optimization analysis was deemed suitable for this study case as an approximate spokes shape and material use minimization is desired.

*Figure 5: Default Car Model*

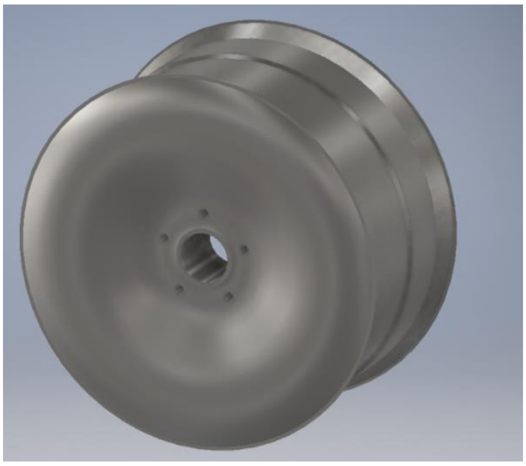

*Figure 6: Initial Geometry*

## Objectives

The main intent of the optimization process is to find the optimal frontal shape with the minimum amount of material used while meeting the loading specifications and staying well below the material's yield stress limit.

## Problem Specification

The relevant problem parameters are detailed in Table 6.

*Table 6: Problem parameters*

| Parameter | Value |
|---|---|
| Car weight | 1500 Kg |
| Pressure on wheel | 100 kPa |
| Moment applied | 300 N.m |
| Material | Magnesium Alloy |

General wheel dimensions and specifications for the selected car model are detailed below.

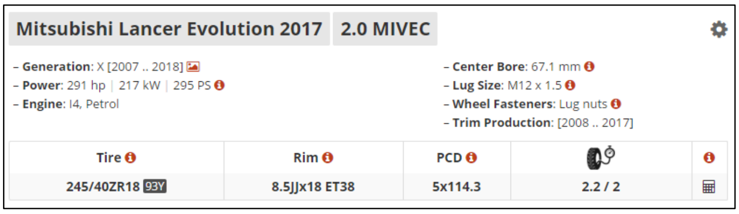


*Figure 7: Wheel specifications (www.wheel-size.com)*

## I. Start Up and Geometry Export

- The CAD model for the initial geometry was created in Autodesk Inventor. The model is directly exported to Ansys from Inventor via its embedded Ansys 18.0 Options Tab using the **Workbench** option.

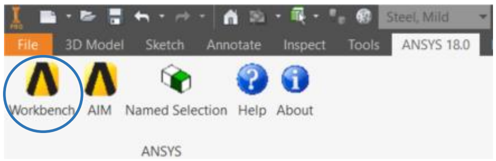


*Figure 8: Ansys interface*

- The model is automatically opened in Ansys 18.

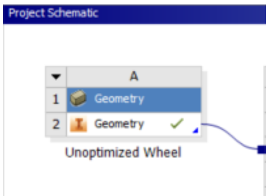


*Figure 9: Geometry tab*

## II. Static Structural Analysis

- Run a **Static Structural** study by dragging the desired study from the **Analysis Systems** column into the **Project Schematic** region.

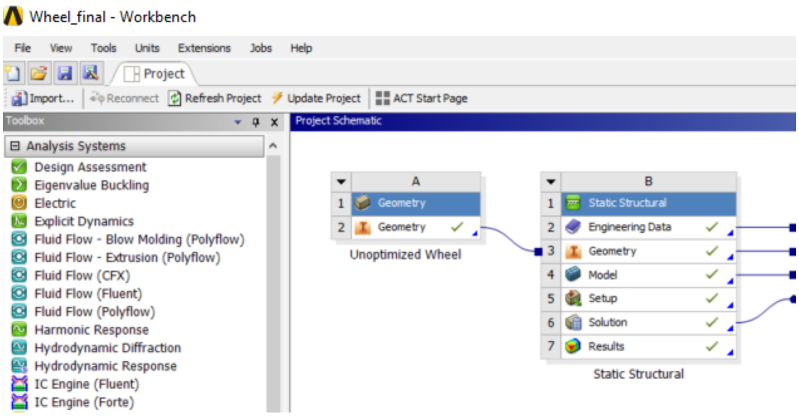


*Figure 10: Structural Study*

- Link the imported geometry to the Geometry Tab of the Static Structural study and open the **Model** Tab.

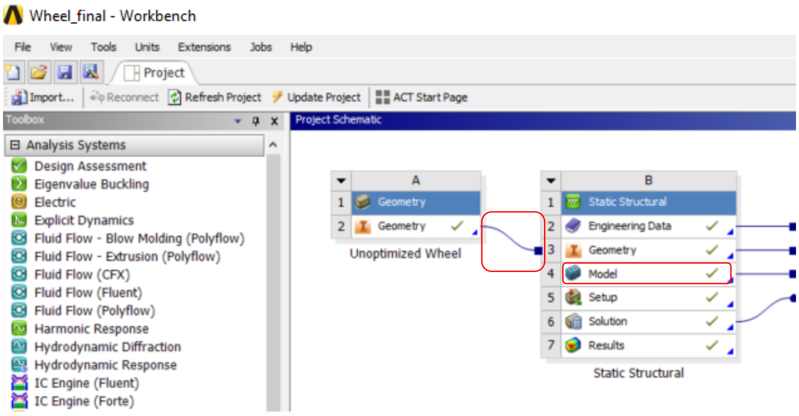


*Figure 11: Link to Model tab*

- The first step is to define a suitable mesh, in this case **edge Sizing** and **curvature Sizing** functions were implemented. Use edge and face sizing methods with sensible values for minimum size. The finer the mesh, the more accurate the results. A relatively fine mesh takes approximately 5 minutes to generate. If further sizing and methods are implemented with finer mesh, it can take more than 30 minutes to complete.

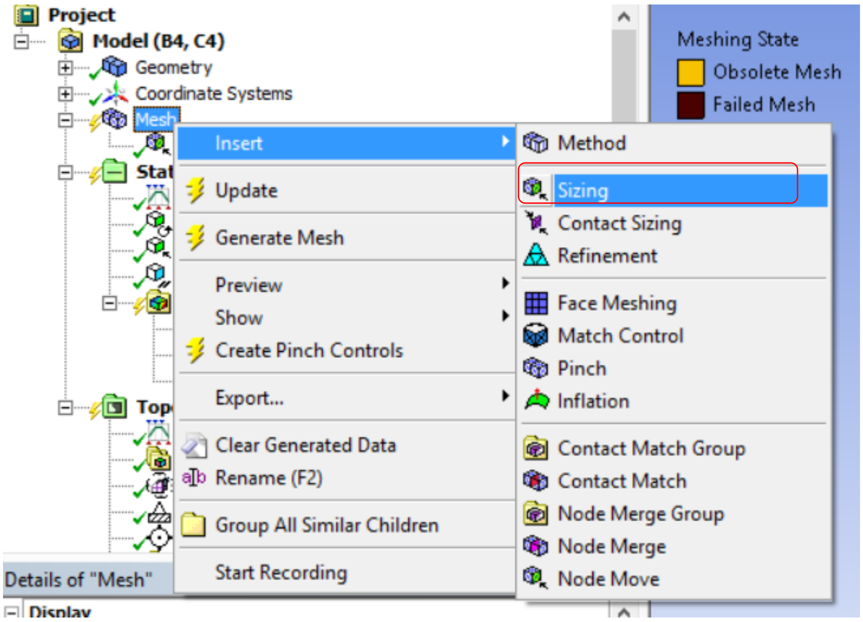


*Figure 12: Sizing function*

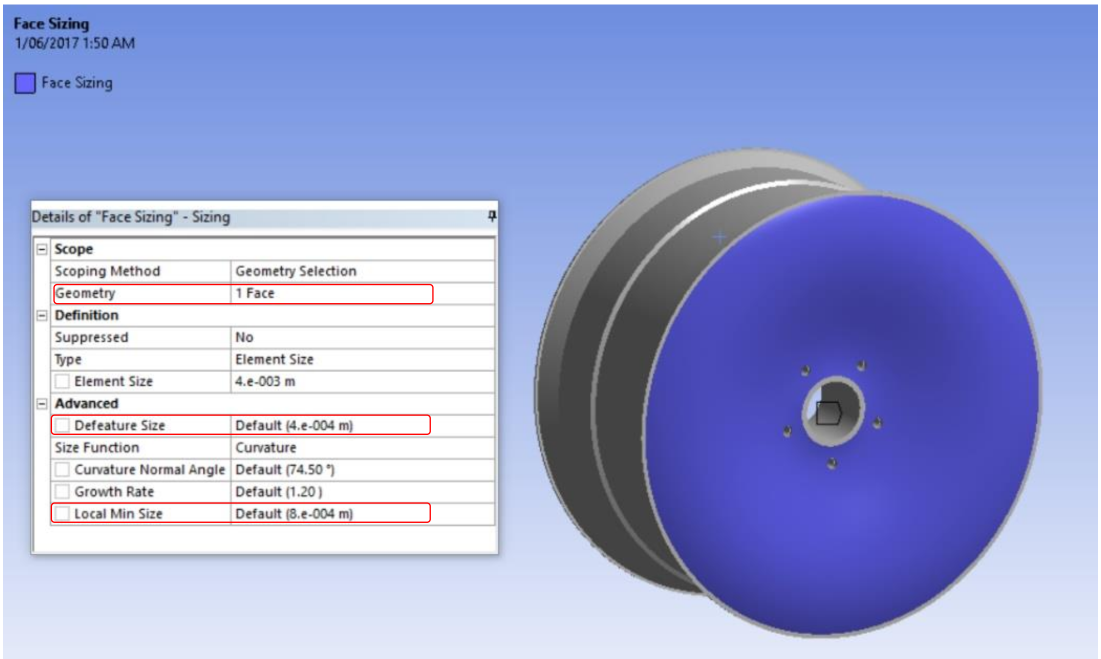


*Figure 13: Face sizing*

- A relatively fine mesh will provide more accurate results.

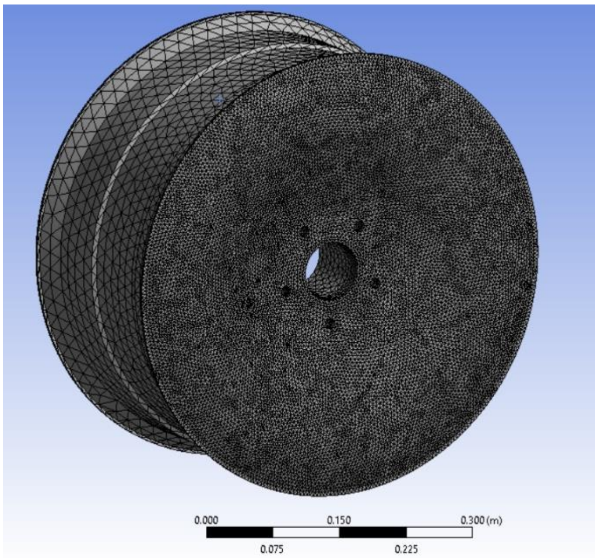


*Figure 14: Wheel Mesh*

- By clicking on the **Static Structural** element of the model tree; loads, supports and other various options appear on the top ribbon. Click on **Loads → Pressure** to add a pressure load on the surface of the wheel which will simulate the weight of the vehicle.

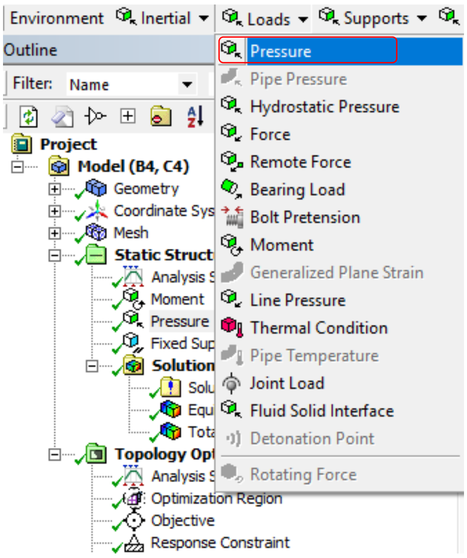


*Figure 15: Pressure definition*

- Fixed **cylindrical supports** are selected for the centre bore and bolt holes of the geometry. Additionally, a rolling resistance **Moment** of 300 N.m is added (computed by multiplying the approximate driving force applied times the wheel radius around centre bore). Likewise, the effective **Pressure** on wheel-tyre contact that includes the weight of the vehicle is approximately 150000 Pa per wheel, assuming the car is moving at a constant speed in a rectilinear trajectory.

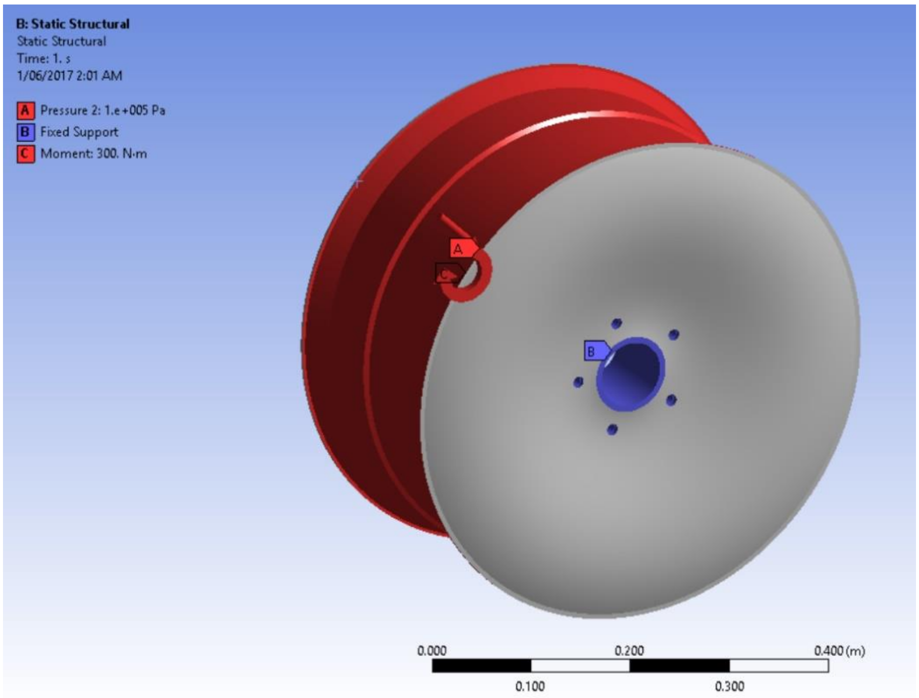


*Figure 16: Pressure on Wheel*

- Subsequently, **Stress** and total **Deformation** analyses are performed. By clicking on the **Solution** Tab, the desired results can be selected.

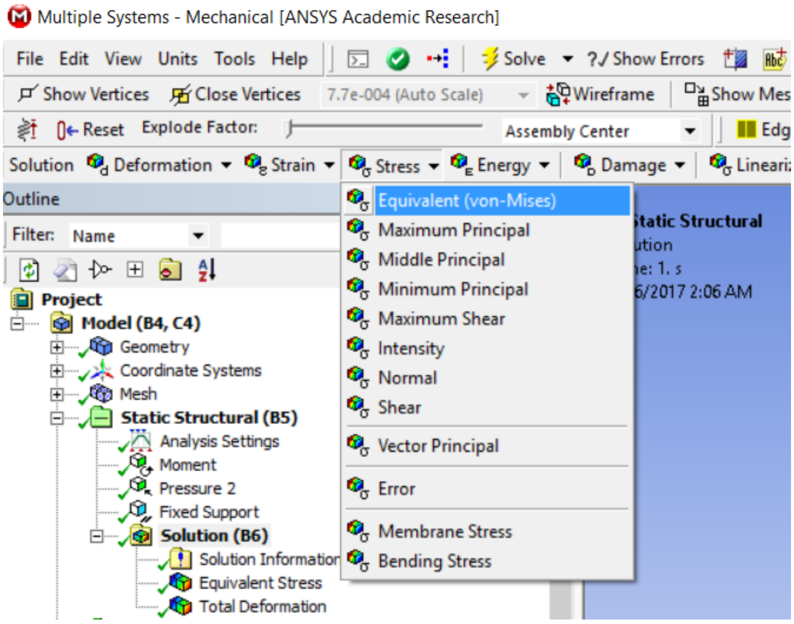

*Figure 17: Stress definition*

- The respective solutions for the Equivalent Stress and Deformation studies are displayed after the analysis is solved.

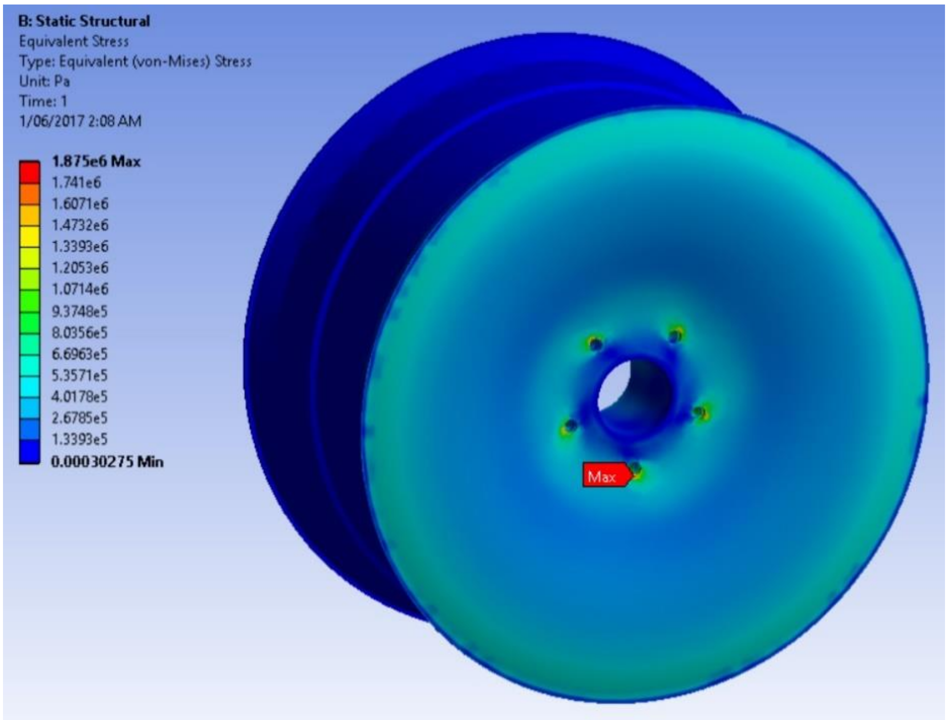


*Figure 18: Von Mises Stress results*

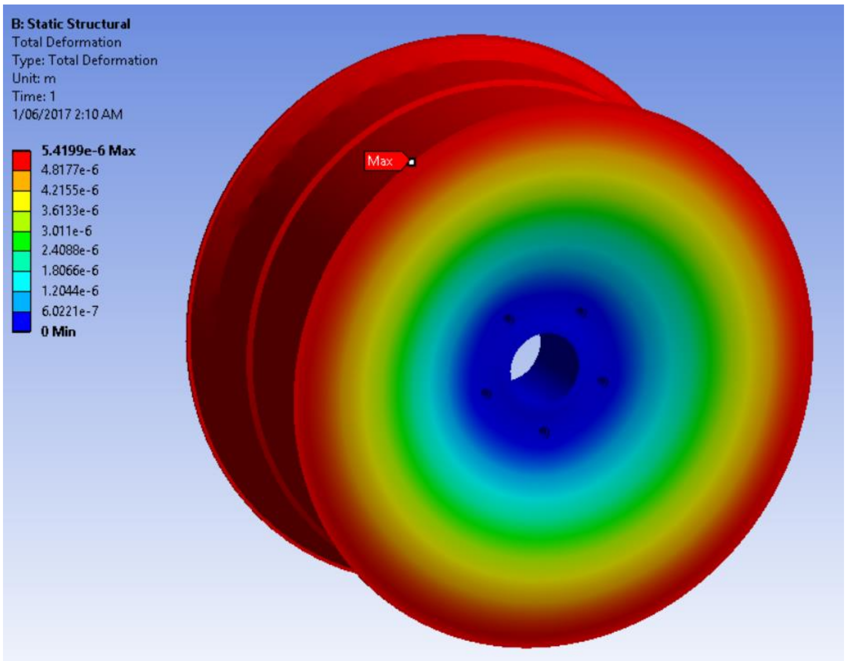


*Figure 19: Deformation results*

- The preliminary results are used as the reference criteria for the subsequent optimization process.

## III. Optimization

- To begin with, a **Topology Optimization** study is dragged from the **Analysis Systems** column. The Topology module is then linked to the static analysis. Engineering data, geometry and Model tabs are directly joined. It is also advisable to link static results to Topology optimization setup in order to simplify the process. This step already defines a default design space, objective functions, and constraints.

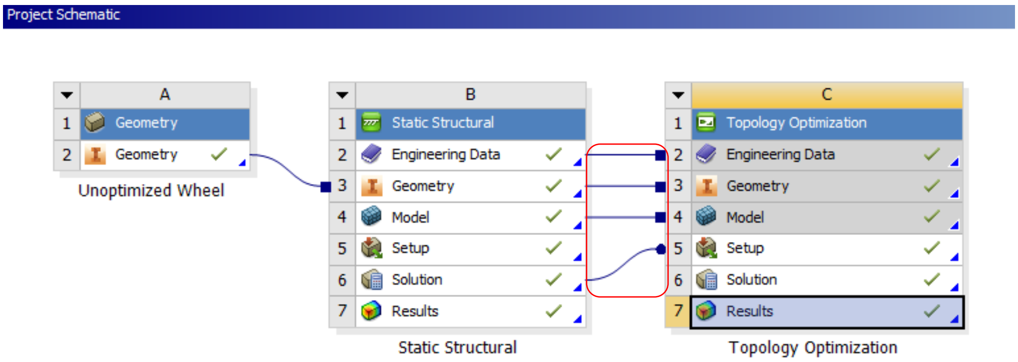


*Figure 20: Optimization module*

- Open the **Setup** Tab from the Topology Optimization menu. A new Module will be added to the previous workspace which includes Topology Optimization parameters and analysis settings.

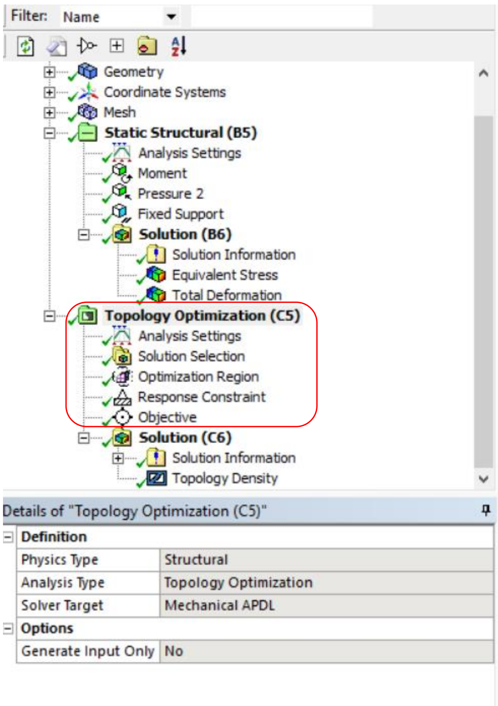


*Figure 21: Optimization options*

- Under **Analysis Settings**, a maximum number of iterations, convergence accuracy and type of solver can be defined. For this exercise, the default values are kept.

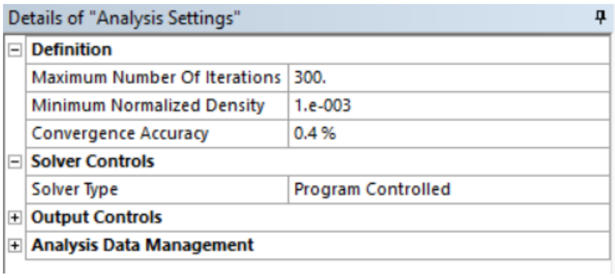

Details of "Analysis Settings"

| | |
|---|---|
| **Definition** | |
| Maximum Number Of Iterations | 300. |
| Minimum Normalized Density | 1.e-003 |
| Convergence Accuracy | 0.4 % |
| **Solver Controls** | |
| Solver Type | Program Controlled |
| **Output Controls** | |
| **Analysis Data Management** | |

*Figure 22: Solver settings*

- Under the **Topology Optimization** tab, select optimization region. Then, under **Geometry** in the Design Region, select **All bodies**. In **Exclusion Region**, select surface type and choose surfaces that will not be optimized (wheel rim without the front face, bolt pattern and centre bore). The defined regions are expressed in Figure 23.

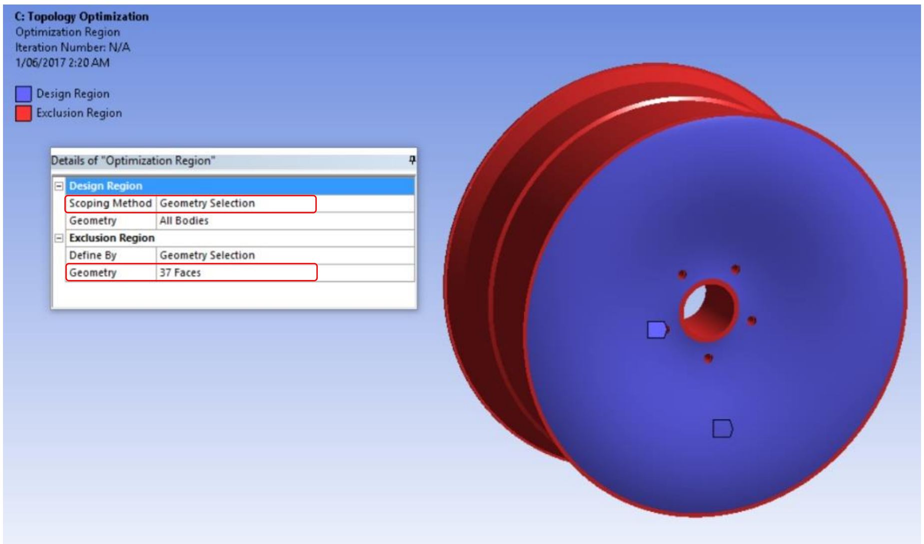


*Figure 23: Optimization region*

- **Manufacturing** constraints can be added from the top left ribbon in order to define a minimum or maximum permissible size for a specific member. It is set as program controlled for this exercise.


*Figure 24: Manufacturing parameters*

- Under **Response Constraint**, select mass or volume, depending on the optimization objective. In this case, a mass response constraint is selected with a retain value of 18 %. This value is arbitrarily set, and it's limited by the maximum amount of material that can be removed while complying with the boundary conditions set.

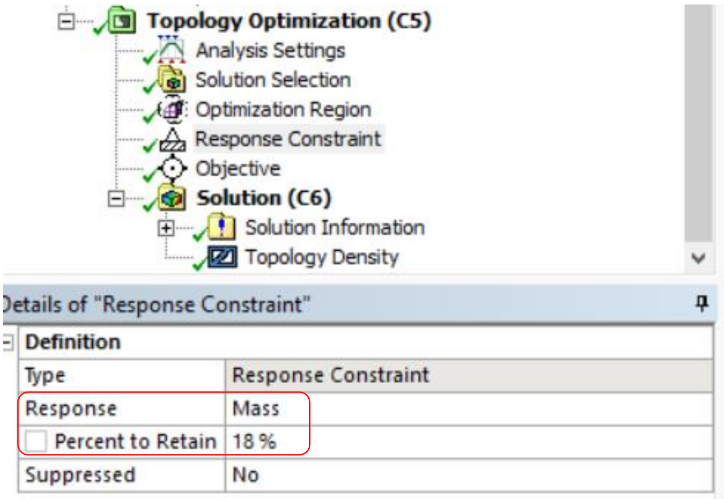


*Figure 25: Constraint definition*

- The **Objective Function** type is automatically set as single. For multi-objective analyses, additional objective functions can be implemented in the same manner. (**Objective → right click → insert → Objective**) The Response type is automatically set to **Minimize Compliance**. A Volume or Mass minimization Objective function can be set but this would over constraint the Optimization analysis (a mass constraint was already set) and the software would produce an error.

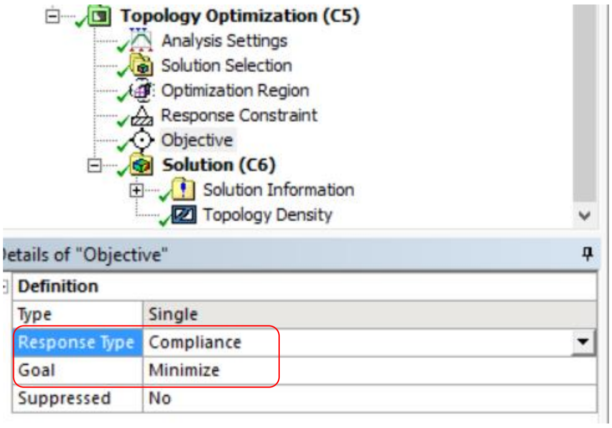


*Figure 26: Objective function definition*

- Once all the optimization parameters are defined, **Run** the analysis simulation. The process running time depends on the complexity of the model. For the specified model, the process takes approximately 5 hours to complete.
- During the analysis, check the results file for convergence. In this case, convergence was reached after 21 iterations. The number of iterations needed to reach convergence depends on the type of analysis and model's complexity.

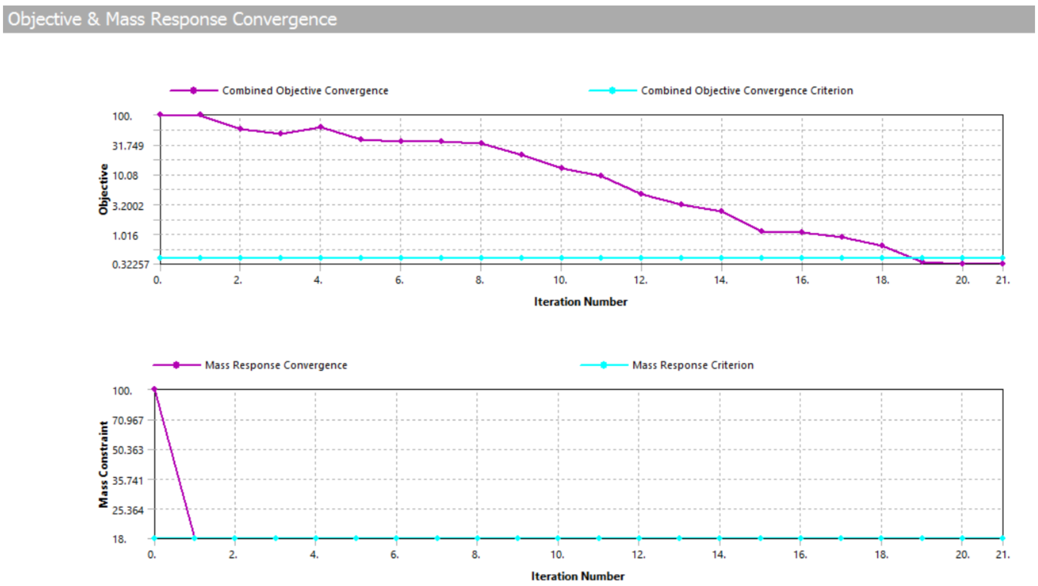


*Figure 27: Solution convergence criteria*

- Once the Solver is finalized and convergence is reached, the details of the Topology Optimization solution can be observed.

Details of "Topology Density"

| | |
|---|---|
| **Scope** | |
| Scoping Method | Optimization Region |
| Optimization Region | Optimization Region |
| **Definition** | |
| Type | Topology Density |
| By | Iteration |
| Iteration | Last |
| Retained Threshold | 0.5 |
| Exclusions Participation | Yes |
| Suppressed | No |
| **Results** | |
| Minimum | 1.e-003 |
| Maximum | 1. |
| Original Volume | 9.1555e-003 $m^3$ |
| Final Volume | 3.3114e-003 $m^3$ |
| Percent Volume of Original | 36.169 |
| Original Mass | 16.48 kg |
| Final Mass | 5.9606 kg |
| Percent Mass of Original | 36.169 |
| **Visibility** | |
| Show Optimized Region | Retained Region |
| **Information** | |
| Iteration Number | 21 |

*Figure 28: Optimization results*

- The resulting shape can be viewed in topology density under **Solution → Topology Density**.

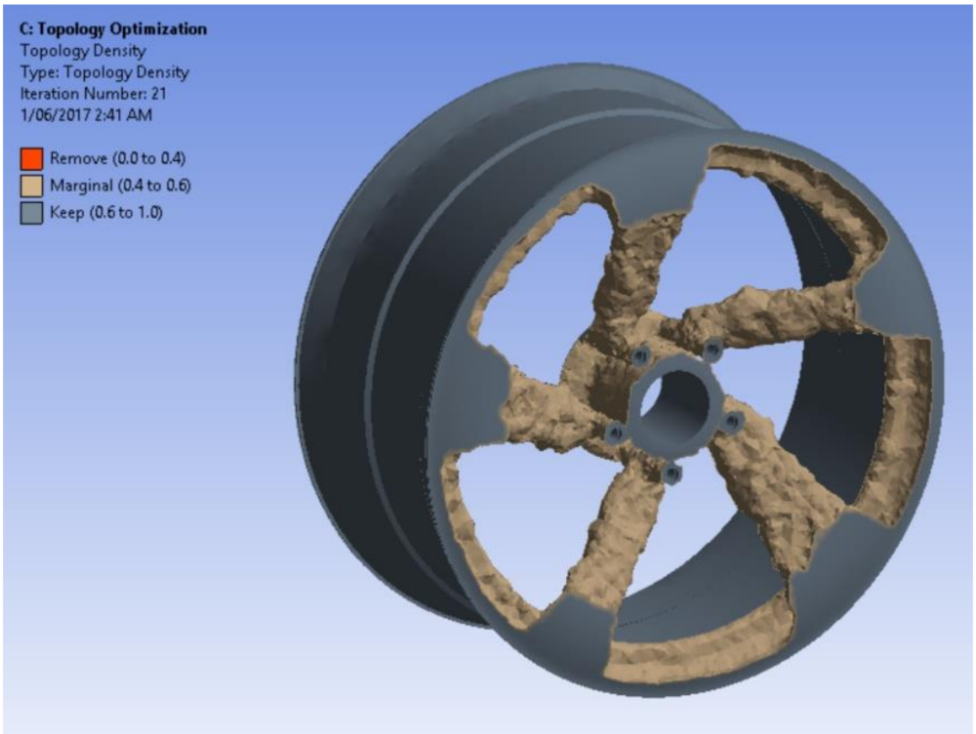


*Figure 29: Wheel shape after optimization*

## IV. Post-processing

- A post processing technique is implemented in order to smooth out the rough shapes of the optimized model. The **SpaceClaim** module of Ansys offers useful tools for this type of analyses. Similarly, **Autodesk Inventor** is also a good tool for surface finishing and post processing results.

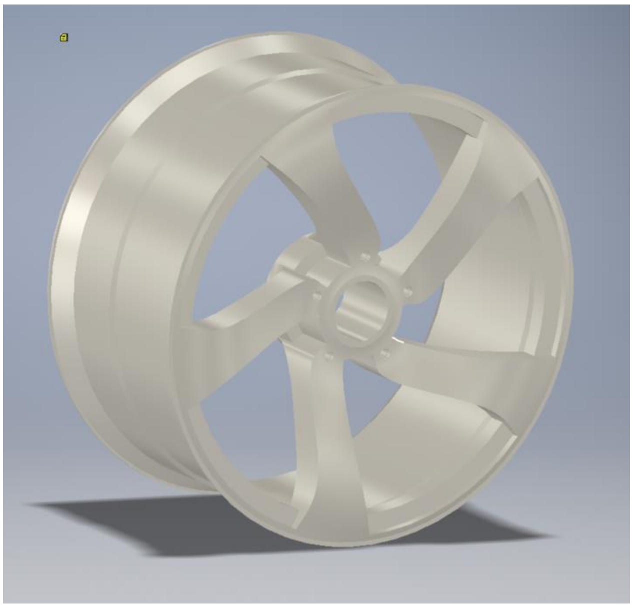

*Figure 30: Post processed model*

- After the model is processed with smoothing features and symmetry tools, it can be exported back to Ansys® 18 for a new Static Structural Analysis so the results of the optimized model can be effectively compared to those of the preliminary model.

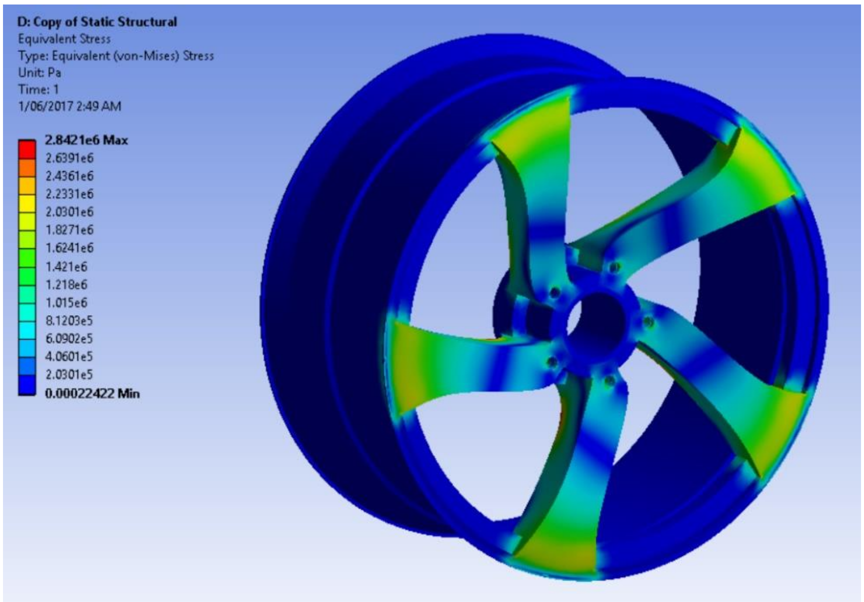


*Figure 31: Equivalent stress after optimization*

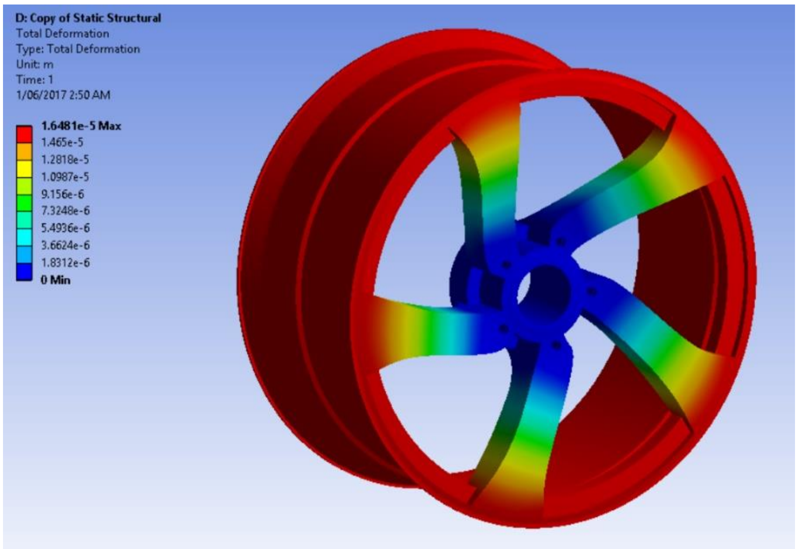


*Figure 32: Deformation after optimization*

## V. Results

The Static Structural results of the optimized model are identified in Table 7.

*Table 7: Optimization results*

| Parameter | Initial Model | Optimized Model |
|---|---|---|
| Total Stress (Von-Mises MPa) | 1.875 | 2.842 |
| Deformation (m) | 5.42e-6 | 1.65e-5 |

Literature suggests that the yield stress of Magnesium alloy is between 70 and 100 MPa which validates our analysis. The total stress acting on the wheel increased by almost 60% but such increase will not affect the fatigue life or performance of the wheel in any aspect. The deformation is also observed to be minimal with a maximum value of approximately 0.02 mm. Moreover, approximately 65% of mass was removed. The initial and optimized geometries are illustrated below.

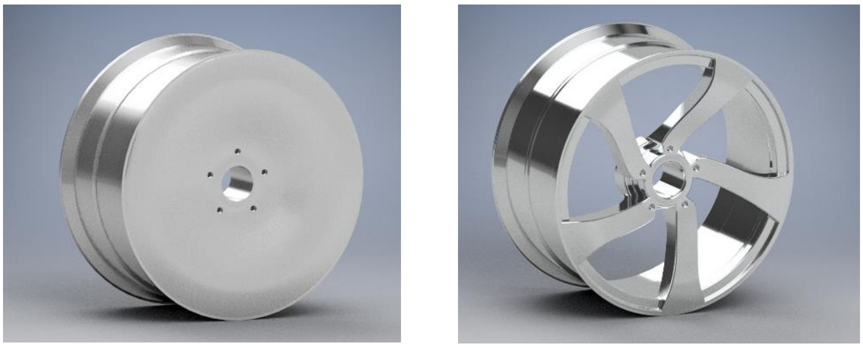

*Figure 33: End results*

### 3.2.2 Optimization Case 2 – Indoors Jib Crane

PROBLEM DESCRIPTION

Jib cranes are one of the most versatile types of cranes with a broad range of applications. Jib cranes are especially suitable for lifting tasks in relatively small or indoor areas. The Jib member is an operational arm which extends from the main body of the crane and supports a fixed pulley system. The main objective of a Jib crane is to lift and/or move heavy masses. Therefore, its Jib requires a high strength to effectively support cycling loads and a low weight to maximize the loads it can lift. An optimal strength to weight ratio would significantly enhance the operational limits of the Jib and would ensure the minimum amount of material is used.

There is a wide variety of Jib crane types used in industry. For this analysis, a standard indoors Jib crane model as suggested in Figure 34 is considered.

*Figure 34: Jib crane model (image from purposeof.com.au)*

The starting geometry, as suggested by Figure 35, presents a solid rectangular mass of steel which denotes the Jib of the crane. This component is the main optimization region for which the amount of material used is intended to be minimized. Similar to the previous study case, a topological optimization method is implemented.

*Figure 35: Initial geometry*

### OBJECTIVES

As previously mentioned, the main objective of the optimization process is to effectively minimize the amount of material used in the Jib of the crane while meeting the load and material limits. The final shape of the Jib is not constrained so an increased versatility to the optimization solver is enabled.

Relevant parameters of the case study are set following real operational limits and loads of existing similar-sized Jib cranes. Such parameters are detailed in Table 8.

*Table 8: Problem parameters*

| **Parameter** | **Value** |
|---|---|
| Material | Stainless steel |
| Test load | 5 tonnes |
| Jib length | 4.5 meters |
| Crane height | 5 meters |
| Jib thickness | 0.2 meters |

## I. Start Up and Geometry Export

- Select a Static Structural analysis from the Toolbox in Workbench and drag it to the project schematic.

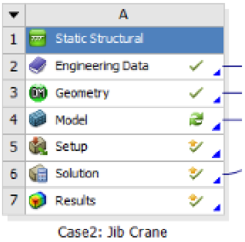


*Figure 36: Static Structural analysis*

- The initial geometry is created in **Autodesk Inventor** and exported to Ansys Workbench. The export can be done directly from the Inventor-Workbench interface tab or the model can be saved as *.iges* and opened as a new Geometry in Workbench.

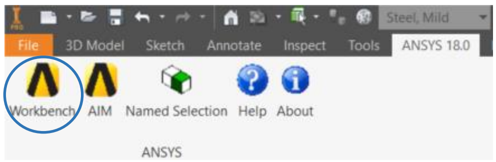


*Figure 37: Inventor interface*

- Before the static structural or optimization studies can be carried out, appropriate **named selections** need to be assigned to relevant sections of the crane. Named selections can later be used to assign loads, constraints or conditions to specified sections of the model. The main named selection to be created is the **optimization region** being the Jib of the crane. In order to create a named selection, select a type of geometry (body, face, edge or point) → select the desired geometry (Jib) → right click and create named selection. In this case, the named selection is called *Optimization_region*

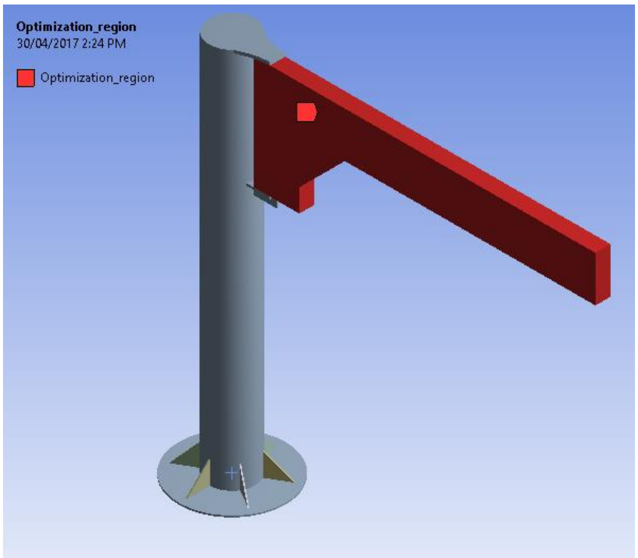


*Figure 38: Optimization region*

- An additional step is implemented in which a surface is created at the bottom end of the Jib where the test load will be placed, simulating real operation. The first step is to create a **sketch** at the end of the Jib. Select lower Jib surface → create **new plane** from face → create rectangular sketch on new plane.

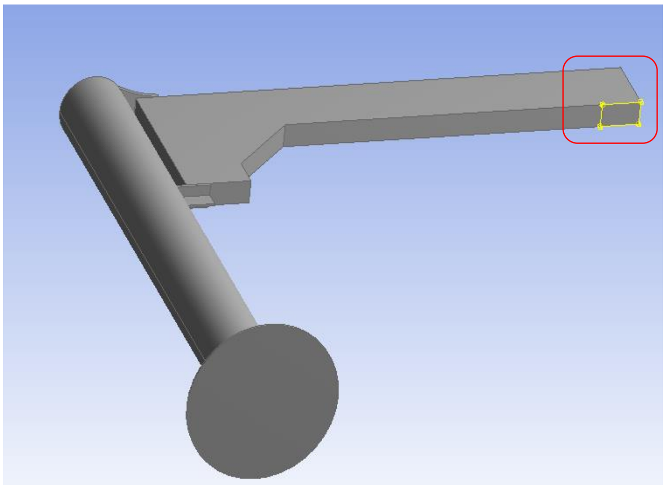

*Figure 39: Jib sketch*

- Then, from the new sketch, a surface is created. Click on **Concept** on the top left menu → Surfaces from Sketches. Assign the surface to the previously created sketch and click on **Generate**.s

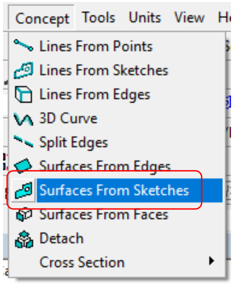


*Figure 40: Surface from sketch*

- The surface body will be created right at the end of the bottom surface of the Jib where the test load is applied.

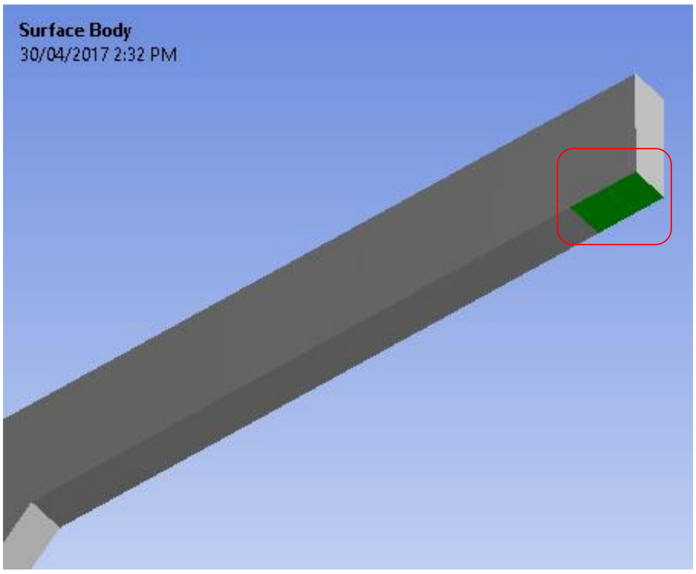


*Figure 41: Surface body*

## II. Static Structural Analysis

Once the geometry is successfully created, and the named selections are defined, the next step involves the implementation of a structural analysis under the previously defined loads and constraints. The results from this analysis will be compared to the results of the optimized model.

- An appropriate mesh needs to be assigned to the model. Right click on Model → Edit.

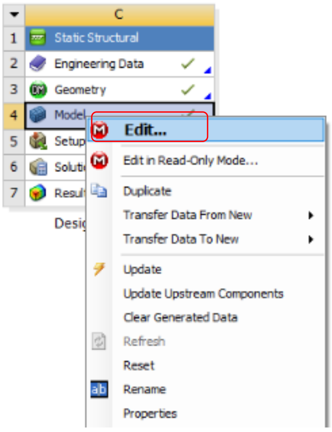


*Figure 42: System's mesh*

- In order to obtain a relatively fine mesh with smaller elements where higher accuracy is desired, two **sizing functions** are created. (mesh → right click → insert → sizing). The first sizing function will be created for the optimization region. Choose named selection from the **scope** option and indicate the section named “Optimization region”. Select an element size type and provide an element size value. The size function can be set as uniform as the optimization region does not have special features as curves or holes.

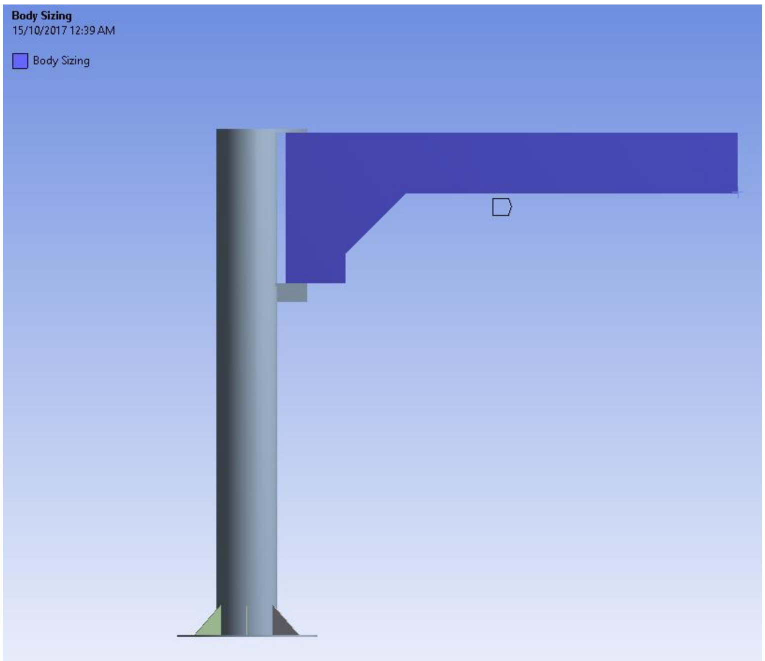


*Figure 43: Optimization region sizing*

- The same procedure is followed for the second **sizing function** assigned to the Jib supports. A relatively smaller element size is set because most of the load is carried by the structural supports and a finer mesh would output more reliable results. The final mesh is illustrated in Figure 44.

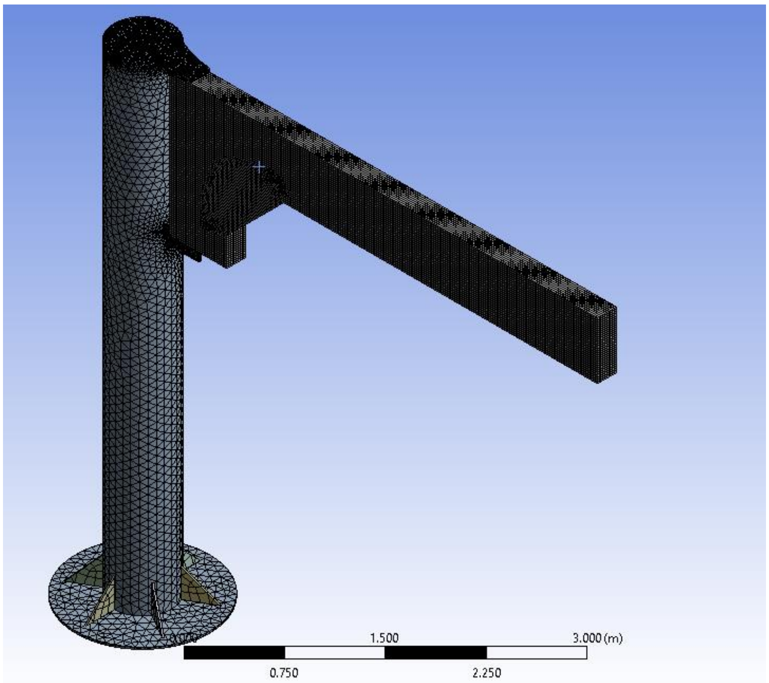


*Figure 44: Final Mesh*

- Now, the **static structural** analysis can be carried out. Click on the static structural tab → on the top ribbon select **Supports** and choose a **fixed support**. Select the relevant geometry (bottom face of base) and **apply**.

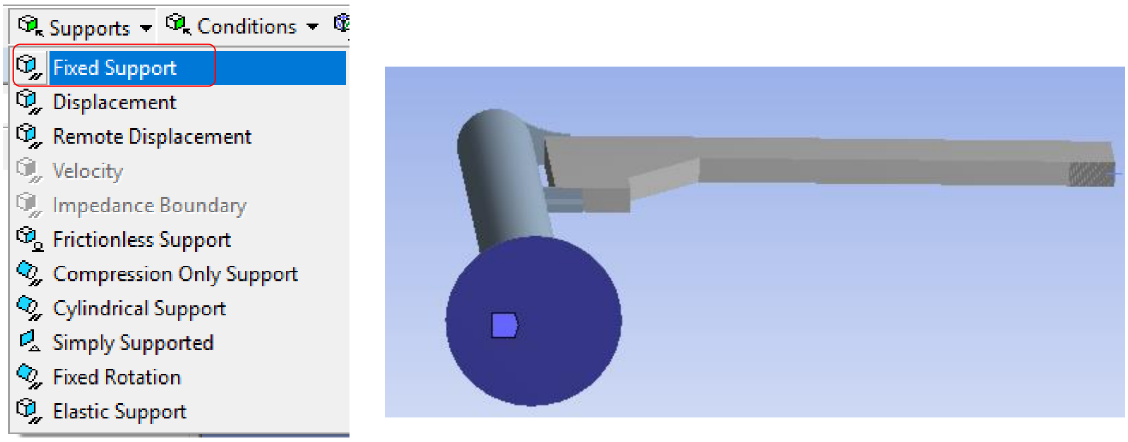


*Figure 45: Fixed base*

- Under **Loads,** on the top ribbon, select **Force** and choose the previously created surface located at the bottom end of the Jib. For this example, a maximum load of 5 tonnes (50000 [N]) is defined (general case for this type of cranes)

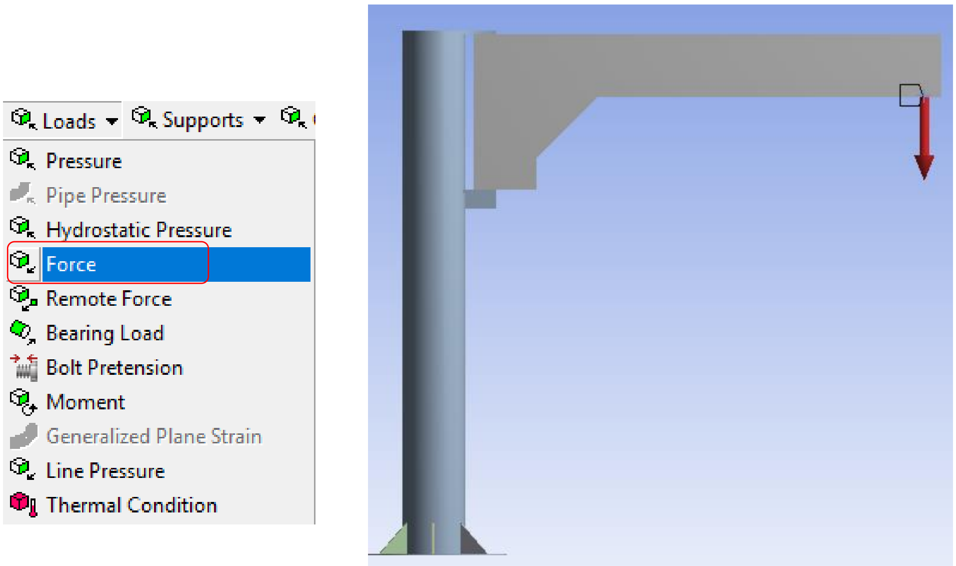


*Figure 46: Load definition*

- Click on the **Solution** tab → the possible solution types that can be implemented appear on the top ribbon. Select **Deformation** → Total Deformation, then, select **Stress** → Equivalent (Von-Mises) which are the most pertinent results required for this analysis.

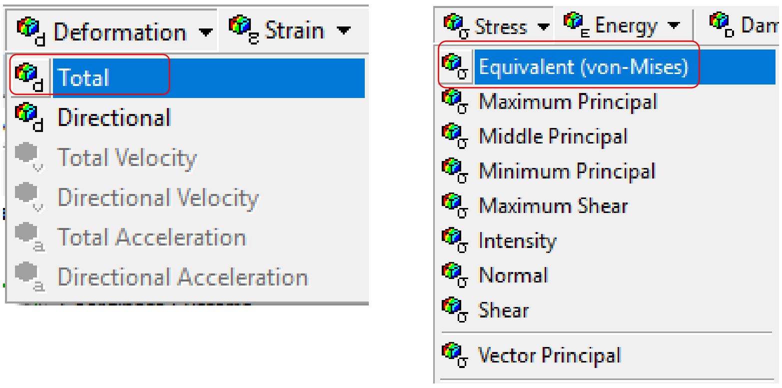


*Figure 47: Study types*

- Once the loads/constraints and study types are set, the model can be solved (**Solution** → right click → **Solve**). The solution process takes about 30 minutes (depending on the mesh quality and problem size). The results are described by Figures 48 and 49.

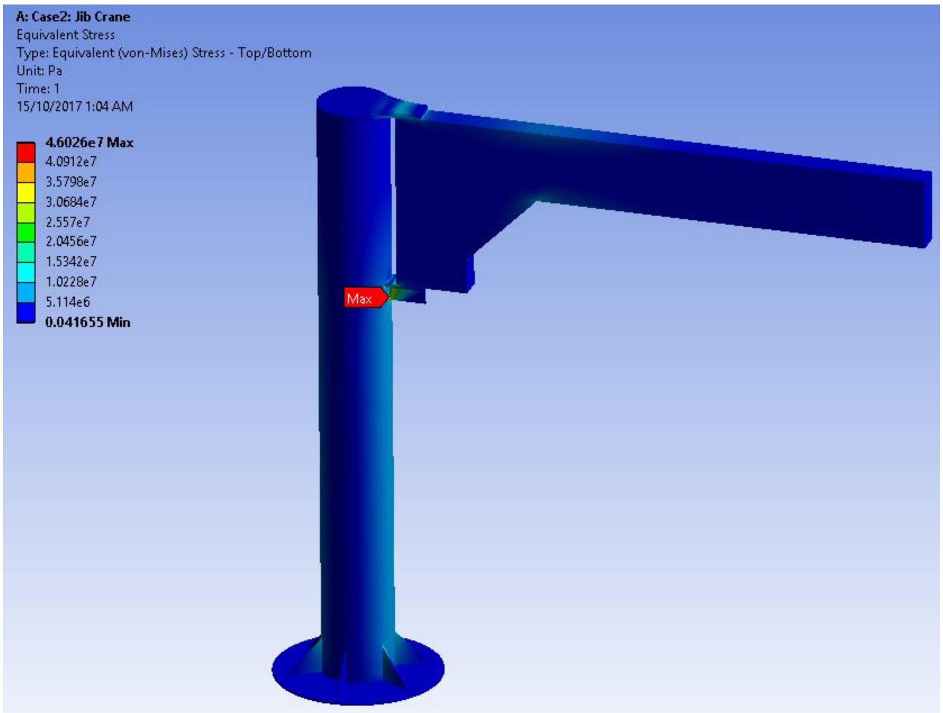


*Figure 48: Von Mises Stress*

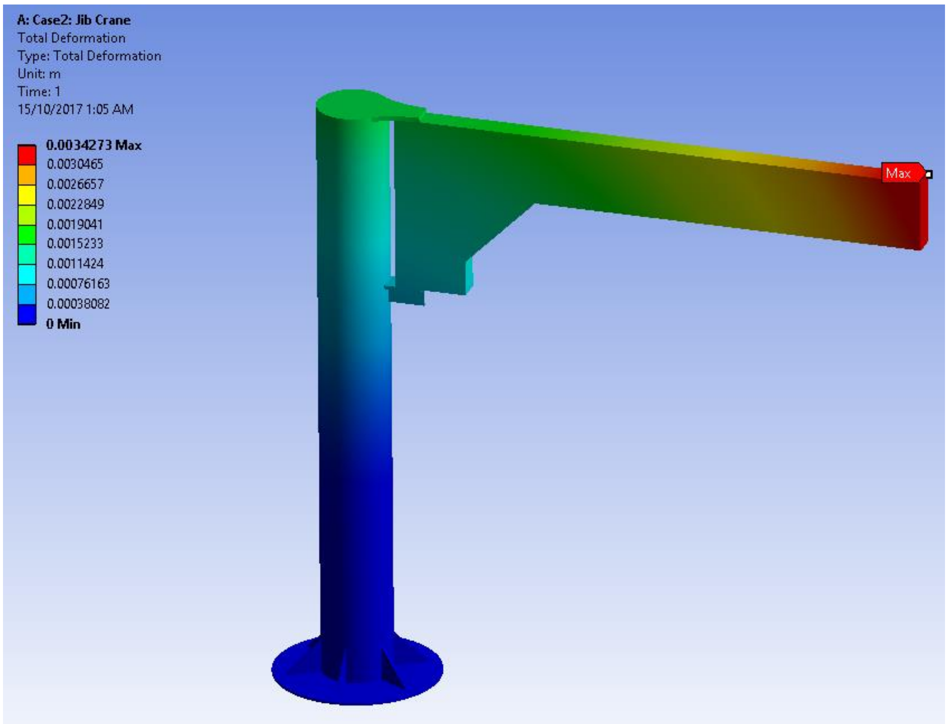


*Figure 49: Deformation*

## III. Optimization

Once the stress and deformation studies are completed, the topology optimization procedure is carried out. This process is similar to the first optimization case performed.

- The structural analysis is linked to a topology optimization study (similar to the first study case) with the **Engineering Data, Geometry** and **Model** as shared tabs. Additionally, the solution tab of the structural analysis can be linked to the **Setup** tab of the optimization study, so the results obtained in Static Structural study are kept.

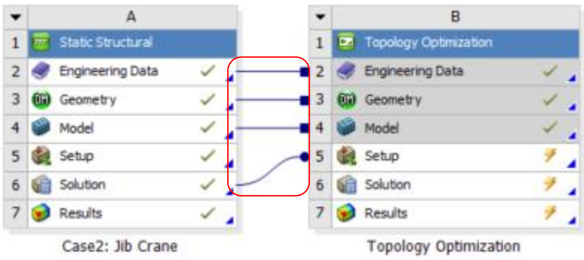


*Figure 50: Optimization study*

- Open the **Setup** tab on the optimization study. Under Topology Optimization, click on **Analysis Settings** and check the parameters as per Figure 51. The solver is chosen to be **Program Controlled** which means the software selects the most suitable solution method for the problem. The **convergence accuracy** can be increased or decreased according to the desired precision of the study. The default value is 0.1%, a higher value can be applied to studies that require improved accuracy.

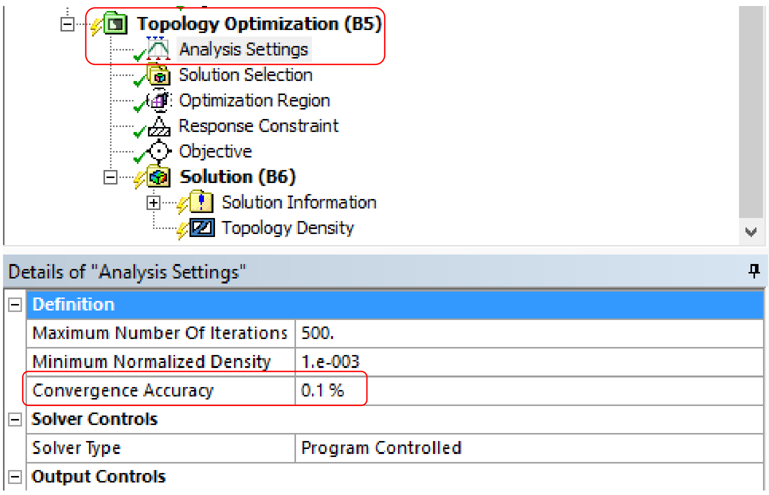


*Figure 51: Analysis settings*

- Under the **Optimization Region** option, the entire model is set as a design region by default. However, in this case, we only wish to optimize the Jib of the crane. One of the named selections created when defining the geometry was called “Optimization region”. This named selection is now useful for setting the design region.

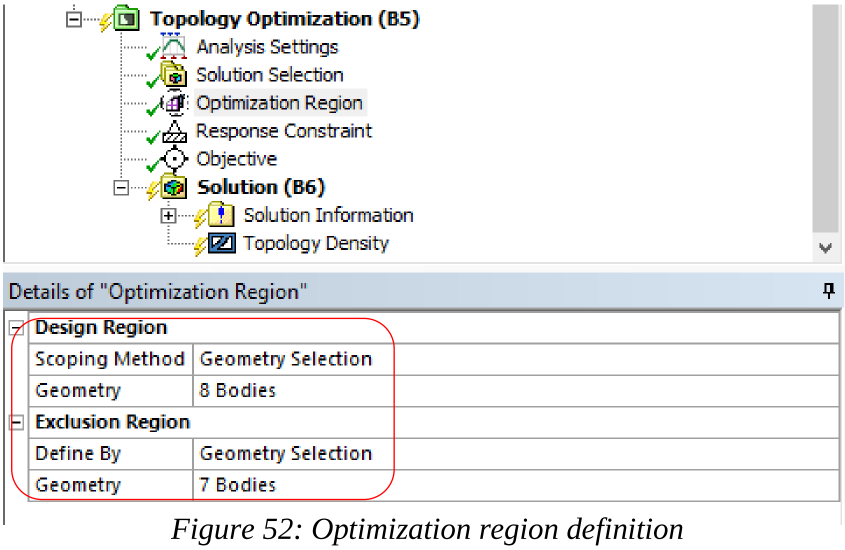


*Figure 52: Optimization region definition*

- The optimization region (Jib) and the exclusion region are illustrated in Figure 53.

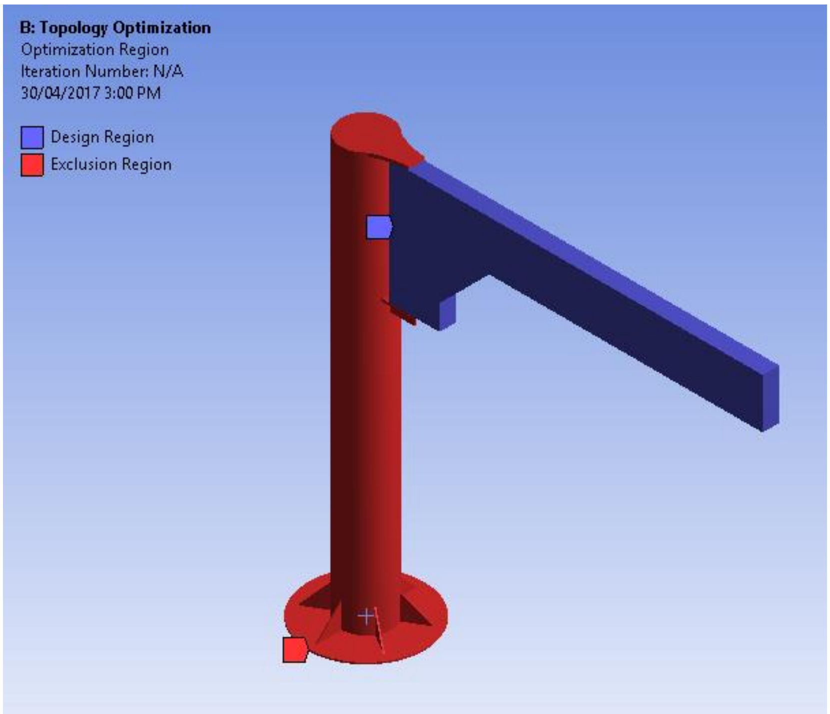


*Figure 53: Optimization region*

- As in the previous study, **Manufacturing** constraints can be added from the top left ribbon in order to define a minimum or maximum permissible size for a specific member. It is set as program controlled for this exercise.


*Figure 54: Manufacturing constraints*

- Under **Response Constraint**, the mass of the model is selected to be the main constraint as we wish to carry out our study around it. The **Percent to Retain** value can be arbitrarily set but an unrealistically low value will yield unfeasible results or errors in the solution of the model. Thus, a 30% mass retention value is chosen. Additionally, the Percent to Retain value can be set as a parameter. This feature will be studied in the following case studies regarding Parametric Optimization.

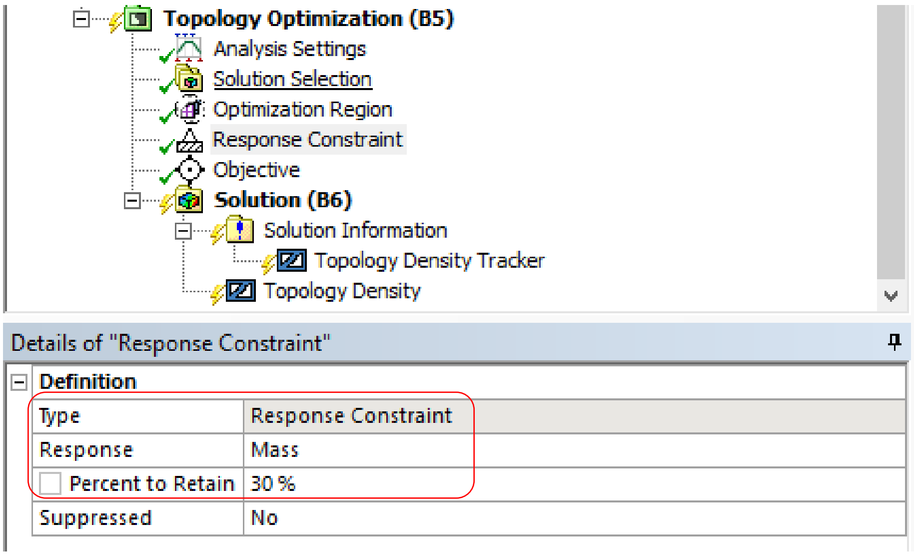


*Figure 55: Constraints*

- Subsequently, the **Objective function** of the optimization study is defined. As in the wheel case, a compliance objective function type is deemed suitable. As previously explained, compliance indicates that the system will be able to sustain the defined loads and boundary conditions once the optimization process is completed. To insert an objective function, **Objective → right click → insert → Objective**. The Response type is automatically set to **Minimize Compliance**.

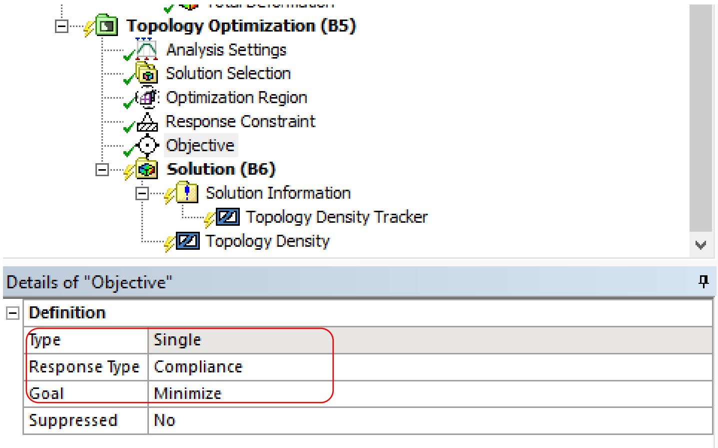


*Figure 56: Objective function*

- Under **Solution** → right click → **Solve**. The running time depends on the complexity of the model. For the specified case and mesh quality, the process takes approximately 6 hours to complete.

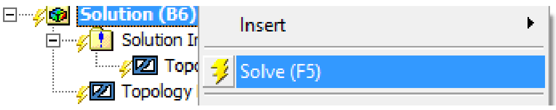


*Figure 57: Solve model*

- The solution process can be tracked under the **Solution Information** tab where we can manually check for **Convergence** during the analysis as explained in Figure 58. In this case, convergence was reached after 20 iterations. The number of iterations needed to reach convergence depends on the type of analysis, model complexity and mesh quality.

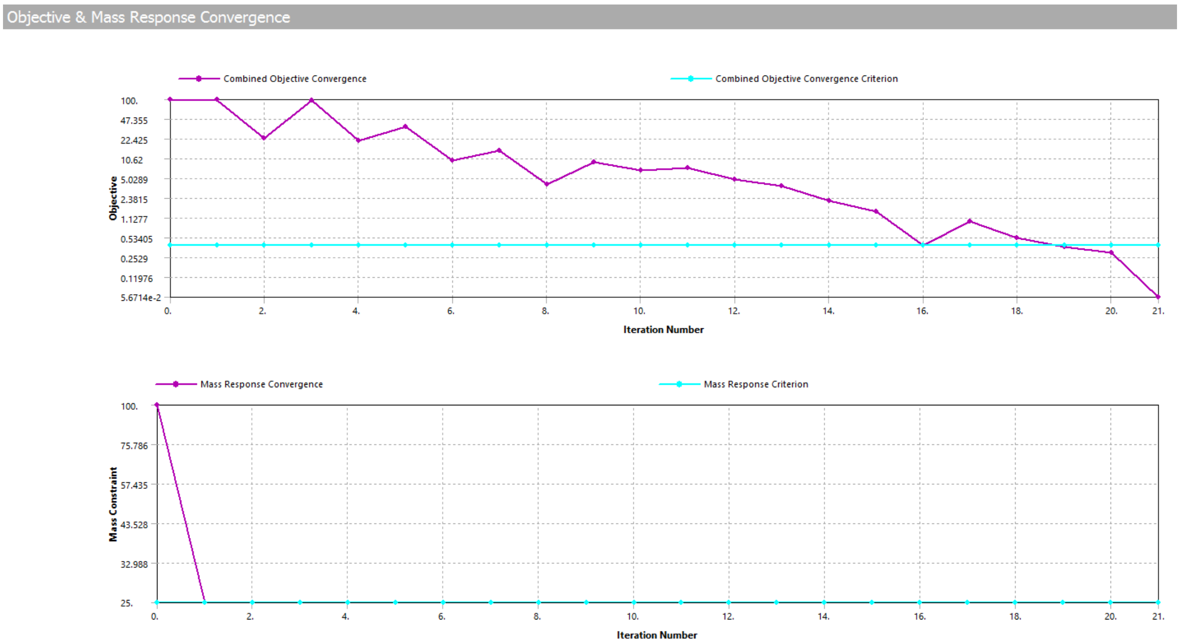


*Figure 58: Convergence plot*

- Once the Solver is finalized and convergence is reached, the details of the Topology Optimization solution can be observed.

| Details of "Topology Density" | |
|---|---|
| **Scope** | |
| Scoping Method | Optimization Region |
| Optimization Region | Optimization Region |
| **Definition** | |
| Type | Topology Density |
| By | Iteration |
| Iteration | Last |
| Retained Threshold | 0.5 |
| Exclusions Participation | Yes |
| Suppressed | No |
| **Results** | |
| Minimum | 2.e-003 |
| Maximum | 1. |
| Original Volume | 2.1501 $m^3$ |
| Final Volume | 1.6305 $m^3$ |
| Percent Volume of Original | 75.833 |
| Original Mass | 16878 kg |
| Final Mass | 12799 kg |
| Percent Mass of Original | 75.833 |

*Figure 59: Optimization results*

- The resulting shape (Figure 60) can be viewed in topology density under **Solution → Topology Density**.

*Figure 60: Resulting topology*

## IV. Post-processing

- A similar post processing technique as for the wheel study case is implemented in order to smooth out the rough shapes of the optimized model. The SpaceClaim module of Ansys offers useful tools for this type of analyses. Similarly, **Autodesk Inventor** is a good tool for surface finishing and post processing results.

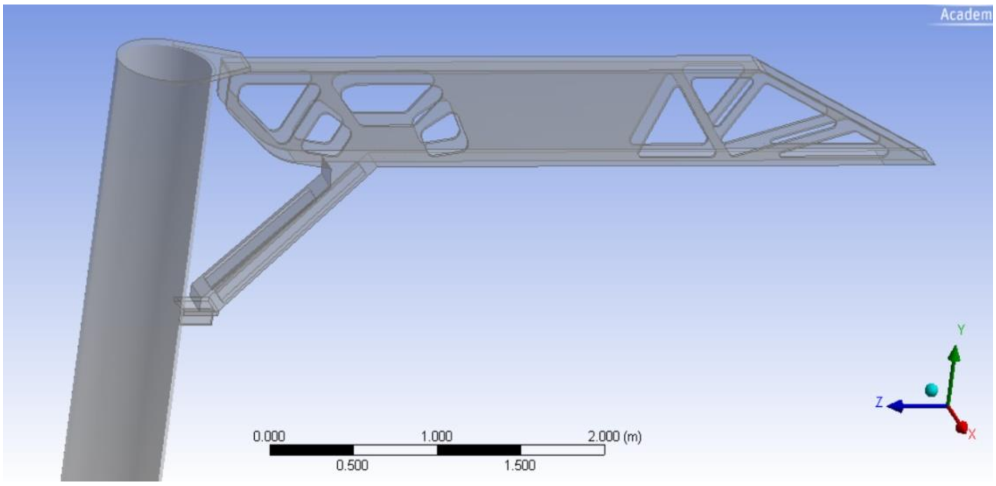


*Figure 61: Post processed model*

*Figure 62: Optimized model*

- After the model is processed with smoothing features and symmetry tools (Figure 62), it can be exported back to Ansys® 18 for a new Static Structural Analysis so the results of the optimized model can be effectively compared to those of the preliminary model. This step works as a validation method for the optimization process. Results from the structural analysis of the optimized model are illustrated in Figures 63 and 64.

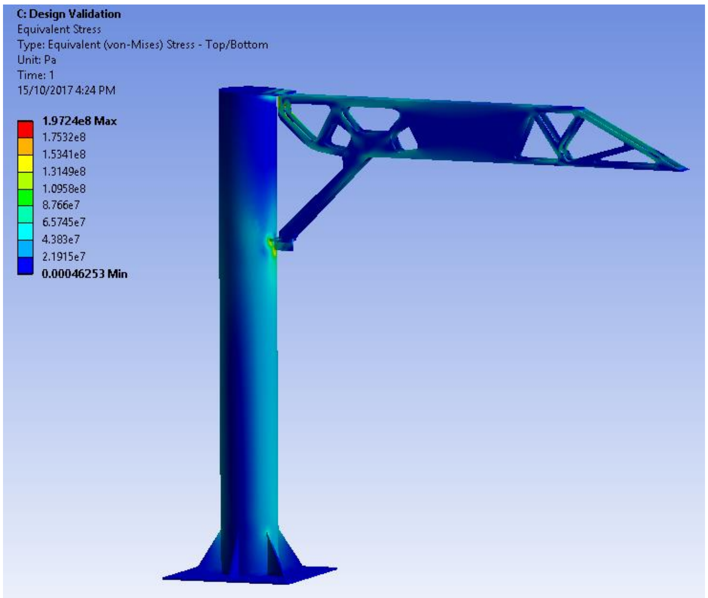


*Figure 63: Equivalent stress*

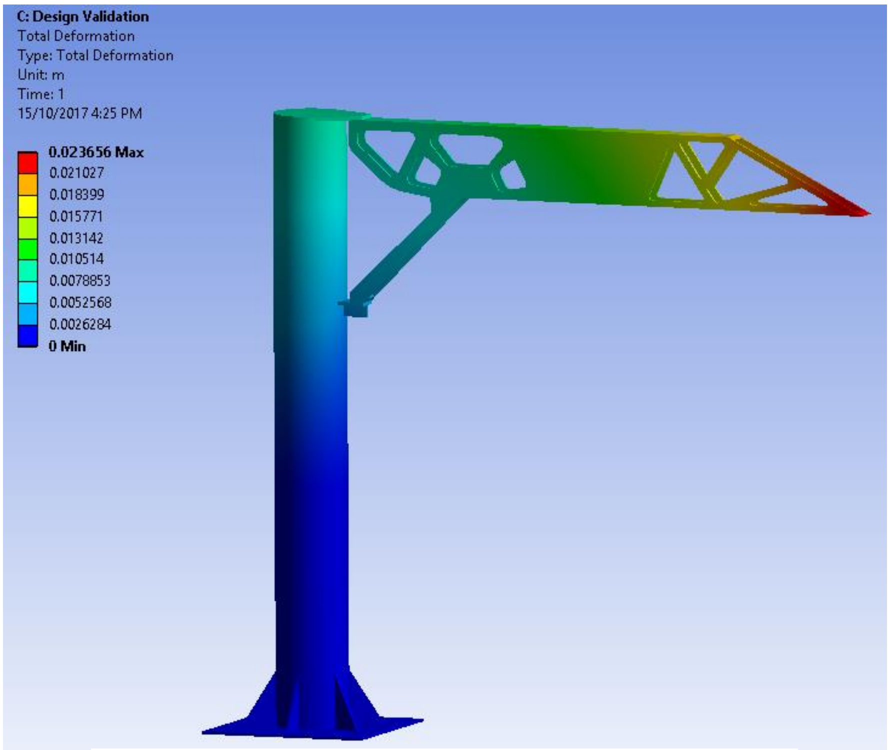


*Figure 64: Total deformation*

## V. Results

The Static Structural results of the optimized model along with those of the initial model are identified in Table 9.

*Table 9: Validation*

| Parameter | Initial Model | Optimized Model |
|---|---|---|
| Total Stress (Von-Mises MPa) | 46.02 | 197.24 |
| Deformation (m) | 0.003 | 0.023 |

Literature suggests that the yield stress of **Stainless Steel** typically lies between 220 and 300 MPa. Structural results strongly suggest that the maximum equivalent stress experienced by the model during operation is below the material's yield strength, validating the optimization results. The deformation suggests a slight increase but is still permissible with a maximum value of approximately 2 cm. Furthermore, nearly 30% of the total mass was removed. The initial and optimized geometries are illustrated in Figure 65.

*Figure 65: End results*

### 3.2.3 Optimization Case 3 – Rocket Nozzle

PROBLEM DESCRIPTION

Rocket engines create thrust by effectively expanding propellant and accelerating it to supersonics speeds. The shape of the nozzle is carefully analysed, tested and optimized so the desired amount of thrust is produced in a sustainable manner. This optimization case considers a medium size bell-shaped rocket nozzle resembling SpaceX's Merlin 1D Engine as in Figure 66.

The initial 2D geometry is created in Autodesk Inventor and imported to Ansys Workbench 18. Subsequently, a CFD analysis is carried out in order to obtain the preliminary exit flow conditions. Critical dimensions such as the throat and exit areas, nozzle length and chamber pressure are parametrized for the optimization study. The mentioned optimization parameters are illustrated in Figure 67.


*Figure 66: Merlin rocket engine (image from nasaspaceflight.com)*

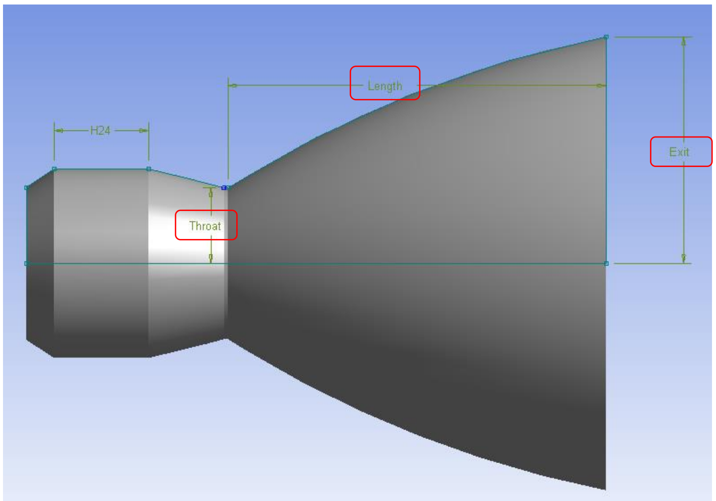


*Figure 67: Initial Nozzle Geometry*

### OBJECTIVES

As previously stated, the main optimization objectives include:

- Achieving a sonic flow speed (Mach 1) at the throat of the nozzle and a subsequent flow expansion to supersonic speeds in the diverging section of the nozzle.
- Obtaining a perfect (or close to perfect) flow expansion where the pressure of the flow exiting the nozzle equals the back (ambient) pressure.

### ASSUMPTIONS

Rocket science is a thorough and complex field that requires several design, simulation, test and optimization analyses to obtain a reliable model. Thus, a number of assumption and approximations are made to simplify the analysis keeping in mind that the study focuses on testing the optimization capabilities of the FEA software rather than the rocket engine performance itself. Relevant assumptions include:

- The working fluid is ideal air at constant temperature.
- Pressure generated by combustion in real engines is simulated as a constant chamber pressure whose nominal value will be optimized.
- The ambient (back) pressure is constant with a nominal value of one atmosphere (1 bar)
- Heat transfer through the nozzle walls is negligible.

### PROBLEM SPECIFICATION

The initial parameters taken into account for this analysis are detailed In Table 10. Such parameters are preliminary as the optimization process will suggest the optimum values that will need to be used in order to effectively meet the aims of the study.

*Table 10 Study parameters*

| **Parameter** | **Value** |
|---|---|
| Chamber pressure (kPa) | 200.0 |
| Ambient pressure (kPa) | 101.2 |
| Throat diameter (m) | 0.4 |
| Exit diameter (m) | 1.2 |
| Nozzle length (m) | 1.0 |

## I. Start Up and Geometry Export

- A **Fluid Flow (Fluent)** study is selected from the **Analysis Systems** toolbox and dropped in the Project Schematic as per Figure 68.

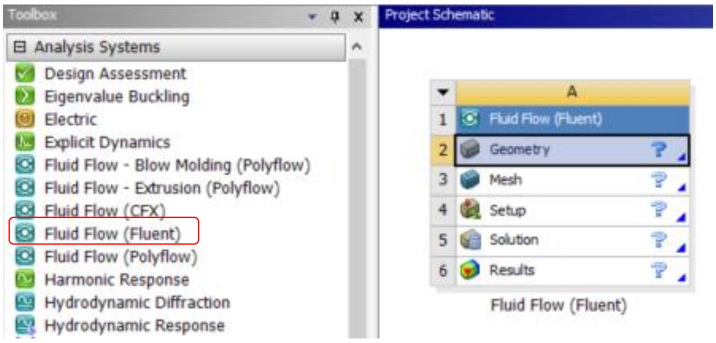


*Figure 68: Analysis selection*

- The initial geometry created in **Autodesk Inventor** is directly exported to Workbench 18

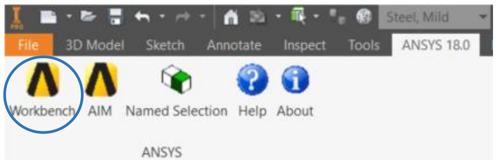


*Figure 69: Geometry export*

- The initial geometry created includes the nozzle with previously stated dimensions, as well as a flow domain at the exit of the nozzle of approximately 10 meters so the flow exiting the nozzle can be observed and the performance of the nozzle tested. The geometry exported to Workbench is illustrated in Figure 70.

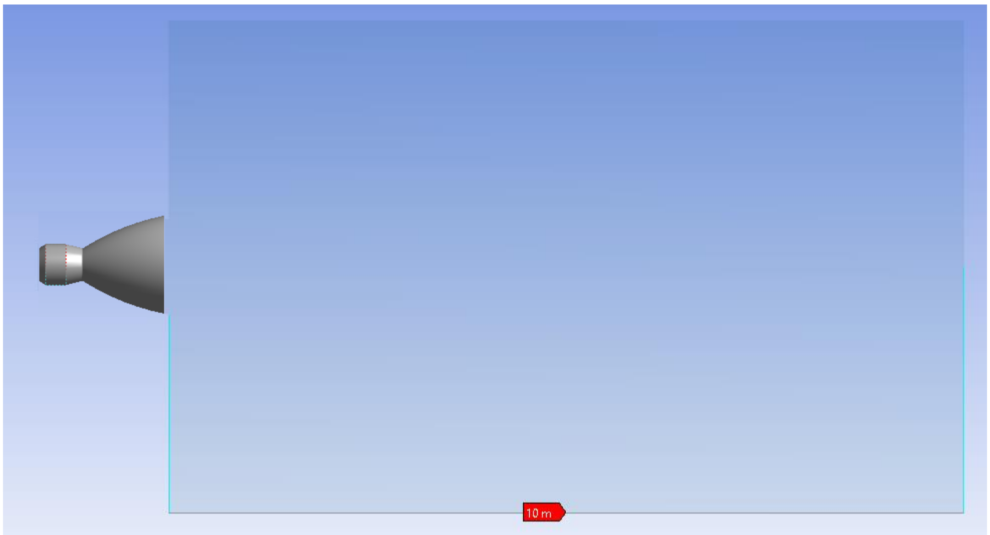


*Figure 70: Initial Geometry*

- PARAMETERS 1 TO 3: The **parameters** defined during the geometry generation process, as previously mentioned, are the exit radius, throat radius, and Nozzle length.

| Dimensions: 4 | |
|---|---|
| D Exit | 0.6 m |
| H24 | 0.25 m |
| D Length | 1 m |
| D Throat | 0.2 m |

*Figure 71: Geometry parameters*

- Once the parameters are defined, a *Parameter set* box will automatically appear in the **Project Schematic** window.

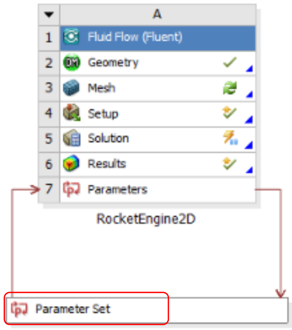


*Figure 72: Input Parameters*

- An important step is to name relevant faces/edges (using the **Named Selection** option) to which appropriate boundary conditions will be allocated during the CFD analysis. Relevant features to name include the inlet, outlet and the analysis domain (entire model). Additionally, the throat and exit edges were named as per Figure 73.

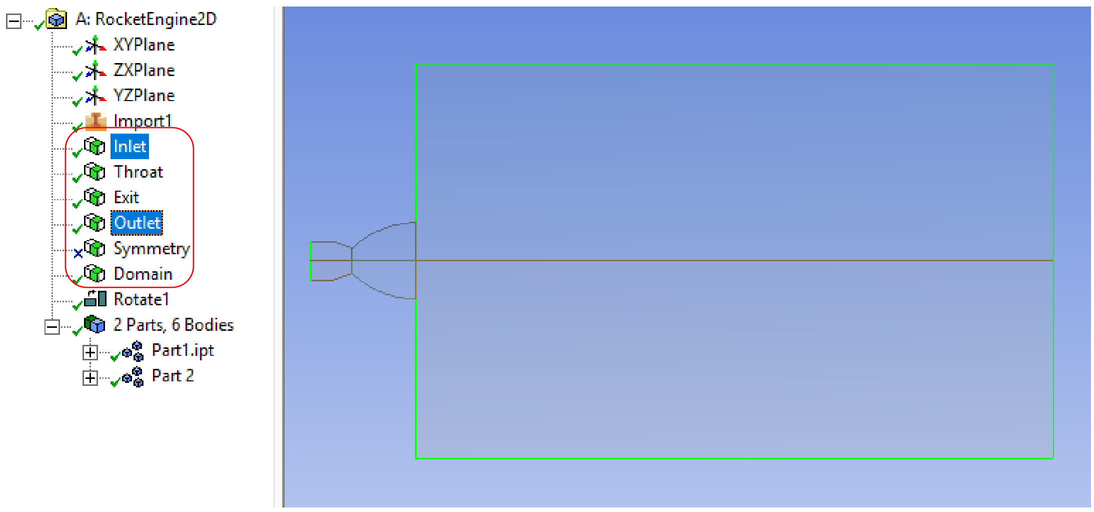


*Figure 73: Named Selections*

- The created geometry represents the flow domain. Thus, the body is set as a **Fluid**.

| Details of Body | |
|---|---|
| Body | Nozzle |
| Volume | 0.36673 $m^3$ |
| Surface Area | 3.6315 $m^2$ |
| Faces | 12 |
| Edges | 26 |
| Vertices | 16 |
| Fluid/Solid | Fluid |
| Shared Topology Method | Automatic |
| Geometry Type | DesignModeler |

*Figure 74: Body type*

## II. Meshing

The next step involves the generation of a suitable **Mesh**, similar to previous study cases. A fine mesh is desirable especially along the boundaries and small sectional areas of the nozzle. However, a very fine mesh takes a considerable amount of computational time to generate and therefore is not recommended for this study which does not require an exceedingly high accuracy. As mentioned, the most sensible sections of the model are the boundaries (place of boundary layer formation) the inlet, outlet and the throat section.

- A curvature **sizing function** is appropriate for the model due its highly curved shape. A fine relevance centre is also defined for more precise results.

| Details of "Mesh" | |
|---|---|
| Export Format | Standard |
| Element Order | Linear |
| Sizing | |
| Size Function | Curvature |
| Relevance Center | Fine |
| Max Face Size | 4.e-002 m |
| Mesh Defeaturing | Yes |
| Defeature Size | 8.7996e-004 m |
| Growth Rate | Default (1.20 ) |
| Span Angle Center | Fine |
| Min Size | 1.7599e-003 m |
| Curvature Nor... | Default (18.0 °) |
| Bounding Box Di... | 12.0550 m |
| Minimum Edge L... | 0.20 m |

*Figure 75: Mesh definition*

- For the boundaries of the model, an **inflation** feature is implemented (mesh → right click → inflation) where the number of layers, growth rate, inflation algorithm and other parameters can be set according to the desired accuracy. The **maximum layers** value for the inflation feature is arbitrarily set as 10. This value is deemed suitable for the purpose of the study.

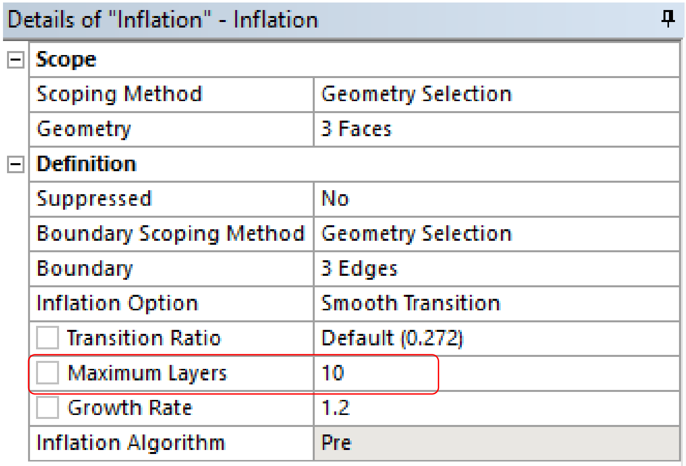


*Figure 76: Inflation feature*

- Additionally, an edge sizing feature (mesh → right click → sizing) is also implemented so a relatively fine and consistent mesh is generated across the nozzle. The mentioned sizing function is applied to the outlet and throat of the nozzle.

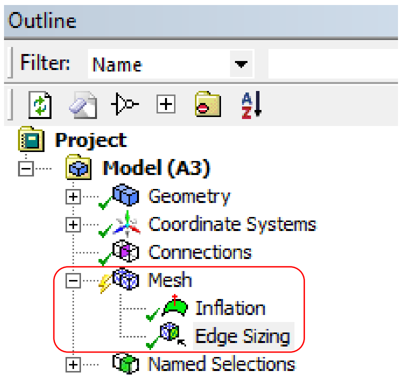


*Figure 77: Mesh functions*

- The final mesh is illustrated in Figure 78.

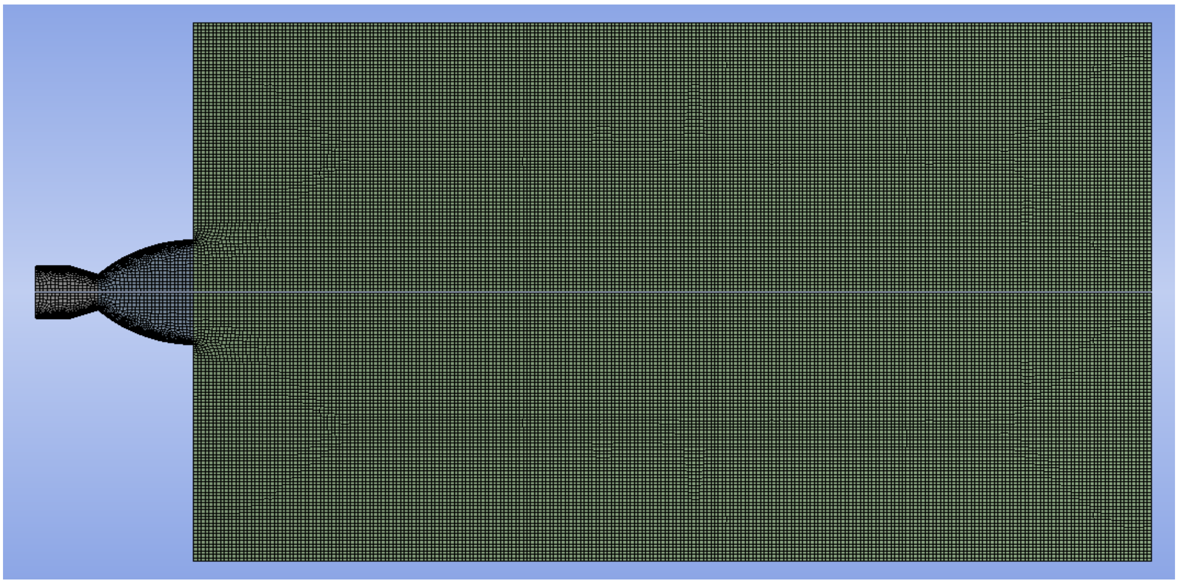

*Figure 78: Final mesh*

## III. CFD Study

- Once a suitable mesh is generated, the CFD analysis can be initiated. The first step is to open the **Setup** tab.

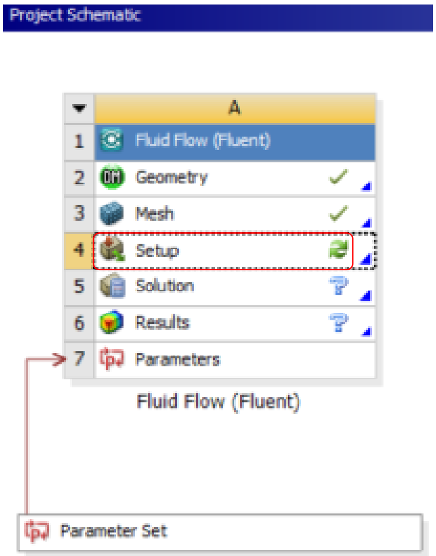


*Figure 79: Analysis setup*

- A **settings** window will appear where the default display and processing options can be observed. The **Double Precision** option is selected for this analysis as compressible flow studies require a relatively more precise analysis.

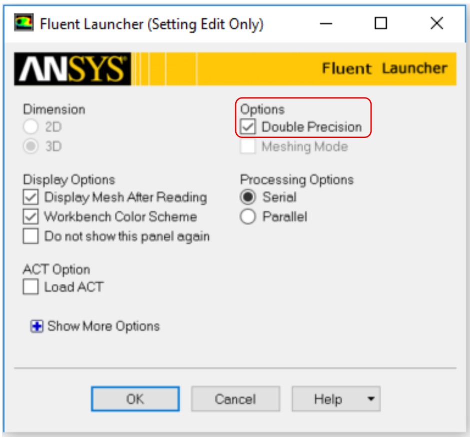


*Figure 80: Analysis settings*

- The **Fluent Module** is then launched, and the model is automatically imported and displayed as per Figure 81.

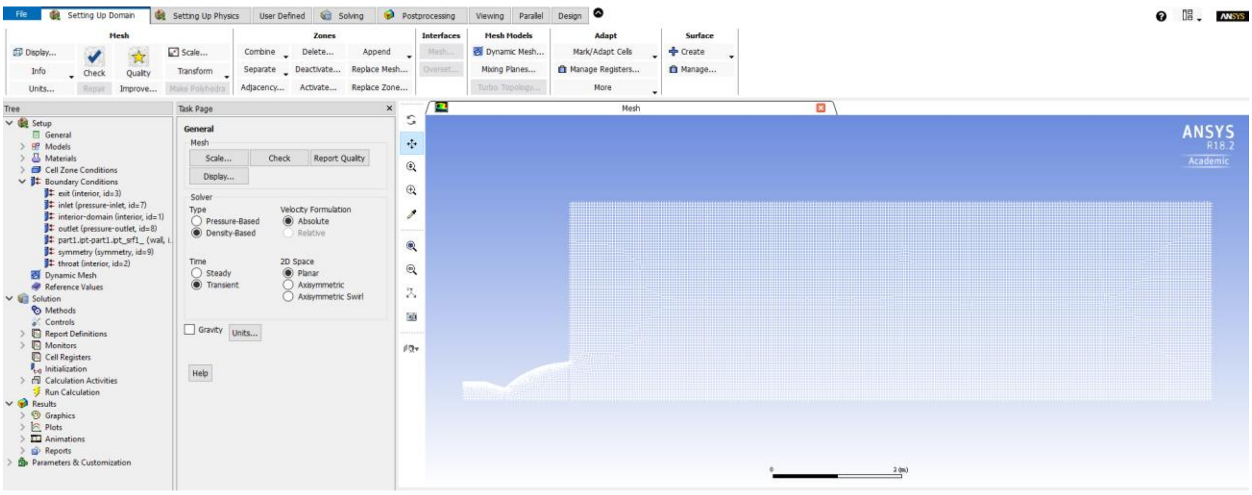

*Figure 81: Model imported to Fluent*

- The subsequent CFD Analysis is highly systematic as the **Fluent Module** offers a simplified and organized technique for carrying out the study following a series of steps towards the final solution. Such steps include the **Setup**, **Solution** and **Results** which comprise the model parameters, boundary conditions, solver types, results preferences, and are detailed on the far-left column of the screen as per Figure 82.

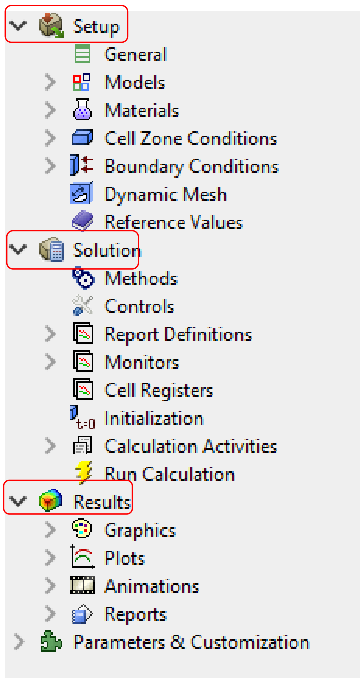


*Figure 82: Analysis components*

- Selecting the **General** tab, a **density-based** solver type is chosen since compressibility effects are a major feature of the analysis. Furthermore, a **transient** Time is preferred as we wish to observe the transient characteristics of the nozzle. Finally, gravity can be safely neglected due to the far higher pressure and acceleration forces being dominant in the rocket engine.

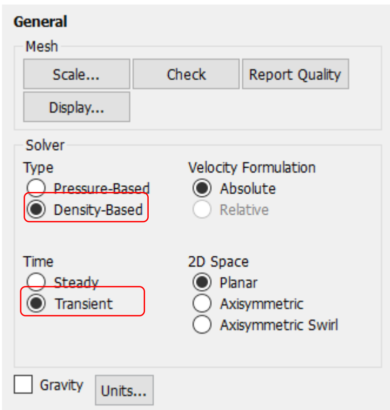


*Figure 83: General settings*

- Following the model tree, the next tab contains the available **Models** for the system. Under this tab, the **Energy** model is turned on (Energy → double click → tick energy equation) which implements an energy conservation approach besides the mass and momentum conservation methods already employed by the solver.

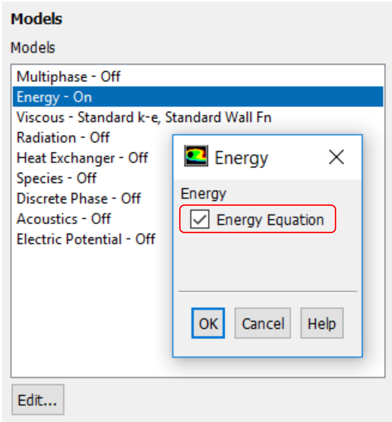


*Figure 84: Energy equation*

- Additionally, the default viscous model consists of a laminar flow approach which is not appropriate for this analysis. Therefore, a more suitable model that effectively takes turbulence into account must be implemented. A standard **two-equation k-omega SST** model is deemed suitable for the current analysis as it incorporates modifications for low-Reynolds-number effects, compressibility, and shear flow spreading. The SST (shear stress transport) model selected accounts for shear stress turbulence in transonic flows as suggested by the Ansys Fluent Theory guide.

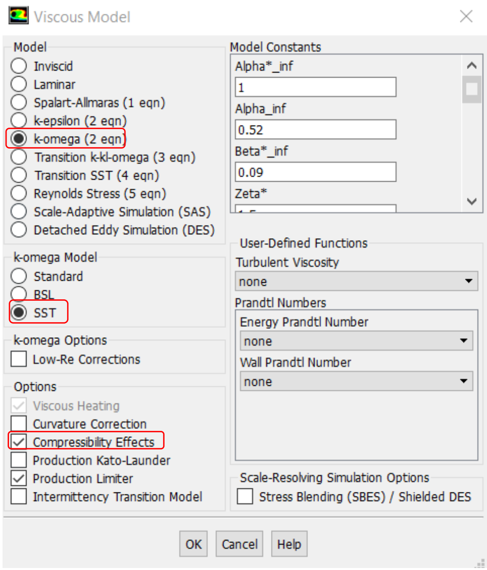


*Figure 85: Viscous Model*

- The next tab down the model tree involves the **Materials** to be considered for the analysis. For this study, ideal air is incorporated as the baseline fluid. Its properties can be viewed or modified by clicking on Materials → air → Properties. Under **Density**, the ideal-gas option is thus selected. A more detailed combustion analysis can be carried out with the desired fuel and oxidizer types by defining chemical equations, species, ratios and other necessary parameters.

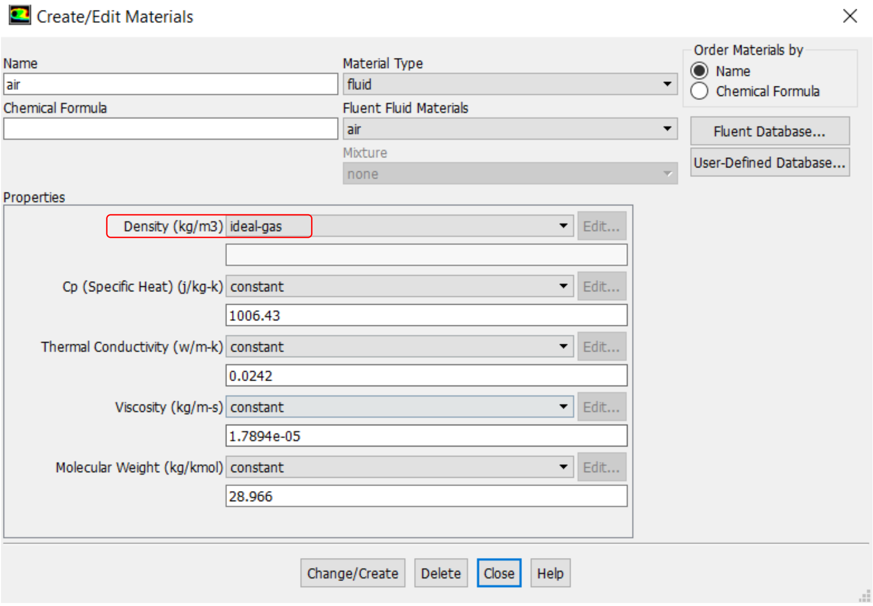


*Figure 86: Fluid properties*

- The most relevant section of the CFD analysis is the definition of suitable boundary conditions for the model. Under the **Boundary Conditions** tab, the sections that were previously named and stored are automatically imported to the Fluent solver along with other conditions generated by the module. The most relevant zones are the **inlet** and **outlet**, the **exit** and **throat** regions are set as interior and suitable conditions are automatically set to the remaining zones.

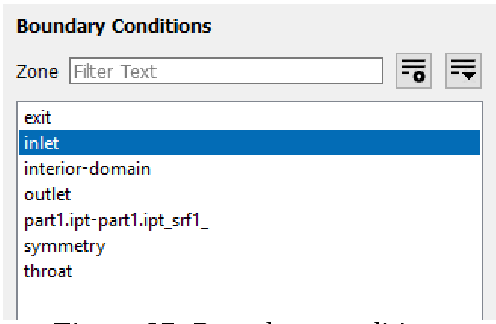


*Figure 87: Boundary conditions*

- PARAMETER 4: The inlet zone represents the combustion chamber of the rocket engine. Thus, it is set as **Pressure inlet,** which becomes one of the design parameters for the subsequent optimization process. An initial value of 200kPa is arbitrarily set and parametrized by clicking on constant → **New Input Parameter.**

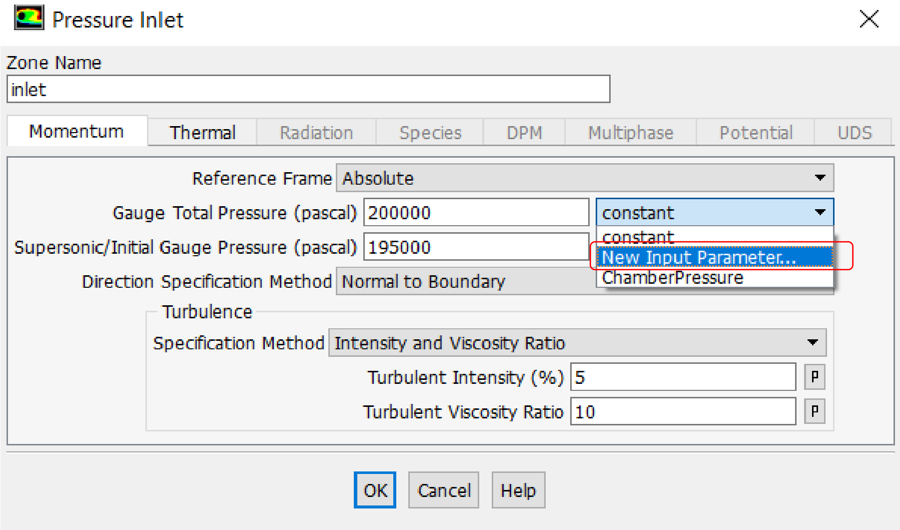


*Figure 88: Inlet condition*

- The new input parameter is named, and an initial value is defined as per Figure 89.

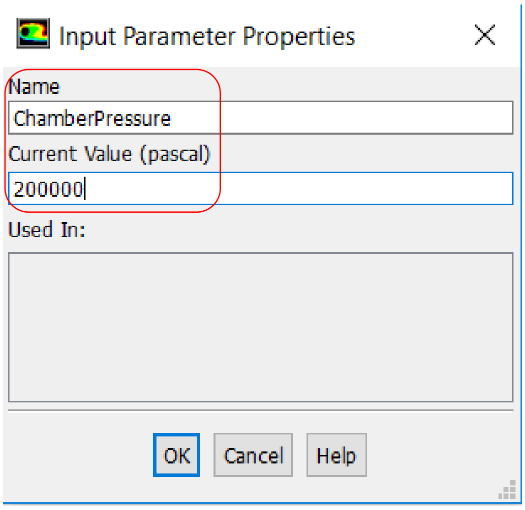


*Figure 89: Chamber pressure parameter*

- Similarly, the outlet zone that represents the ambient surrounding the nozzle, is set as a **Pressure outlet** type with a gauge pressure value of zero which suggests that the nozzle is operating at standard atmospheric pressure.

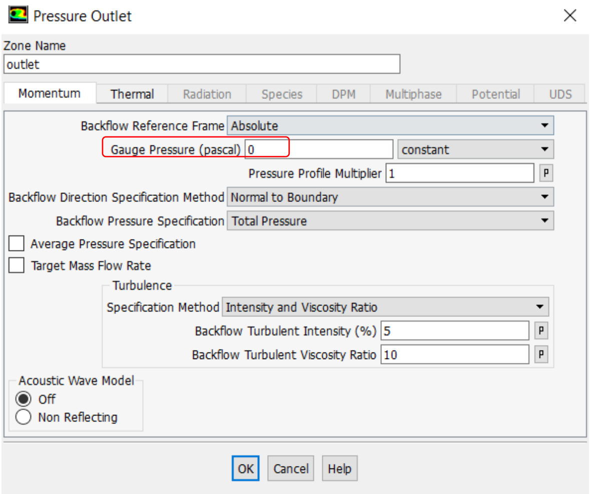


*Figure 90: Outlet pressure condition*

- The software automatically recognizes the flow domain and adds a wall type boundary condition around it. The material, thickness and thermal properties of the wall can also be modified.

- Additionally, under **Reference Values**, the solution is set to be computed from the **Inlet**. This facilitates a systematic approach where the solver is initialized at the inlet and works along the engine until it reaches the exit. The reference values are suggested by the solver and are kept constant.

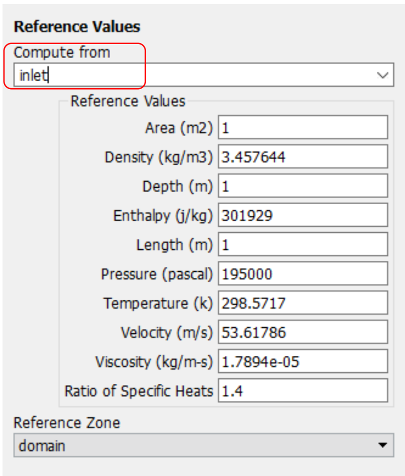


*Figure 91: Reference values*

- The boundary conditions are now set, and the solver type, methods and controls can be defined. Under **Methods**, the Turbulent Kinetic Energy is defined by a Second Order Upwind Discretization method for better accuracy (will slightly increase simulation time) Additionally, solution control values are kept constant but can be modified depending on the type of analysis and desired outcomes.

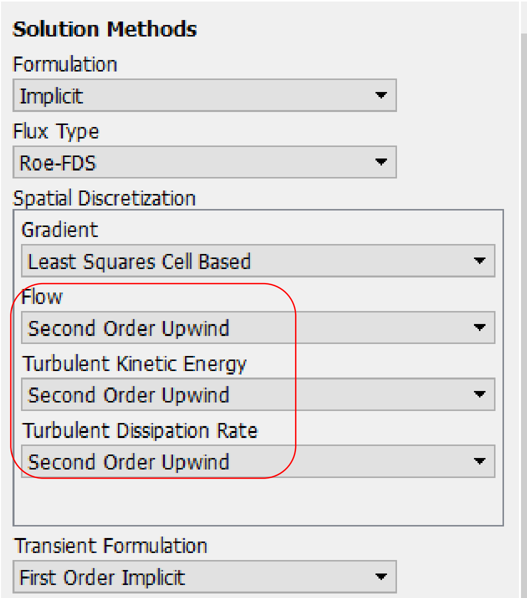


*Figure 92: Solution methods*

- Once all the solver parameters and conditions are set, a solution initialization is recommended as this tool evaluates potential issues with the model prior to the actual solution process. A **Hybrid Initialization** is selected. Subsequently, the solution is initialized.

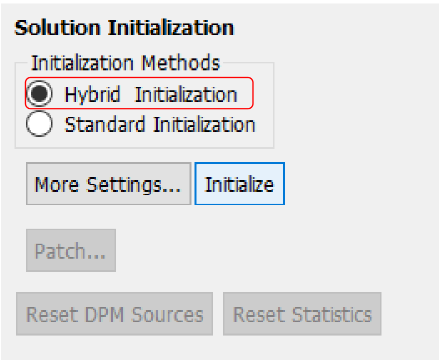


*Figure 93: Solution initialization*

- Finally, under **Run Calculation**, the time step size is kept as 0.01 seconds with a value of 300 time steps arbitrarily set. Additionally, the number of maximum iterations per time step is set to 40 but can be increased depending on the desired output accuracy. Subsequently, click on **Calculate** to run the simulation.

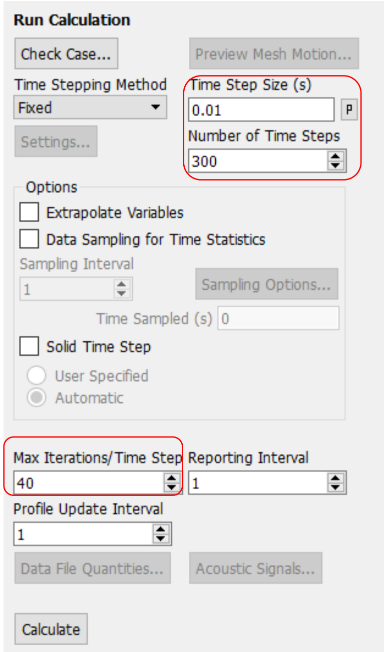


*Figure 94: Calculation parameters*

## IV. CFD Results

- The calculation converged after approximately 1500 iterations and nearly 4 hours as suggested by Figure 95.

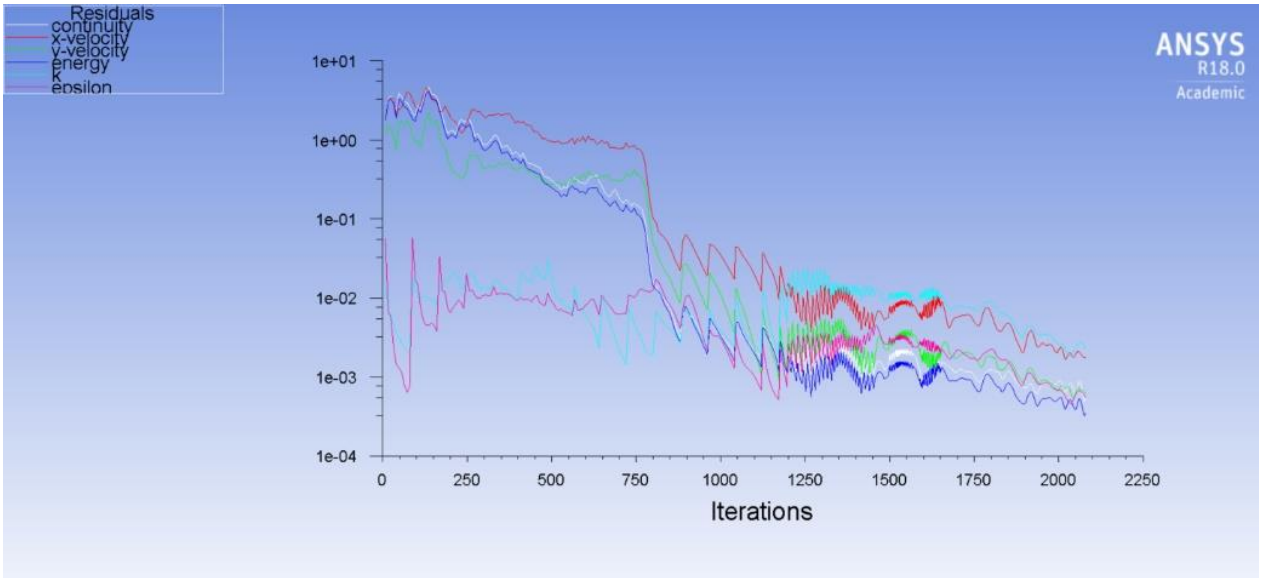


*Figure 95: Solution convergence*

- Once the calculation is complete, open the **Results** tab on the Project schematic.

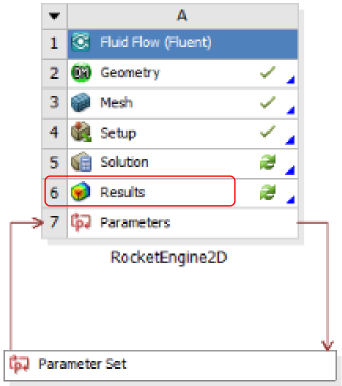


*Figure 96: Results*

- Into the results module, a contour can be created so the Mach number and Pressure values across the nozzle can be easily observed. To create a contour, click on the contour tool on the top ribbon → Select the desired variable (Mach number or Pressure) → Select flow domain → Apply. The Mach number contour across the nozzle is illustrated in Figure 97.

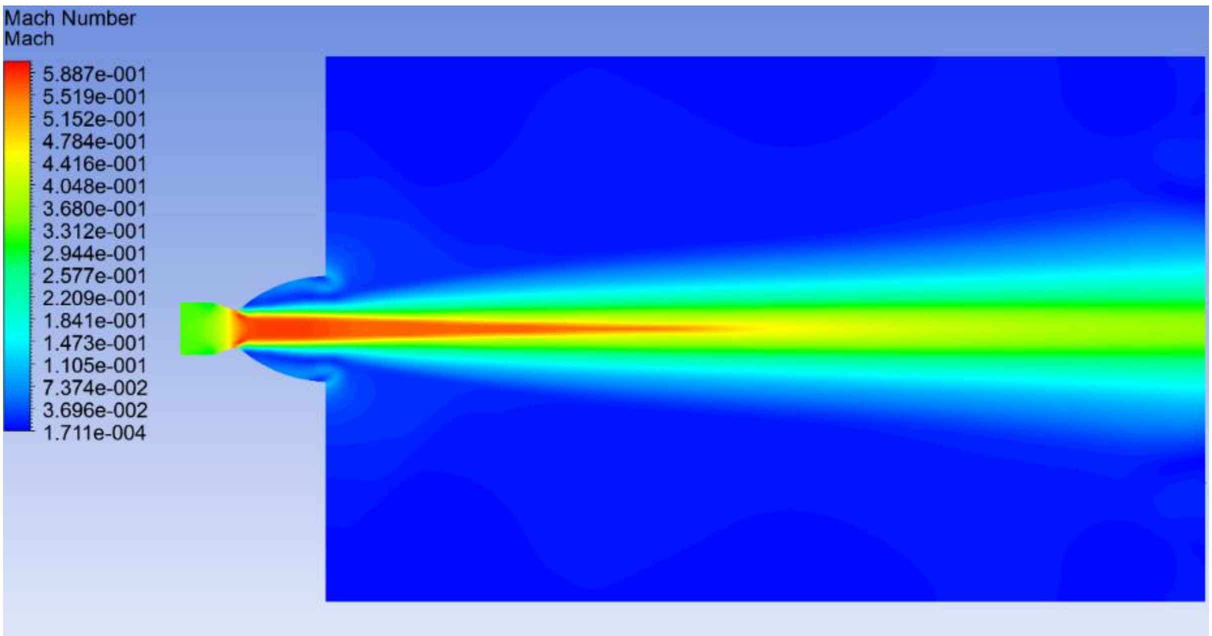


*Figure 97: Mach number*

- Similarly, the Pressure contour is generated. The contour effectively denotes the chamber pressure being expanded to match the ambient pressure.

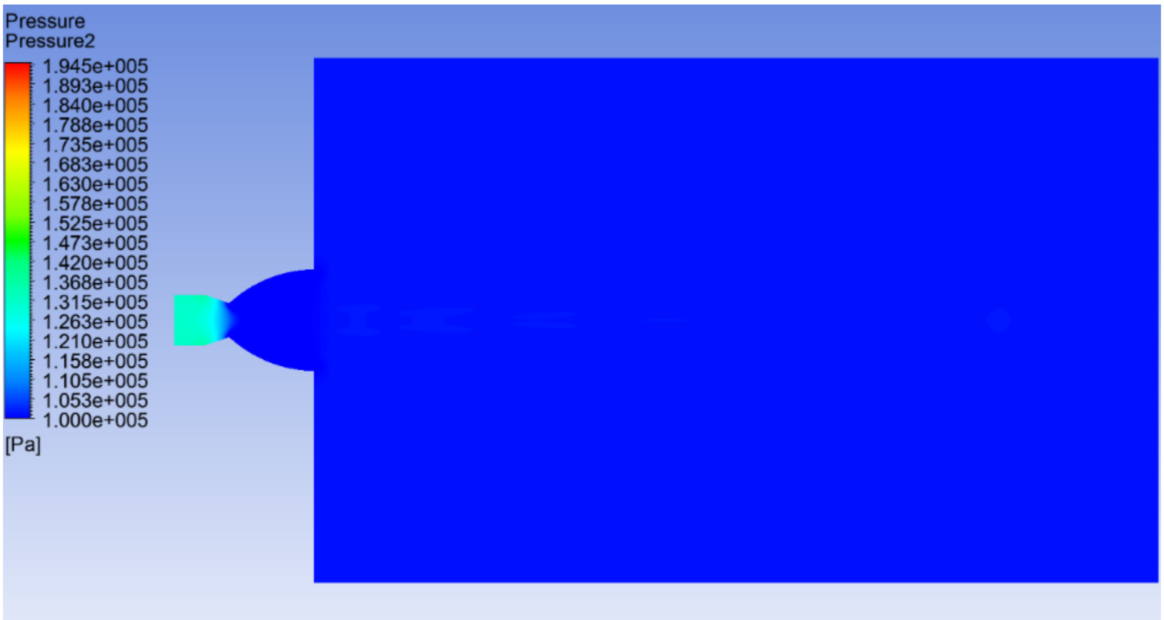


*Figure 98: Pressure distribution*

As it can be clearly seen from Figures 97 and 98, the initial geometry does not meet the elementary requirement of a rocket engine. Figure 97 strongly suggests that the Mach number at the throat of the nozzle is approximately 0.5 which does not let the flow become supersonic at the diverging section. The next phase will intend to optimize the previously set parameters, so the requirements are successfully met.

## V. Optimization

Before the optimization process takes place, the output parameters need to be set. Output parameters are the reference values for which suitable input parameters values will be selected by the optimization module. These parameters are the Mach number at the throat of the nozzle and the pressure at the exit zone.

- Parameters can be set from the Solution module in Fluent. Under Report definitions → create a **new report**.

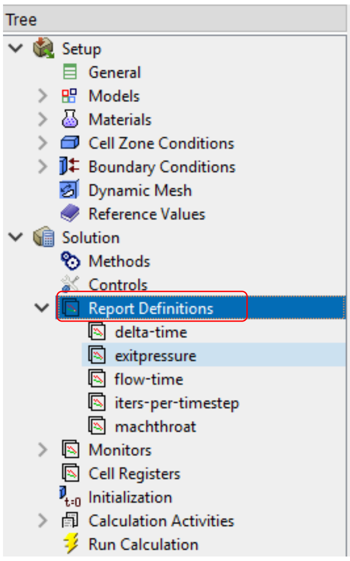


*Figure 99: Report definition*

- When creating the new report → select **surface region** → **Facet average**. This report will output a single value averaged across the specified zone.

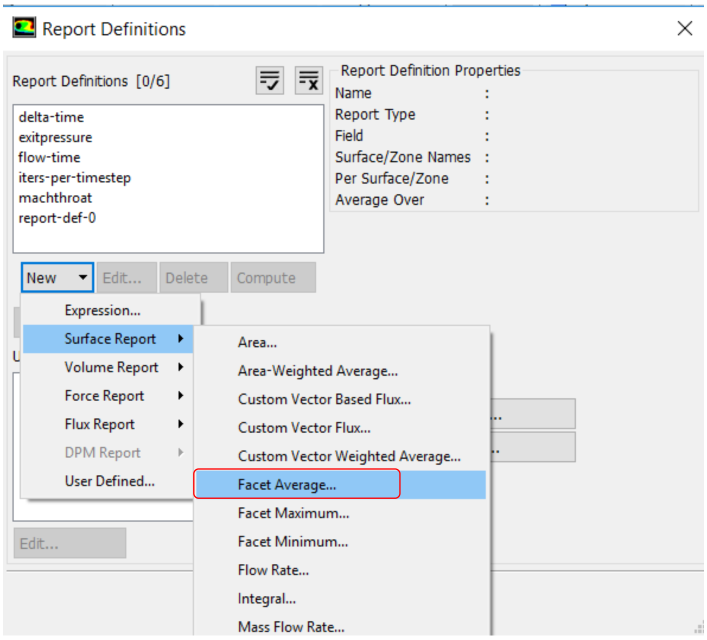


*Figure 100: Parameter definition*

- OUTPUT PARAMETER 1: Once the surface report is defined, the variable type and relevant zones are specified. In this case, the first output parmeter to be defined is the **Mach number**. Thus, select the Mach number variable from the Field variable section, select the throat zone from the surfaces section, name the surface report and tick the **Create Output Parameter** box.

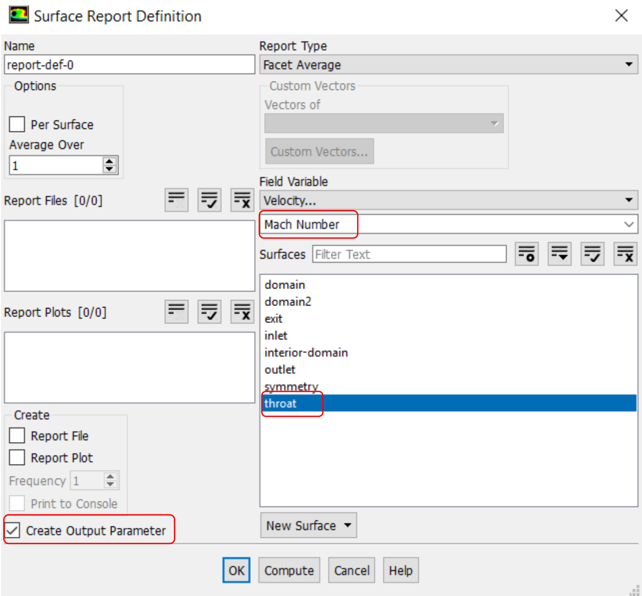


*Figure 101: Output parameter 1*

- OUTPUT PARAMETER 2: Follow the same process to define the exit pressure as an output parameter as detailed in Figure 102.

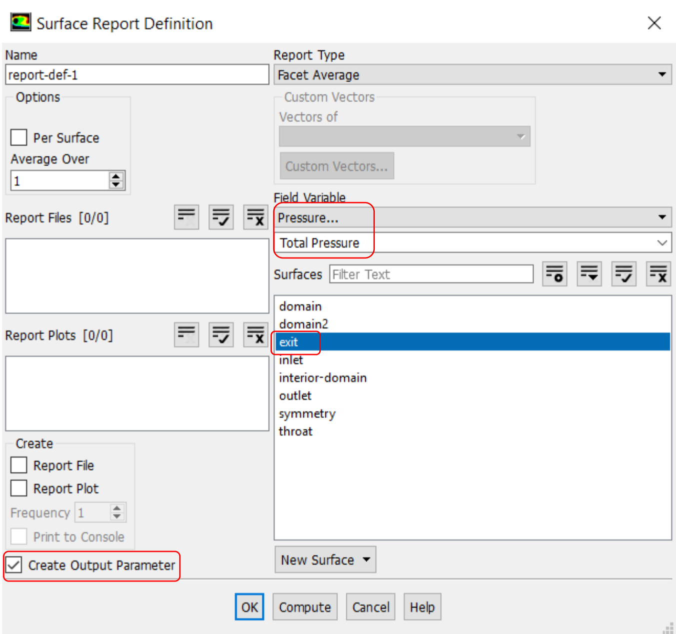


*Figure 102: Output parameter 2*

- The created output parameters can now be observed under the **Parameters and Customization** section in Fluent.

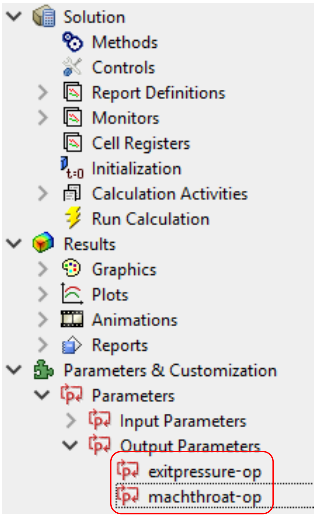


*Figure 103: Output parameters*

- Once the input and output parameters have been set, the project schematic window will automatically include the set of defined parameters.

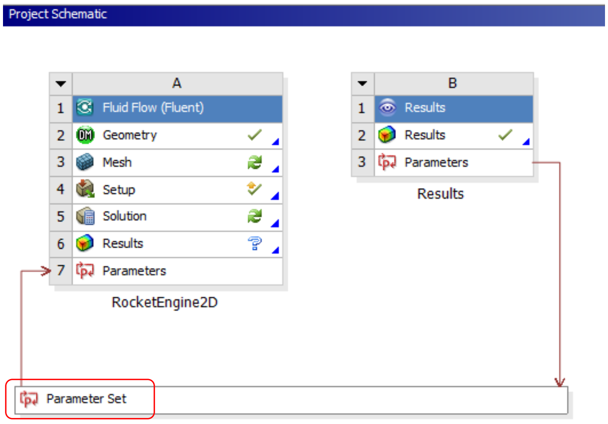


*Figure 104: Parameter set*

- The defined parameters will appear under the Parameter Set tab.

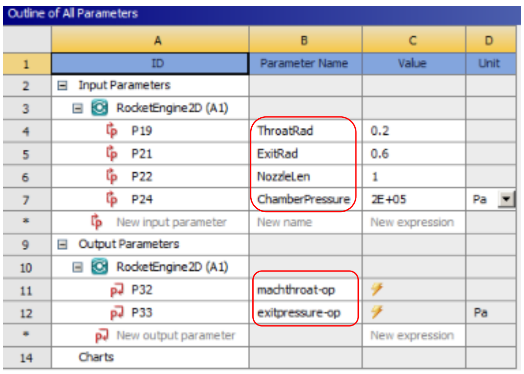
Outline of All Parameters

| | A | B | C | D |
|---|---|---|---|---|
| 1 | ID | Parameter Name | Value | Unit |
| 2 | Input Parameters | | | |
| 3 | RocketEngine2D (A1) | | | |
| 4 | P19 | ThroatRad | 0.2 | |
| 5 | P21 | ExitRad | 0.6 | |
| 6 | P22 | NozzleLen | 1 | |
| 7 | P24 | ChamberPressure | 2E+05 | Pa |
| * | New input parameter | New name | New expression | |
| 9 | Output Parameters | | | |
| 10 | RocketEngine2D (A1) | | | |
| 11 | P32 | machthroat-op | | |
| 12 | P33 | exitpressure-op | | Pa |
| * | New output parameter | | New expression | |
| 14 | Charts | | | |

*Figure 105: Defined parameters*

- The optimization process contemplated in this study starts with a **parameter correlation** analysis. A parameter correlation analysis identifies input parameter that are strongly related to the output variables that we seek to obtain. The result of this analysis is a correlation matrix or a sensitivity graph that identifies input parameters with large effects on the output parameters of the study. This analysis is useful when a large number of input parameters exists and using all these parameters in the optimization process would significantly increase the computational time or would not be handled appropriately by the optimization software.

*Note: The parameter correlation analysis is optional as it does not have any effect on the optimization process. However, it provides useful insight into the relationship between input and output parameters.*

- The first step is to connect the **Parameter Set** in the Project schematic with a **Parameter Correlation** study from the Design Exploration Toolbox.

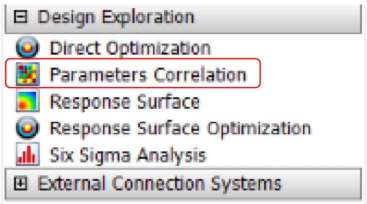


*Figure 106: Design Exploration studies*

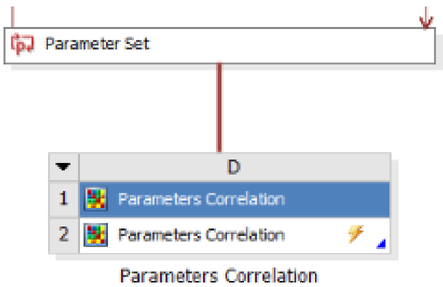


*Figure 107: Parameter correlation study*

- Opening the **Parameters Correlation** tab (Figure 107), it can be observed that lower and upper bounds for each input parameter are automatically set by the software but can be easily modified to suit design purposes. The bounds for the throat radius are described by Figure 108. The **Nozzle length** bounds are set from 0.9 to 1.1 meters, the **exit radius** from 0.4 to 0.8 meters and the chamber pressure from 200 kPa to 8 MPa.

Properties of Outline A5: P5 - ThroatRadius

| | A | B |
|---|---|---|
| 1 | Property | Value |
| 2 | General | |
| 3 | Units | m |
| 4 | Type | Design Variable |
| 5 | Classification | Continuous |
| 6 | Values | |
| 7 | Lower Bound | 0.1 |
| 8 | Upper Bound | 0.4 |

*Figure 108: Throat radius bounds*

- Once the input parameter bounds are defined, the Parameter Correlation properties can be set. The default correlation properties define a **Spearman** correlation type with 100 samples and a mean accuracy of 1%. These parameters can be modified but the default values are suitable for this analysis.

Properties of Outline A2: Parameters Correlation

| | A | B |
|---|---|---|
| 1 | Property | Value |
| 2 | Design Points | |
| 3 | Preserve Design Points After DX Run | ☐ |
| 4 | Failed Design Points Management | |
| 5 | Number of Retries | 0 |
| 6 | Parameters Correlation | |
| 7 | Reuse the samples already generated | ☑ |
| 8 | Correlation Type | Spearman |
| 9 | Number Of Samples | 100 |
| 10 | Auto Stop Type | Enable Auto Stop |
| 11 | Mean Value Accuracy | 0.01 |
| 12 | Standard Deviation Accuracy | 0.02 |
| 13 | Convergence Check Frequency | 10 |
| 14 | Correlation Status | |
| 15 | Size of Generated Sample Set | 0 |
| 16 | Converged | No |

*Figure 109: Correlation type*

- The correlation study can now be **Run**.

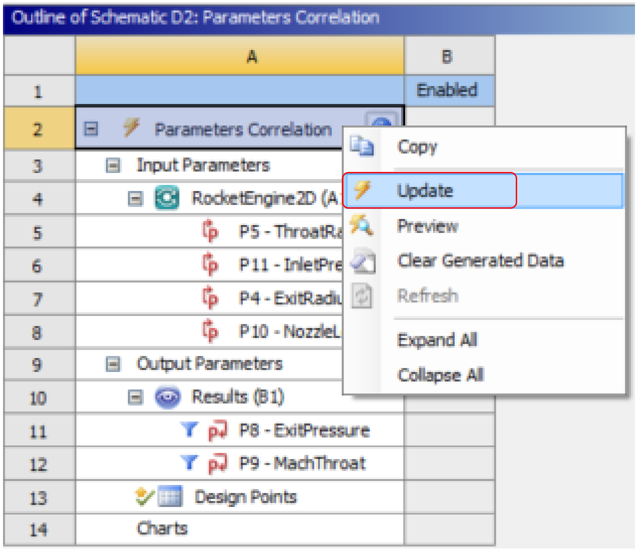


*Figure 110: Correlation solution*

- Once the study is finalized, a number of correlation and sensitivity graphs become available which effectively provide a graphical representation of how input parameters are related to output parameters.

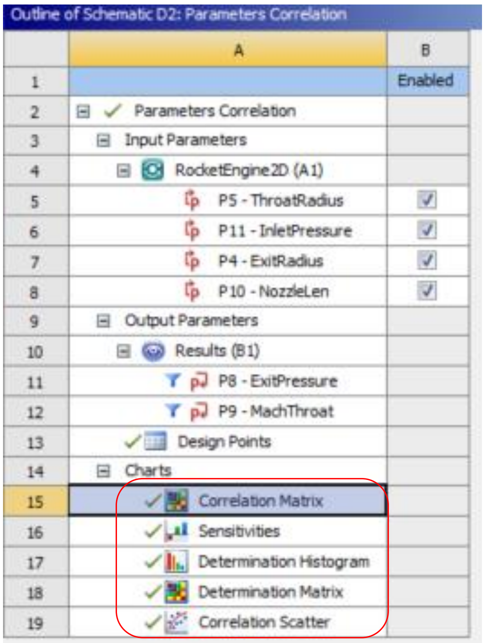


*Figure 111: Correlation results*

- A very effective graphical representation method is a **Sensitivity plot**, which illustrates the relationship between input and output parameters in a bar graph methodology as per Figure 112. The graph suggests that there is a strong correlation between all the selected input parameters and the specified output parameters. Additionally, the graph proposes that the input parameters with major effect on the output values are the chamber pressure and throat radius, while the nozzle length has the lowest effect on the output parameters.

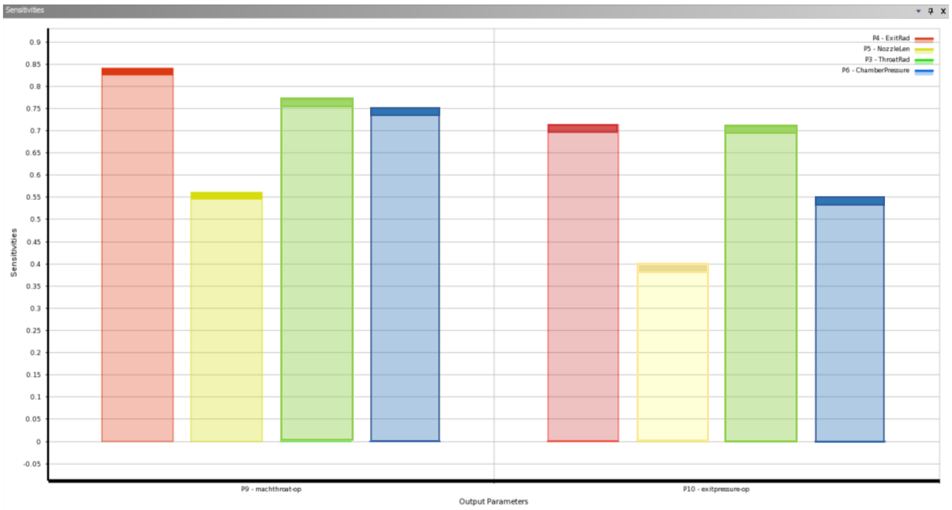


*Figure 112: Sensitivity Analysis*

- Now that the relationships between input and output parameters have been identified, the Optimization analysis can be carried out. From the Design Exploration section in the Analyses Toolbox, a **Direct Optimization** module is selected and linked to the existing Parameter Set tab in the Project Schematic.

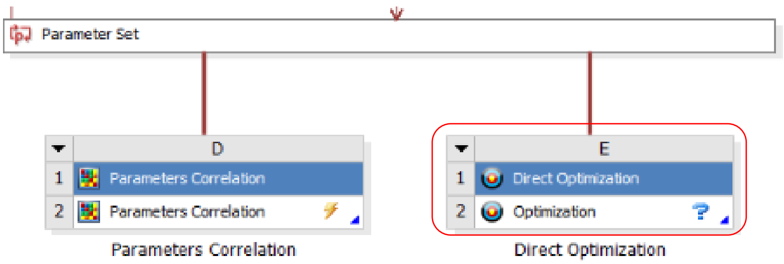


*Figure 113: Direct optimization module*

- Once into the Optimization module, the objective and constraints of the optimization process need to be defined.

Outline of Schematic D2: Optimization

| | A | B |
|---|---|---|
| 1 | | Enabled |
| 2 | Optimization | |
| 3 | Objectives and Constraints | |
| 4 | Domain | |
| 5 | RocketEngine2D (A1) | |
| 6 | P24 - ChamberPressure | ☑ |
| 7 | P19 - ThroatRad | ☑ |
| 8 | P21 - ExitRad | ☑ |
| 9 | P22 - NozzleLen | ☑ |
| 10 | Parameter Relationships | |
| 11 | Results | |

*Figure 114: Objectives and constraints*

- When clicking on **Objectives and Constraints**, a table will appear on the left side of the screen in which the optimization objectives and constraints can be defined. Under the Parameter column, a drop-down list of parameters is available from which the first output parameter (Mach number at throat) is selected. Next, the Objective type is defined as **Seek Target** as a specific Mach number at the throat of the nozzle is required. Other objective types include minimize or maximize a parameter value. Subsequently, a constraint type is specified under the Constraint column. The selected constraint type intends to obtain values that lie within set upper and lower bounds. For the Mach number parameter, the upper and lower bounds defined are 1.2 and 1 respectively as a Mach number lower than 1 would not result in a supersonic flow exiting the nozzle. Subsequently, the same definition process is followed for the second output parameter being the exit pressure.

Table of Schematic E2: Optimization

| | A | B | C | D | E | F | G |
|---|---|---|---|---|---|---|---|
| 1 | Name | Parameter | Objective | | Constraint | | |
| 2 | | | Type | Target | Type | Lower Bound | Upper Bound |
| 3 | Seek P32 = 0; 1 <= P32 <= 1.2 | P32 - machthroat-op | Seek Target | 0 | Lower Bound <= Values <= Upper Bound | 1 | 1.2 |
| 4 | Seek P33 = 0 Pa; 98000 Pa <= P33 <= 1.05E +05 Pa | P33 - exitpressure-op | Seek Target | 0 | Lower Bound <= Values <= Upper Bound | 98000 | 1.05E+05 |
| * | | Select a Parameter | | | | | |

*Figure 115: Objective definition*

- The defined objectives and constraints will now be displayed in the main optimization screen.

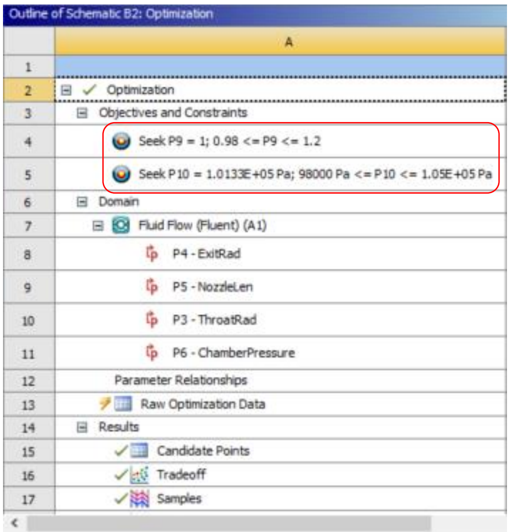


*Figure 116: Optimization objectives*

- The next step has to do with setting the optimization method and other parameters to be taken into consideration by the optimization module. The selected optimization method is a Multi-Objective Genetic Algorithm (**MOGA**) A MOGA optimization supports multiple objectives/constraints and aims to find a global optimum. Other optimization methods include Screening, Nonlinear Programming Quadratic LaGrangian (NLPQL) Mixed Integer Sequential Quadratic Programming (MISQP) as explained in the literature review section. Such methods intend to find a local optimum but require additional user input.

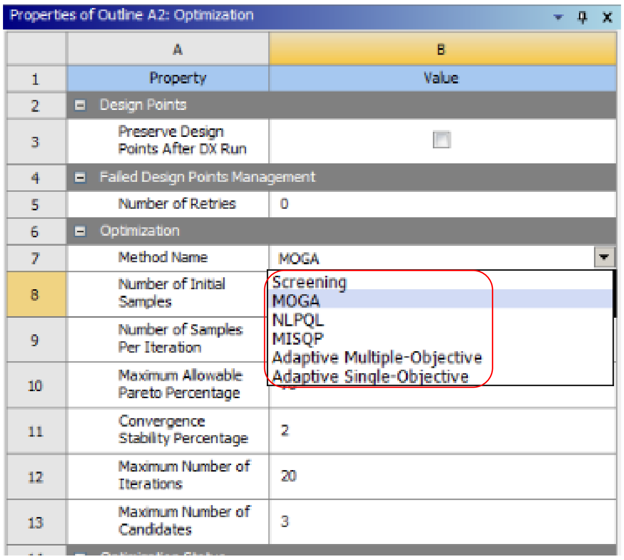


*Figure 117: Optimization Methods*

- Once the optimization method is selected, the number of **sample points** are defined. The default value of 100 initial sample points is kept as well as iteration parameters and allowable Pareto percentage. A solution is said to be pareto efficient if the objective functions can no longer be improved without degrading other objective values.

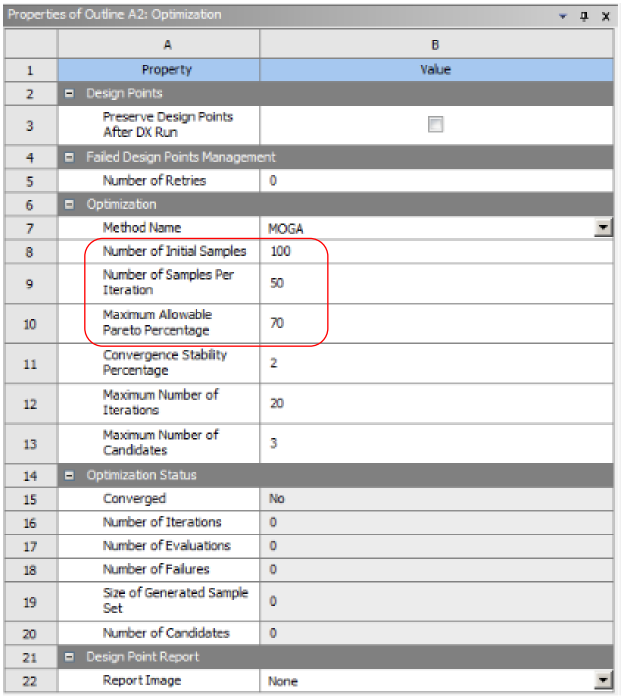

Properties of Outline A2: Optimization

| | A | B |
|---|---|---|
| 1 | Property | Value |
| 2 | Design Points | |
| 3 | Preserve Design Points After DX Run | ☐ |
| 4 | Failed Design Points Management | |
| 5 | Number of Retries | 0 |
| 6 | Optimization | |
| 7 | Method Name | MOGA |
| 8 | Number of Initial Samples | 100 |
| 9 | Number of Samples Per Iteration | 50 |
| 10 | Maximum Allowable Pareto Percentage | 70 |
| 11 | Convergence Stability Percentage | 2 |
| 12 | Maximum Number of Iterations | 20 |
| 13 | Maximum Number of Candidates | 3 |
| 14 | Optimization Status | |
| 15 | Converged | No |
| 16 | Number of Iterations | 0 |
| 17 | Number of Evaluations | 0 |
| 18 | Number of Failures | 0 |
| 19 | Size of Generated Sample Set | 0 |
| 20 | Number of Candidates | 0 |
| 21 | Design Point Report | |
| 22 | Report Image | None |

*Figure 118 Optimization parameters*

- After the optimization settings have been defined, the optimization process can be run. Right click on Optimization → Update.

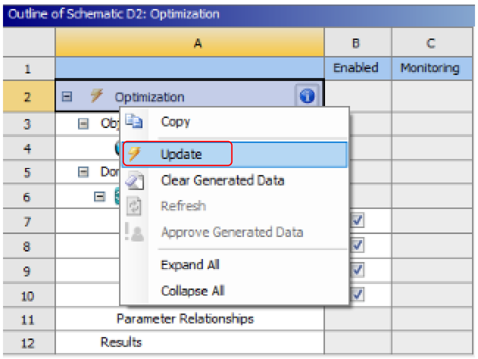


*Figure 119: Optimization Run*

- When the optimization process is run, the initial samples are created and individually solved by the respective module (Fluent, Mechanical, etc) After all the initial samples are solved, the specified optimization algorithm (MOGA) is automatically run and 3 candidates that meet the requirements are suggested by the optimization module when the process is completed. Some samples may have issues while being solved and output values would not be updated by the optimization module as per Figure 120.

Table of Schematic B2: Optimization

| | A | | B | C | D | E | F | G |
|---|---|---|---|---|---|---|---|---|
| 1 | Name | | P4 - ExitRad (m) | P5 - NozzleLen (m) | P3 - ThroatRad (m) | P6 - ChamberPressure (Pa) | P9 - machthroat-op | P10 - exitpressure-op (Pa) |
| 2 | 1 | DP 1 | 0.5075 | 0.905 | 0.181 | 2.325E+05 | 0.78503 | 1.0133E+05 |
| 3 | 2 | DP 1 | 0.5225 | 1.005 | 0.19433 | 4.925E+05 | 1.1676 | 1.0246E+05 |
| 4 | 3 | DP 1 | 0.5375 | 0.955 | 0.20767 | 7.525E+05 | 1.1785 | 1.0133E+05 |
| 5 | 4 | | 0.5525 | 1.055 | 0.18544 | 1.0125E+06 | | |
| 6 | 5 | DP 1 | 0.5675 | 0.93 | 0.19878 | 1.2725E+06 | 1.1951 | 1.5391E+05 |
| 7 | 6 | | 0.5825 | 1.03 | 0.21211 | 2.845E+05 | | |
| 8 | 7 | DP 1 | 0.5975 | 0.98 | 0.18989 | 5.445E+05 | 1.1905 | 1.0133E+05 |
| 9 | 8 | DP 1 | 0.6125 | 1.08 | 0.20322 | 8.045E+05 | 1.1906 | 1.0133E+05 |
| 10 | 9 | DP 1 | 0.6275 | 0.9175 | 0.21656 | 1.0645E+06 | 1.1773 | 1.0133E+05 |
| 11 | 10 | DP 2 | 0.6425 | 1.0175 | 0.18248 | 1.3245E+06 | 1.2005 | 1.0609E+05 |
| 12 | 11 | | 0.6575 | 0.9675 | 0.19581 | 3.365E+05 | | |
| 13 | 12 | DP 2 | 0.6725 | 1.0675 | 0.20915 | 5.965E+05 | 1.2088 | 1.1435E+05 |
| 14 | 13 | DP 2 | 0.6875 | 0.9425 | 0.18693 | 8.565E+05 | 1.1789 | 1.0133E+05 |
| 15 | 14 | DP 2 | 0.7025 | 1.0425 | 0.20026 | 1.1165E+06 | 1.2723 | 1.0133E+05 |
| 16 | 15 | DP 2 | 0.7175 | 0.9925 | 0.21359 | 1.3765E+06 | 1.2152 | 1.0291E+05 |
| 17 | 16 | DP 2 | 0.7325 | 1.0925 | 0.19137 | 3.885E+05 | 1.244 | 1.0133E+05 |
| 18 | 17 | DP 2 | 0.7475 | 0.91125 | 0.2047 | 6.485E+05 | 1.2003 | 1.0133E+05 |
| 19 | 18 | DP 2 | 0.7625 | 1.0113 | 0.21804 | 9.085E+05 | 3.3579 | 2.5056E+05 |
| 20 | 19 | DP 2 | 0.7775 | 0.96125 | 0.18396 | 1.1685E+06 | 1.2489 | 1.0394E+05 |
| 21 | 20 | DP 3 | 0.7925 | 1.0613 | 0.1973 | 1.4285E+06 | 1.2603 | 1.0525E+05 |

*Figure 120: Optimization samples*

## VI. Optimization results

The specified number of design candidates (3) are suggested by DesignXplorer once the optimization process is completed. The candidates are displayed along with a performance identifier (stars, crosses, dashes). A candidate with three stars has met all the specified objectives, one or two stars suggest the candidate meets some objectives or constraints, three crosses mean that the optimization analysis failed, and a grey dash means that the design cannot be more efficient that it currently is. In this case, all 3 candidates meet the specified objectives. Candidate number 3 is selected as the optimized design point and the simulation is now run with the suggested input parameters.

Candidate Points

| | Candidate Point 1 DP 1 | Candidate Point 2 DP 1 | Candidate Point 3 DP 2 |
|---|---|---|---|
| P4 - ExitRad (m) | 0.6275 | 0.5375 | 0.6875 |
| P5 - NozzleLen (m) | 0.9175 | 0.955 | 0.9425 |
| P3 - ThroatRad (m) | 0.21656 | 0.20767 | 0.18693 |
| P6 - ChamberPressure (Pa) | 1.0645E+06 | 7.525E+05 | 8.565E+05 |
| P9 - machthroat-op | 1.1773 | 1.1785 | 1.1789 |
| P10 - exitpressure-op (Pa) | 1.0133E+05 | 1.0133E+05 | 1.0133E+05 |

*Figure 121: Design Candidates*

- The input parameter values suggested by the optimization solver are described in Table 11.

*Table 11: Optimized input parameters*

| **Input Parameter** | **Value** |
|---|---|
| Chamber pressure (MPa) | 0.856 |
| Exit radius (m) | 0.687 |
| Throat radius (m) | 0.187 |
| Nozzle length (m) | 0.943 |

- Using the optimized values for the input parameters, a new simulation is run. The new model successfully meets the case requirements. The Mach number flow profile strongly suggests that a flow speed of Mach one has been reached at the throat of the nozzle and therefore, a supersonic flow profile is observed at the exit where a shockwave can also be identified as per Figure 122.

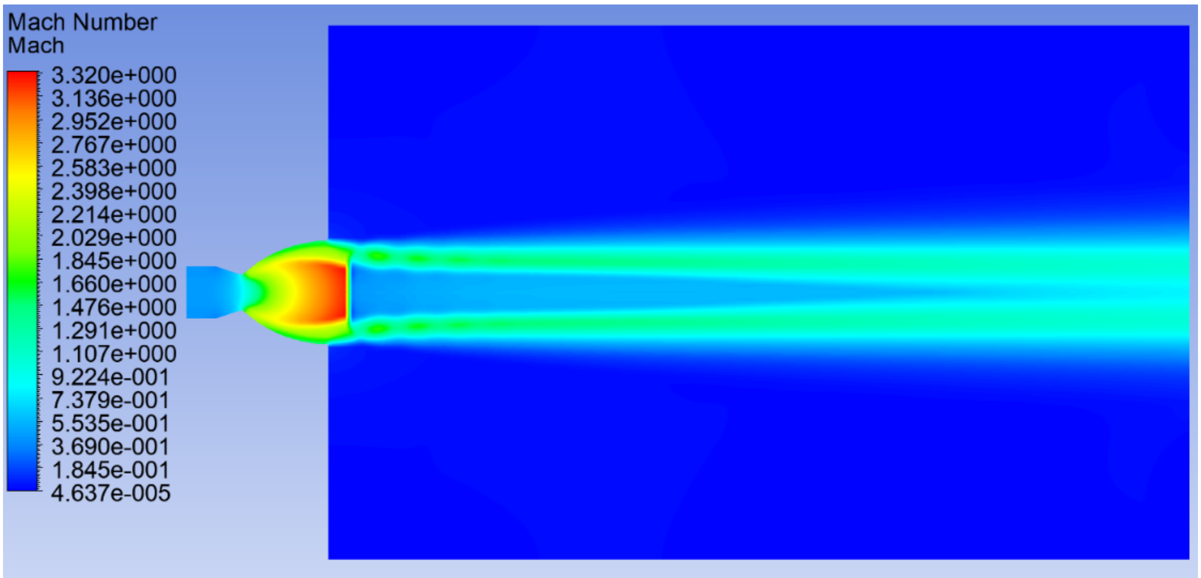


*Figure 122: Mach number results*

- Additionally, the pressure profile is observed in Figure 123. By using the optimized input parameters, the pressure of the flow exiting the nozzle now equals the back (ambient) pressure denoted by the same colour. The shockwave can also be observed.


*Figure 123: Pressure results*

- The problem objectives are effectively attained and demonstrated following the previously specified optimization method. Additionally, the Mach number and Pressure contours agree with those described by various studies in past literature.

### 3.2.4 Optimization Case 4 – Composite Wind Turbine Blade

PROBLEM DESCRIPTION

Wind turbines harness the power generated by the wind. Modern wind turbines exhibit advanced shapes and enhanced designs that offer a versatile and more efficient power generation. The materials from which turbine blades are made, have continuously evolved with fibreglass being the most used material in modern blades. The current study case consists of a wind turbine blade made with composite materials (fibreglass) A parametric optimization study will be carried out, so the preliminary model meets specified requirements and operates efficiently within specified limits.

*Figure 124: Wind Farm (image from digitaltrends.com)*

The initial geometry comprises a 20-meter-long blade divided into 12 sections including the base and root as illustrated in Figure 125. The wing profile considered for the analysis is the NACA 63-412 with an initial pitch angle of zero degrees. Furthermore, the preliminary fibreglass laminate configuration $[\pm45, \pm30, 90, 0]$ is assigned to each section of the blade.

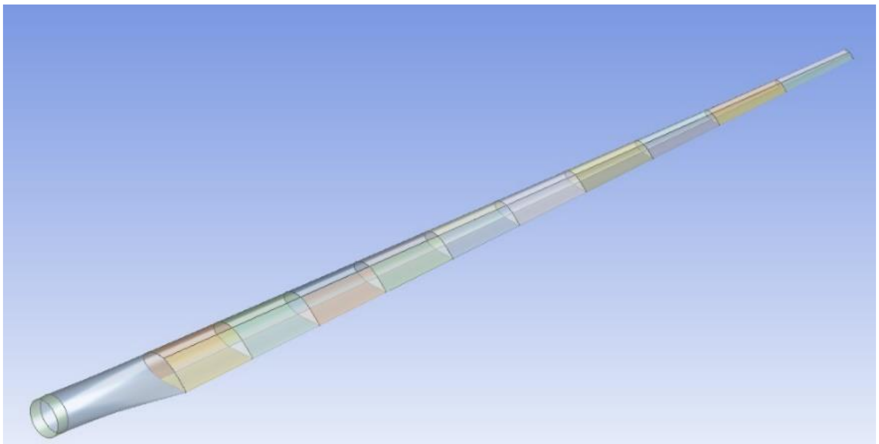

*Figure 125: Initial Blade geometry*

### Objectives

The principal optimization objectives include:

- Running a CFD optimization study in order to maximise the lift to drag ratio by optimizing the pitch angle of the blade.
- Finding the optimum number of fibreglass layers of each orientation in the default laminate configuration $[\pm 45, \pm 30, 90, 0]$ for each section of the blade so that the tip deflection is minimized, and no stress failure occurs in any of the composite layers.

### Assumptions

Wind turbine modelling is a complex field that requires extensive and continuous research, testing and improvement. Therefore, relevant assumptions made for this analysis include:

- Air temperature is constant and ambient changes (rain, dust, snow, etc) are neglected.
- Power conversion analysis, electrical and mechanical components (gearbox, generator, etc) are out of scope.
- The maximum possible loads to be sustained by the blade during operation are considered for the analysis.
- Wind speed is assumed constant at 20 meters per second (the blade's brake mechanism would be set off after this speed limit)
- Blade manufacturing defects and potential irregularities in composite materials are neglected.

### Problem Specification

The initial parameters taken into account for this analysis are detailed In Table 12. Such parameters are preliminary as the optimization process will suggest the optimum values that will need to be used in order to effectively meet the aims of the study.

*Table 12: Model Characteristics*

| Parameter | Value |
|---|---|
| Blade length (m) | 20 |
| Twist angle (degrees) | 15 |
| Pitch angle (degrees) | 0 |
| Blade max width (m) | 1.5 |
| Wind speed (m/s) | 20 |
| Laminate configuration | $[\pm 45, \pm 30, 90, 0]$ |
| Initial number of layers per section | 4 |
| Aerodynamic pressure (Pa) | 700 |

## I. Geometry Modelling

Different types of existing wing profiles are used in wind turbines depending on operational parameters, turbine location, expected loads, size, etc. For this study case, the **NACA 63-412** aerofoil is selected as the default blade profile. *Airfoilstool.com* database offers coordinate files of a great number of wing profiles that can be imported into ANSYS, from where a 3D body can be created.

- The first step is to import the aerofoil's coordinates as a **3D Curve** into ANSYS DesignModeler.

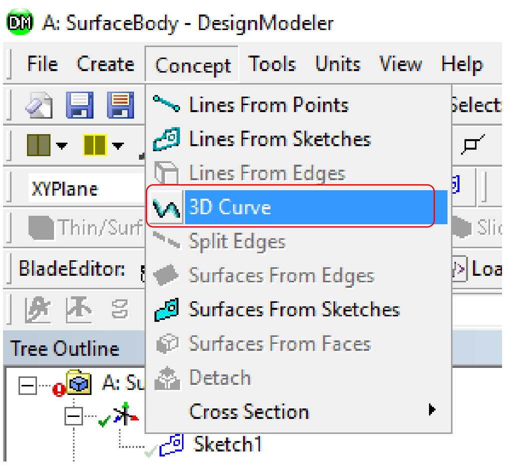


*Figure 126: 3D Curve generation*

- The Definition is set as **From Coordinate File** and the aerofoil file is selected.

Details View

| Details of Curve1 | |
|---|---|
| Curve | Curve1 |
| Definition | From Coordinates File |
| Coordinates File | \\puffball.labs.eait.uq.edu.au\s4344155\Desktop\Airfoil1.txt |
| Coordinates Unit | Meter |
| Base Plane | XYPlane |
| Operation | Add Material |
| Refresh | No |
| Merge Topology? | No |

*Figure 127: Data points import*

- The new **sketch** will be imported as a set of points, such points are joint with spline lines until a closed sketch is achieved.

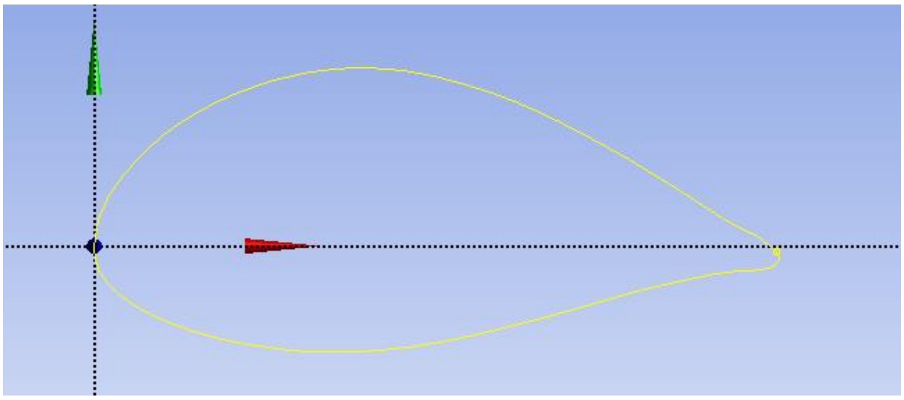

*Figure 128: Wing profile*

- As the initial length of the blade is chosen to be 20 meters, a **new plane** is created 20 meters apart where the same wing profile but smaller is created. This smaller wing profile will become the tip of the blade. A **twist angle** of 15° is applied to the end profile following common industry practices.

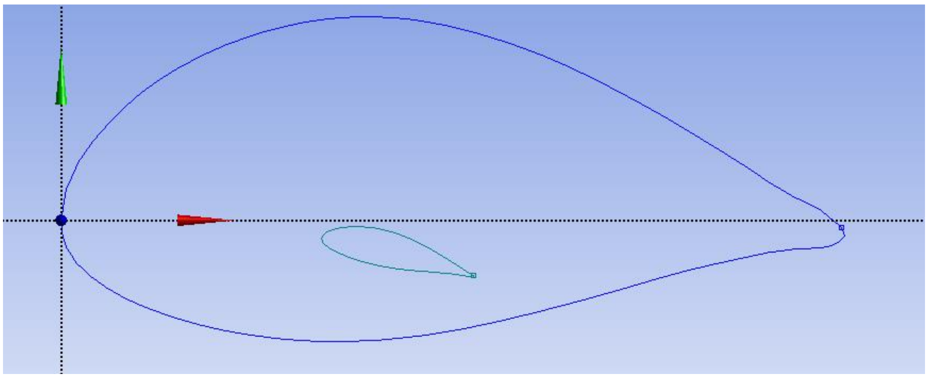

*Figure 129: Twist angle*

- PARAMETER 1: The first input parameter will now be set. The distance of the new plane created for the smaller wing profile from the starting plane becomes a parameter. As mentioned before, the initial value is 20 meters.

| Details of EndPlane | |
|---|---|
| Plane | EndPlane |
| Sketches | 1 |
| Type | From Plane |
| Base Plane | XYPlane |
| Transform 1 (RMB) | Offset Z |
| D FD1, Value 1 | -20 m |
| Transform 2 (RMB) | None |
| Reverse Normal/Z-Axis? | No |
| Flip XY-Axes? | No |
| Export Coordinate System? | No |

*Figure 130: Parameter 1*

- Once the profiles are created, a **Skin/Loft** feature is created between them. As the composite definition will not take place in the DesignModeler, the thickness is set as zero.

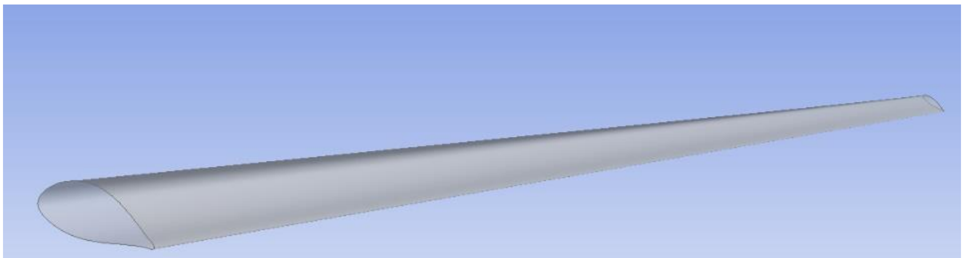

*Figure 131: Blade surface*

- The root of the blade is consequently created by inserting a new Skin/Loft from the initial blade profile to a circle that will become the base of the blade.

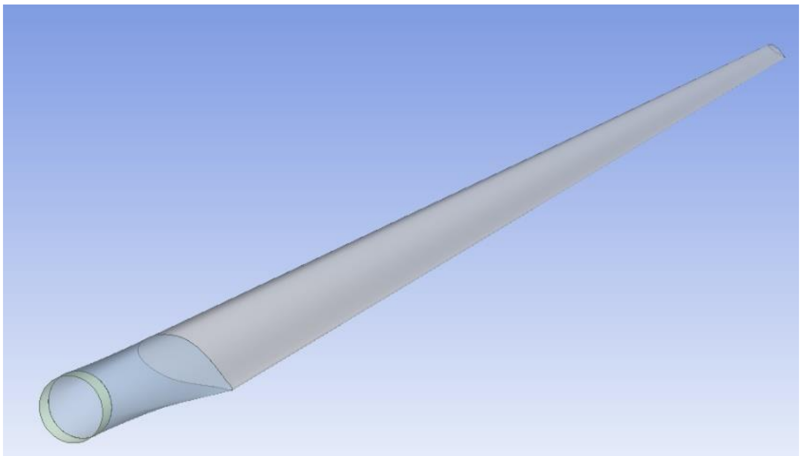

*Figure 132: Blade Model*

- Consequently, the blade is split into sections 2 meters apart using the **Slice** feature. This step takes into account realistic manufacturing limitations as smaller sections with different number of layers would drastically increase manufacturing time and effort. Finally, **Named Selections** are added to each of the faces of the blade.

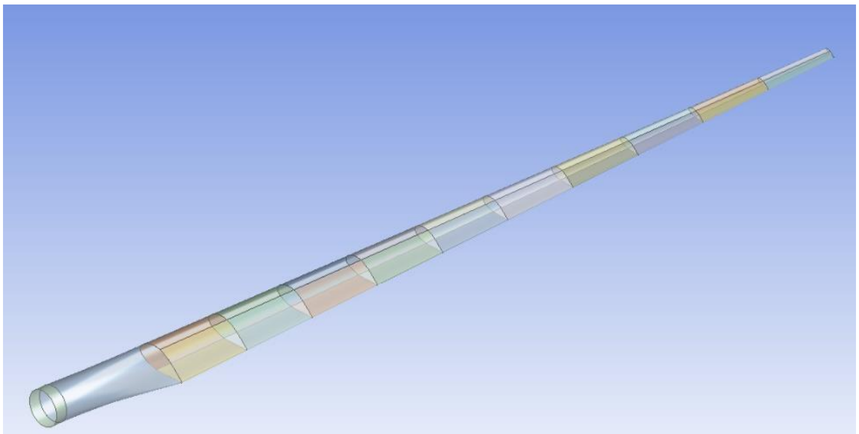

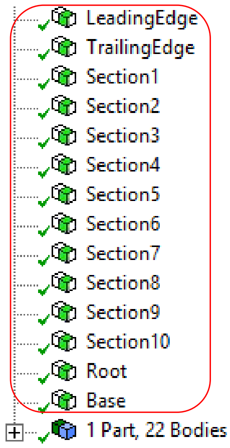


*Figure 133: Blade sections*

## II. Composite modelling

The composite modelling phase works from the shell geometry previously created where a broad number of composite specifications can be applied to said geometry. Single layers with arbitrary fibre orientations, user specified stackups and sub laminates with desired number of layers, orientations, thicknesses, etc. can be easily defined in **ANSYS ACP (Pre)** for subsequent structural or composite performance analyses. More complex composite operations such as draping analyses can also be implemented.

- First, drag an ACP (Pre) analysis tab from the Toolbox Tree and join the created Geometry to the ACP **Geometry** tab.

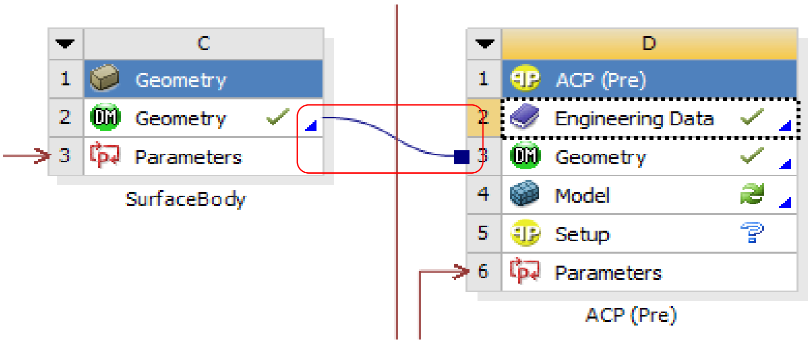


*Figure 134: Ansys composites module*

- Next, right click on the **Engineering Data** tab and select Edit.

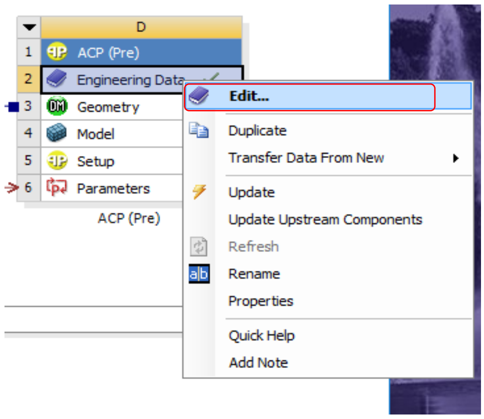


*Figure 135: Engineering Data*

- From the Engineering Data Sources, Select **Composite Materials**. A menu of available materials will appear with the most common composites currently used.

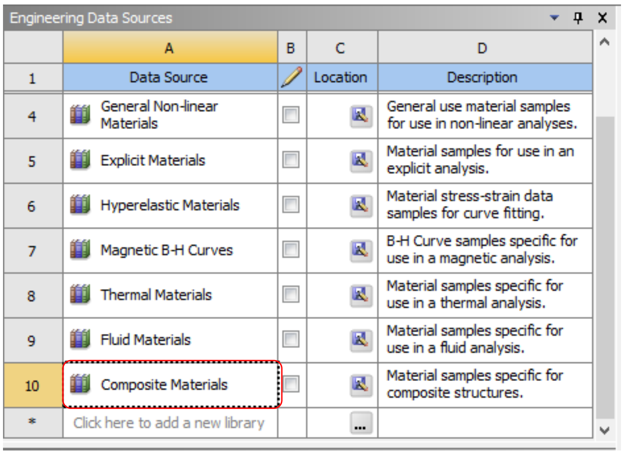


*Figure 136: Composite materials library*

- From the list of available materials, an **Epoxy E-Glass Unidirectional (UD)** composite is selected as the default material for the wind turbine blade. This material is then added to the Engineering Data. The remaining candidates are Epoxy E-Glass Wet and Epoxy S-Glass UD but these materials do not offer the same high-quality properties as suggested by composite materials experts.

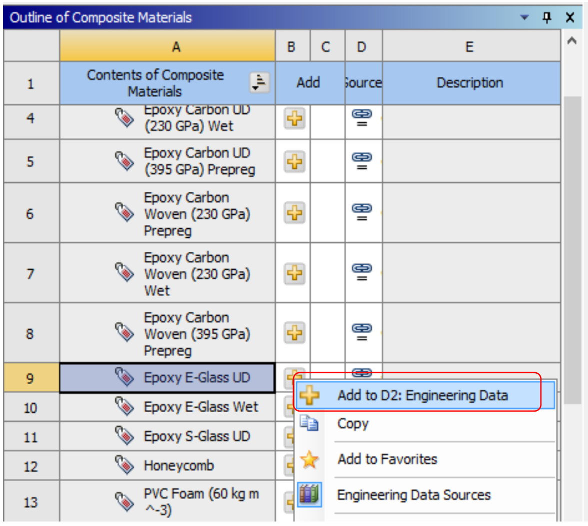


*Figure 137: Epoxy glass fibre selection*

- The next step is to create a suitable **Mesh** for the model. Double click on the Model component of the analysis.

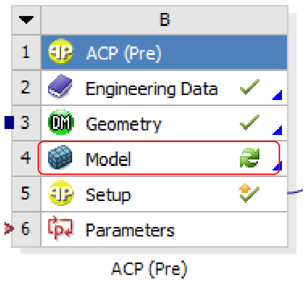


*Figure 138: Model tab*

- A **Proximity** and **Curvature** size function is the main sizing characteristic selected for the current analysis. Furthermore, on the project schematic, a face meshing characteristic with a **Triangles: Best Split** method is implemented in order to obtain a uniform and relatively fine mesh, suitable for the analysis.

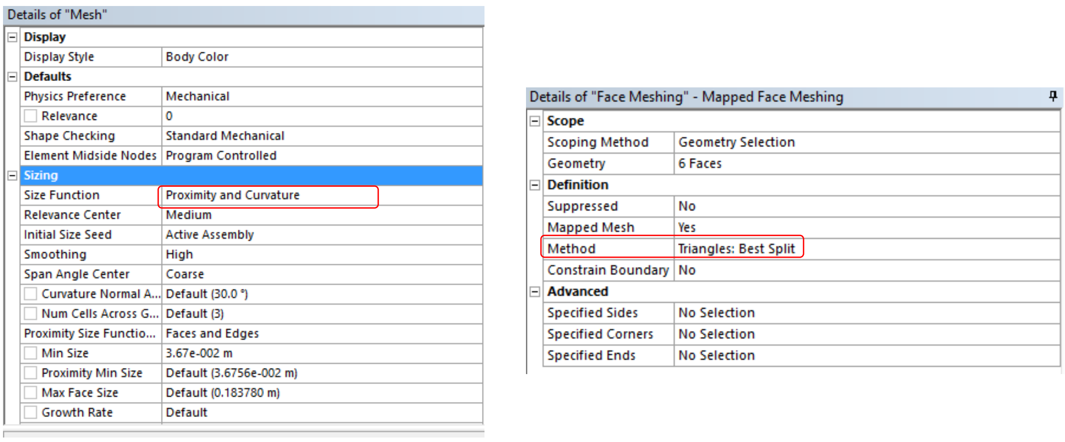


*Figure 139: Mesh configuration*

- A relatively fine and uniform mesh is the result.

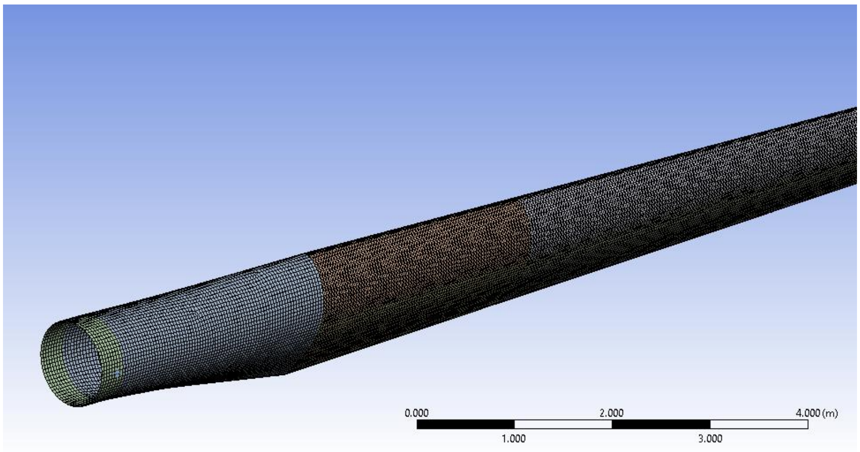


*Figure 140: Final Mesh*

- Once an appropriate mesh is generated, the next step involves the composite material definition. Double click on the **Setup** tab.

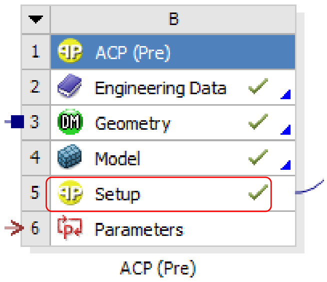


*Figure 141: Setup tab*

- The ACP interface is consistent with Workbench, with a **model tree** and a visualization area.

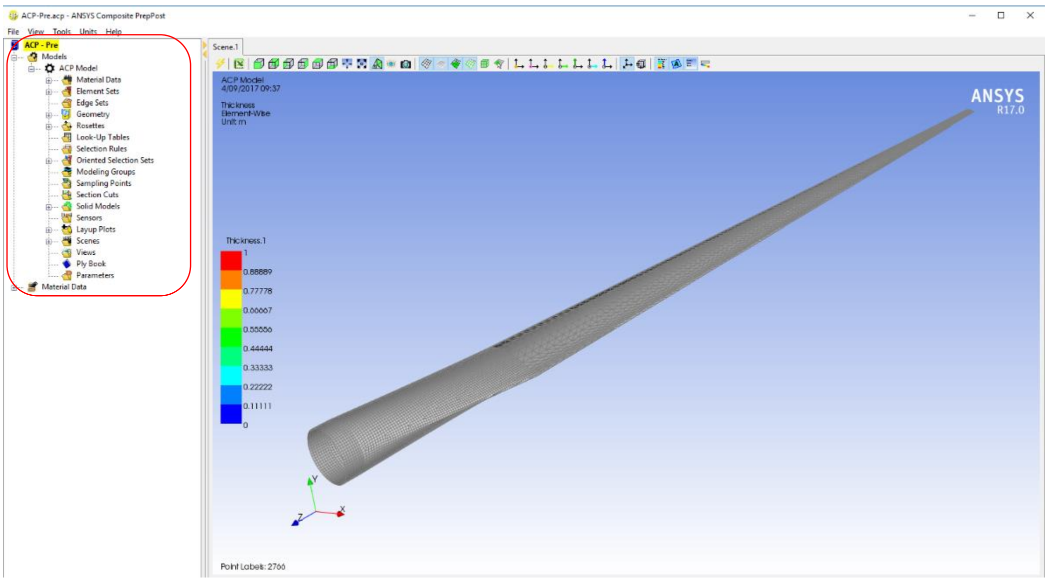


*Figure 142: Ansys ACP (Pre) Interface*

- Ansys ACP (Pre) considers four material classes: Specific materials, **Fabrics**, **Stackups** and **Sublaminates**. The default material (Epoxy Fibreglass UD) was already set in Engineering Data. The fabric type and its properties will be set next. Furthermore, a default stackup will be created for the $[\pm 30]$ and $[\pm 45]$ layers.

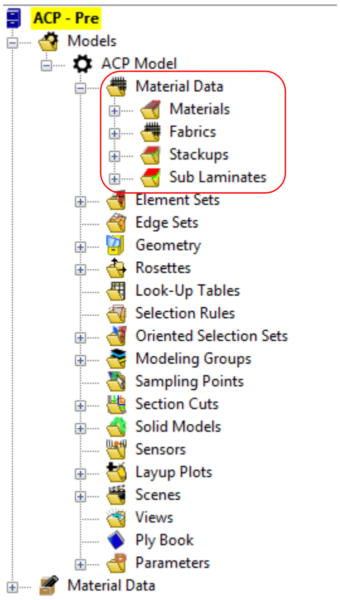


*Figure 143: Material data*

- The default sublaminate configuration taken into consideration is $[\pm 45, \pm 30, 90, 0]$ For the creation of such sublaminate, stackups of $[\pm 45]$and $[\pm 30]$ fibreglass will be defined. Start by creating an initial fabric type. Under **Materials**, the previously selected composite material (Epoxy E-Glass UD) should appear. Under **Fabrics →** right click and select the **Create Fabric** option.

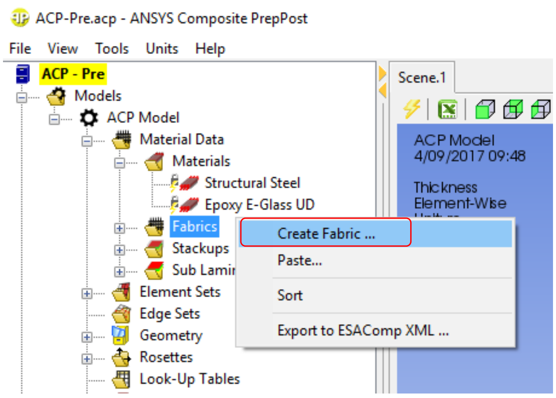


*Figure 144: Fabric definition*

- A sensible name is given to the new fabric and the material is selected from the drop-down menu. Subsequently, a layer thickness needs to be defined. In order to make this analysis as realistic as possible, the thickness of the fibreglass layer considered is obtained from commercially available options. *Swiss-composite.ch* is a worldwide known composite materials supplier, from their product catalogue, the thickness of one of their high-quality fibreglass plies is chosen for this analysis. The selected thickness is 0.45 millimetres for the **UD-Leinwand (plainweave) fibreglass**.

| Glasfilamentgewebe - Tissus de verre - Glass filament fabrics | | | | | | | | | |
|---|---|---|---|---|---|---|---|---|---|
| **190.1006** | VE106 | 106 | 25 g/m² | 22 | 22 | EC 5-5,5 | EC 5-5,5 | Leinwand | 0,03 |
| **190.1058** | VE108 | 108 | 47 g/m² | 23,6 | 18.5 | EC 5-11 | EC 5-11 | Leinwand | 0,06 |
| **190.0070** | 90070 | 7630 | 81 g/m² | 11,8 | 12 | EC 9-34 | EC 9-34 | Leinwand | 0,10 |
| **190.1111** | 91111 | 120 22Z | 105 g/m² | 23.7 | 22.5 | EC 5-11x 2 | EC 5-11x2 | Kreuzköper 1/3 | 0,14 |
| **190.1190** | VE120P | 120 | 103,6 g/m² | 23.6 | 22.8 | EC7-22 | EC7-22 | Kreuzköper 1/3 | 0,12 |
| **190.1106** | 91106 | 116 | 108 g/m² | 24 | 24 | EC 5-11x2 | EC 5-11x2 | Leinwand | 0,14 |
| **190.2105** | 92105 | 7630 | 163 g/m² | 12 | 11.5 | EC 9-68 | EC 9-68 | Leinwand | 0,15 |
| **190.2100** | 92100 | 3715 | 163 g/m² | 6 | 5.8 | EC 9-136 | EC 9-136 | Leinwand | 0,23 |
| **190.1158** | 92110 | | 163 g/m² | 12 | 11.5 | EC 9-68 | EC 9-68 | Köper 2/2 | 0,16 |
| **190.2112** | 92112 | | 200 g/m² | 8 | 6.5 | EC 9-136 | EC 9-136 | Leinwand | 0,20 |
| **190.2115** | 92115 | | 280 g/m² | 7 | 6.5 | EC 9-68x3 t0 | EC 9-204 | Leinwand | 0,30 |
| **190.1358** | 92125 | | 280 g/m² | 7 | 6.5 | EC 9-68x3 t0 | EC 9-204 | Köper 2/2 | 0,35 |
| **190.0745** | 91745 | 181 | 286 g/m² | 22 | 21 | EC 7-22x3 | EC 7-22x3 | Atlas 1/7 | 0,40 |
| **190.2626** | 92626 | 7781 | 296 g/m² | 22 | 21 | EC 6-68 | EC 6-68 | Atlas 1/7 | 0,35 |
| **190.1945** | 91945 | 1581 | 296 g/m² | 22 | 21 | EC 9-34x2 | EC 9-34x2 | Atlas 1/7 | 0,40 |
| **190.2150** | 92150 | | 345 g/m² | 6 | 5.3 | EC 9-68x5 t0 | EC 9-272 | Leinwand | 0,40 |
| **190.1458** | 92140 | | 390 g/m² | 6 | 6.7 | EC 9-68x5 t0 | EC 9-272 | Köper 2/2 | 0,45 |
| **190.2130** | 92130 | | 395 g/m² | 6 | 6.7 | EC 9-68x5 t0 | EC 9-272 | Leinwand | 0,40 |
| **190.9251** | GI 6224/1 | VR447 | 450 g/m² | 6 | 8.5 | EC 9-68x5 t0 | EC13-272 | Scheindreher | 0,65 |
| **190.2145** | 92145 | | 220 g/m² | 6 | 7 | EC 9-68x5 t0 | EC 7-22 | UD-Leinwand | 0,25 |
| **190.2148** | 91135 | 1543 | 288 g/m² | 19 | 12 | EC 9-68x2 | EC 5-11x2 | UD-Köper 1/3 | 0,29 |
| **190.2146** | 92146 | | 425 g/m² | 5.5 | 6.3 | EC 9-136x5 t0 | EC 9-68 | UD-Leinwand | 0,45 |
| **190.1664** | VE664 | | 670 g/m² | 12.8 | 11.6 | EC 9-136x2 | EC 9-136x2 | HD | |
| **190.1000** | VR1000 | | 1005 g/m² | 22.4 | 14 | EC 9-136x2 | EC 9-136x2 | HD | |

*Figure 145: Fibreglass Catalogue from Swiss-composite.ch*

- Thus, the fabric **thickness** is set. The price can also be defined for a total cost estimation. However, financial impacts are not part of the scope of this study.

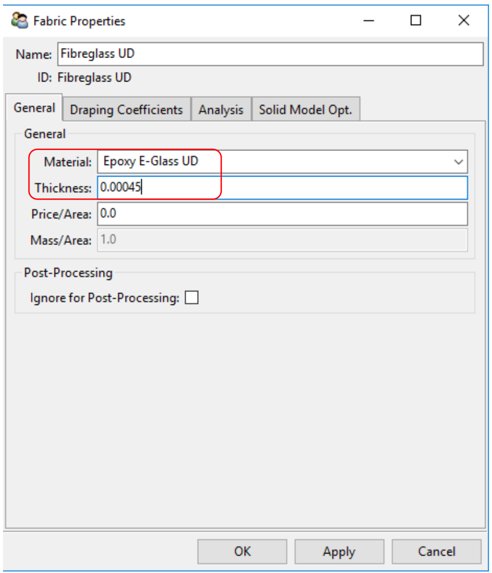


*Figure 146: Fibre thickness definition*

- As previously mentioned, the default laminate configuration is $[\pm45, \pm30, 90, 0]$ where the number of layers for each of the orientations will be parametrised and later optimized for each of the sections of the blade. A stackup needs to be created for the $\pm45$ and $\pm30$ orientations. Thus, right click ***Stackups*** **→ Create Stackup**.

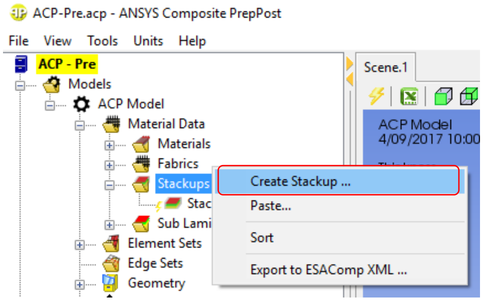


*Figure 147: Stackup definition*

- After naming the new stackup, the layer **materials** and **angles** are defined from the drop-down menus. Hence, the base stackup for the $\pm45$ layer is defined as per Figure 148. The same process is followed for creating a $\pm30$ stackup.

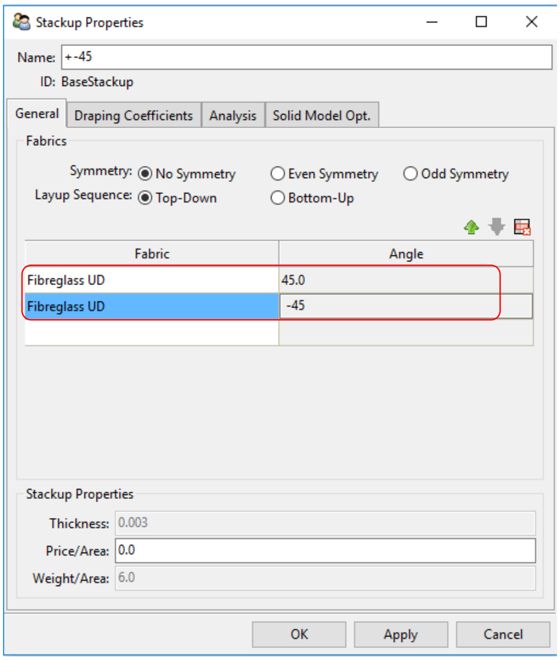


*Figure 148: $\pm45$ Stackup*

- Furthermore, a sub laminate with the default configuration can be created and its polar properties observed under the **Analysis** tab. It's important to mention that this laminate is created for illustration purposes only as individual orientations or number of layers cannot be parametrised for laminates created at this stage. The alternative parametrisation method is described next.

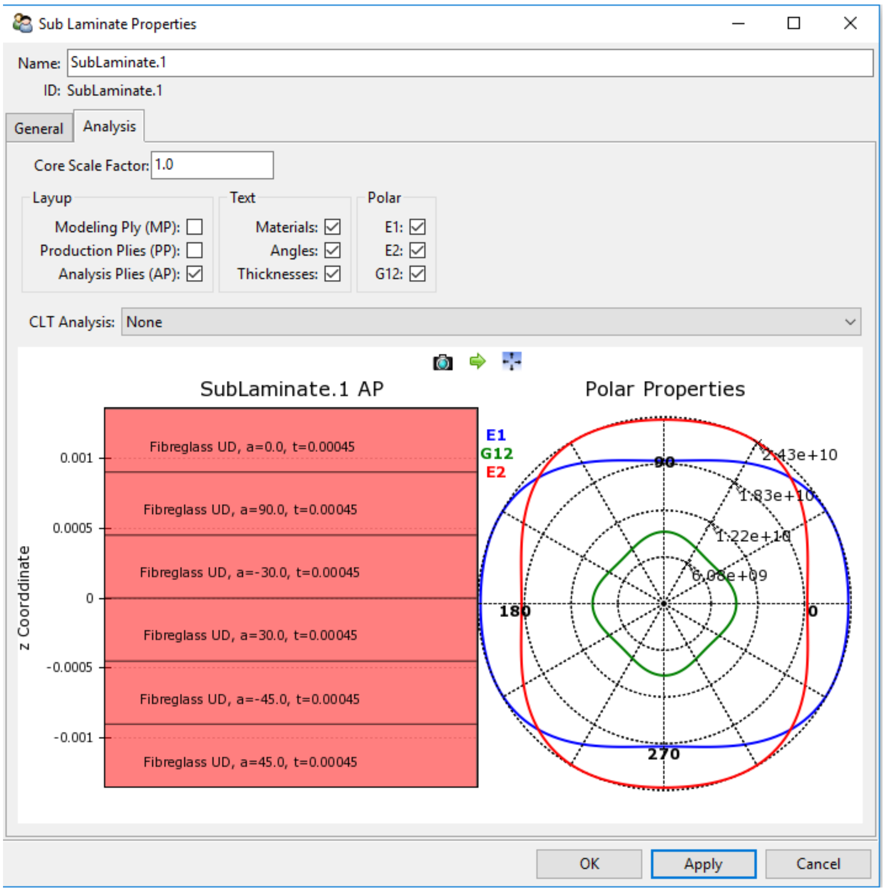


*Figure 149: Polar Properties*

- Working down the model tree, under **Element Sets**, all the surface bodies defined on DesignModeler and named can be observed. Each of these element sets will be assigned to the default laminate configuration.

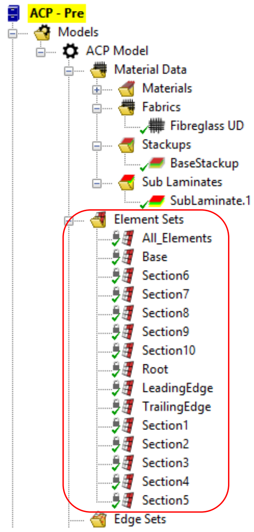


*Figure 150: Element sets*

- The next step, is to create a **Rosette**. Rosettes are coordinate systems that set the Reference Direction for the Oriented Selection Sets that will be created next. Rosettes define the 0° direction for the composite lay-up. A single rosette can be used as reference direction for all element sets or different rosettes can be applied to each element. In this study, as all elements share a similar shape, a single rosette was deemed suitable for defining the lay-up orientation for all the sections of the blade. Therefore, using a point on the base of the blade as the rosette **Origin**, and assigning a **Direction 1** and **Direction 2** (towards the tip of the blade), the new rosette is created. Additionally, a **Cylindrical** rosette type is selected corresponding to the general shape of the blade.

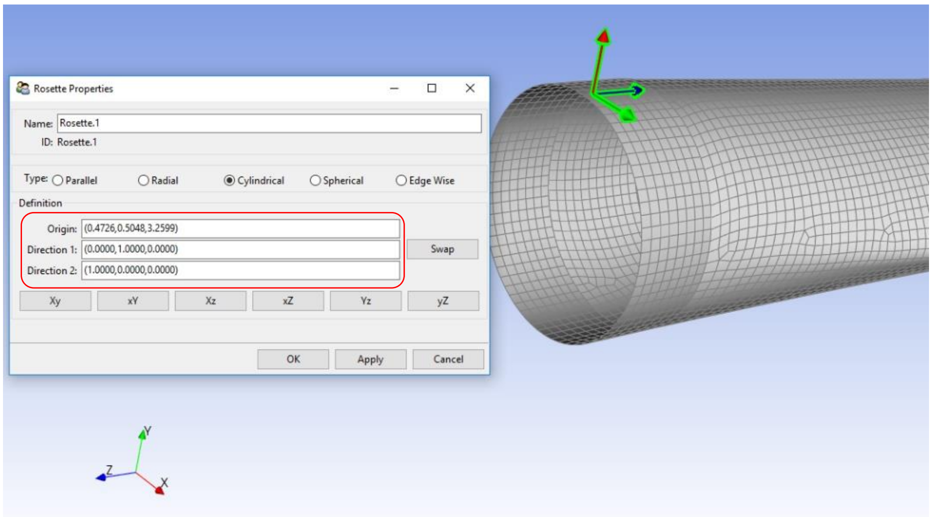


*Figure 151: Rosette definition*

- Subsequently, **Oriented Selection Sets** can be created. An oriented selection set implements the previously defined rosette and a section of the blade in order to generate the reference orientation that the plies will have for said section. Oriented Selection Sets → Create Oriented Selection Set.

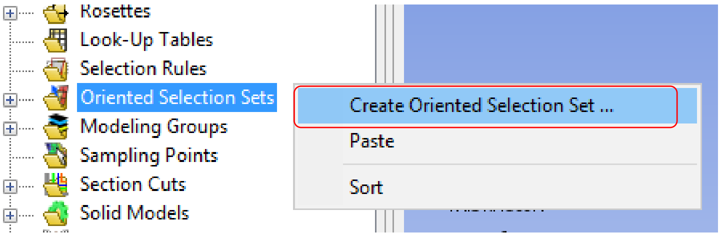


*Figure 152: Oriented selection sets*

- Thus, select an element, which in this case, is the Base. The direction is flipped inwards following industry practises. Select the created rosette. The selection method is set to be **Maximum angle** in order to obtain a uniform fibre orientation.

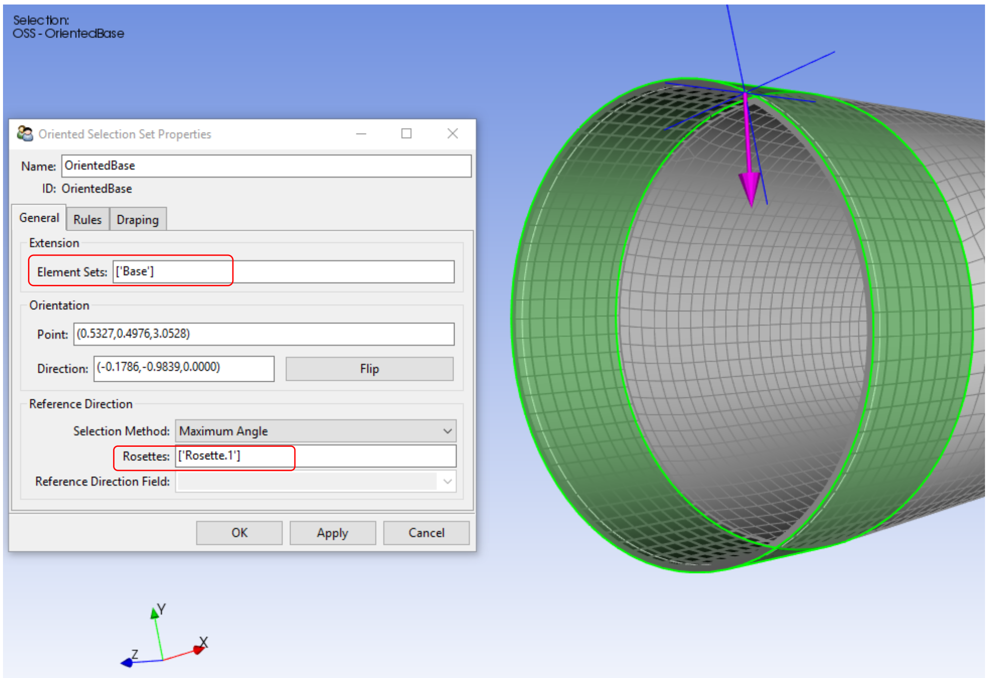


*Figure 153: Oriented element set definition*

- The layup orientation and **reference direction** can be observed. The pink arrows represent the layup direction and the yellow arrows suggest the reference fibre direction angle (a layer of 90° orientation will run perpendicular to the yellow arrows)

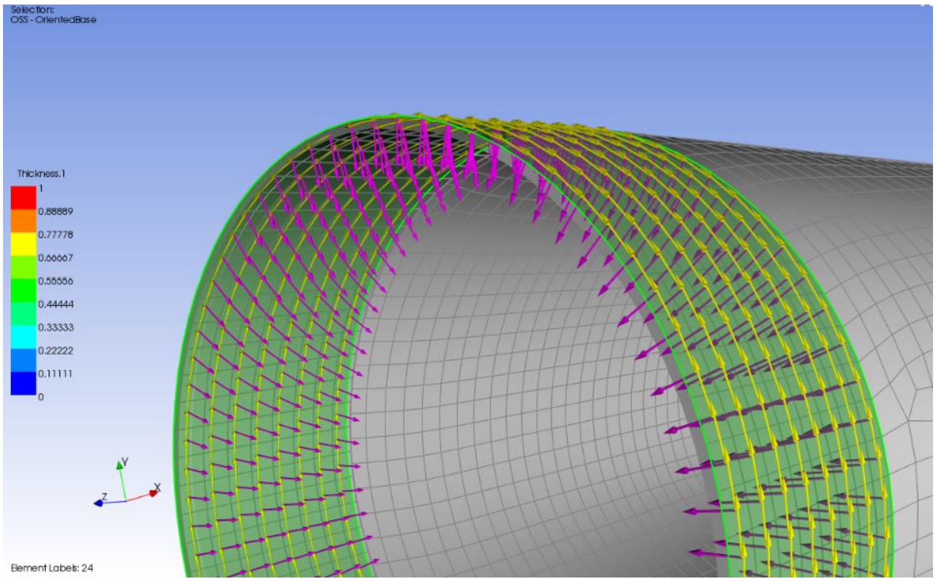


*Figure 154: Reference layup direction*

- The following figure illustrates the layup orientation and **reference fibre direction** applied to one of the sections of the blade. It can be observed that the reference direction runs parallel to the length on the blade, simulating industry practices. The same reference direction and orientation is defined for all the remaining sections.

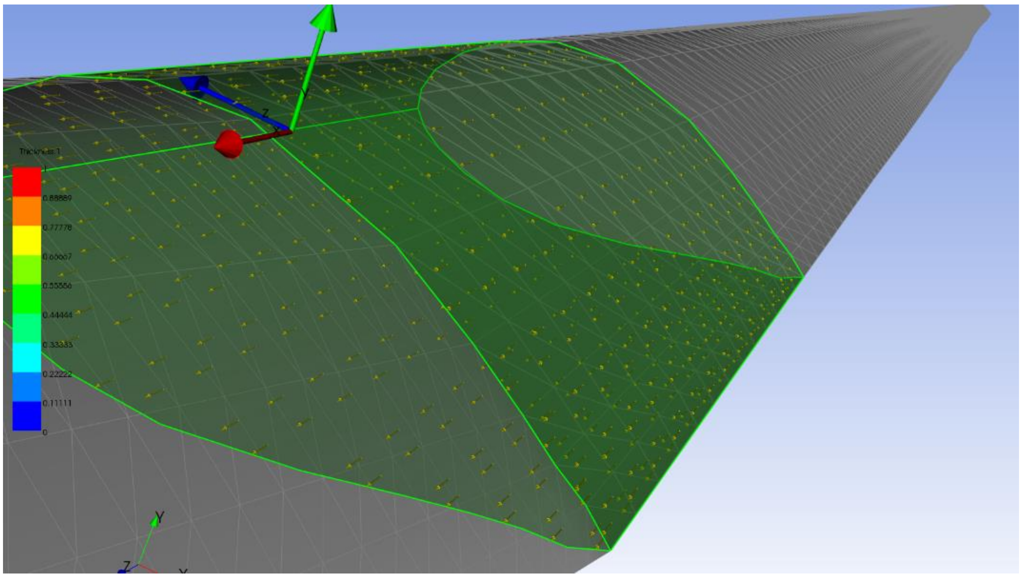

*Figure 155: Reference fibre direction*

- The next step involves the creation of a **Modelling Group.** A Modelling Group is an element set or section where a composite configuration (fabric, stackup or laminate) is assigned to said element, this is the final step towards defining the composite configuration of a model. The initial modelling group is named Base as the modelling will be done starting from the base of the blade onwards. Modeling Groups → Create Modeling Group.

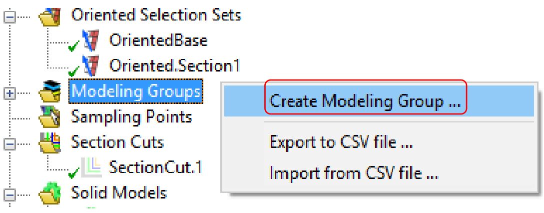


*Figure 156: Modelling group definition*

- A modelling group needs to be created for each of the sections of the blade. Once the modelling group is created and named (in this case is named Base as it defined the composite layers for the Base section) different plies can be assigned to each of the sections. Right click → **Create Ply**.

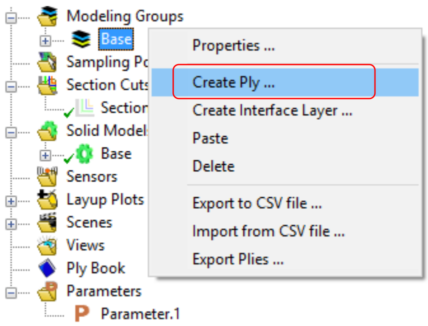


*Figure 157: Ply definition*

- Four plies will be created following the sub laminate configuration $[\pm 45, \pm 30, 90, 0]$. The first ply is named **'0'** as the orientation of the fabric is zero degrees. Additionally, for each ply, the respective **Oriented Selection Set**, **Ply Material** and **Ply Angle** are defined. For this initial layer, the orientation is set as zero degrees and consisting of only 1 layer.

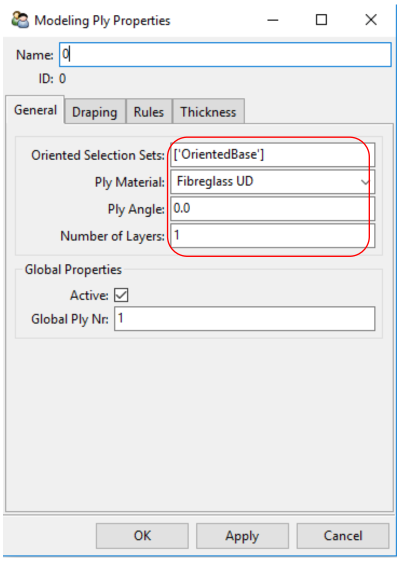


*Figure 158: Ply properties*

- Similarly, the remaining plies for 90, $\pm30$ and $\pm45$ degree orientations are created. The Modelling Group for the Base section will then be defined. As mentioned before, the initial number of layers for each orientation will be 1 as the optimum number of layers are part of the desired outcomes of the optimization process that will follow.

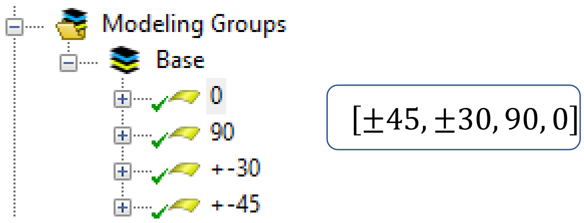


*Figure 159: Base configuration*

- A **solid extrusion** of the shell geometry can now be generated implementing the assigned laminate. The resulting solid model can be exported to a **Static Structural** study in order to analyse its properties followed by the optimization process. Under Solid Models → Create Solid Model.

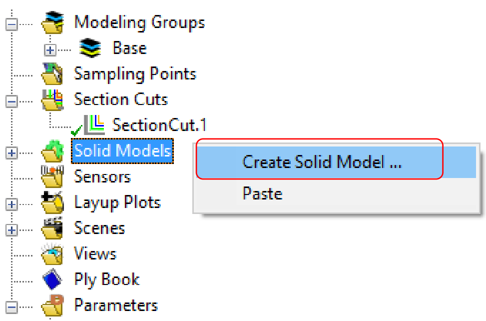


*Figure 160: Solid model generation*

- Then, select the desired **Element Set**, which in this first case is the Base of the blade and **Update** the model. The solid section will now become visible.

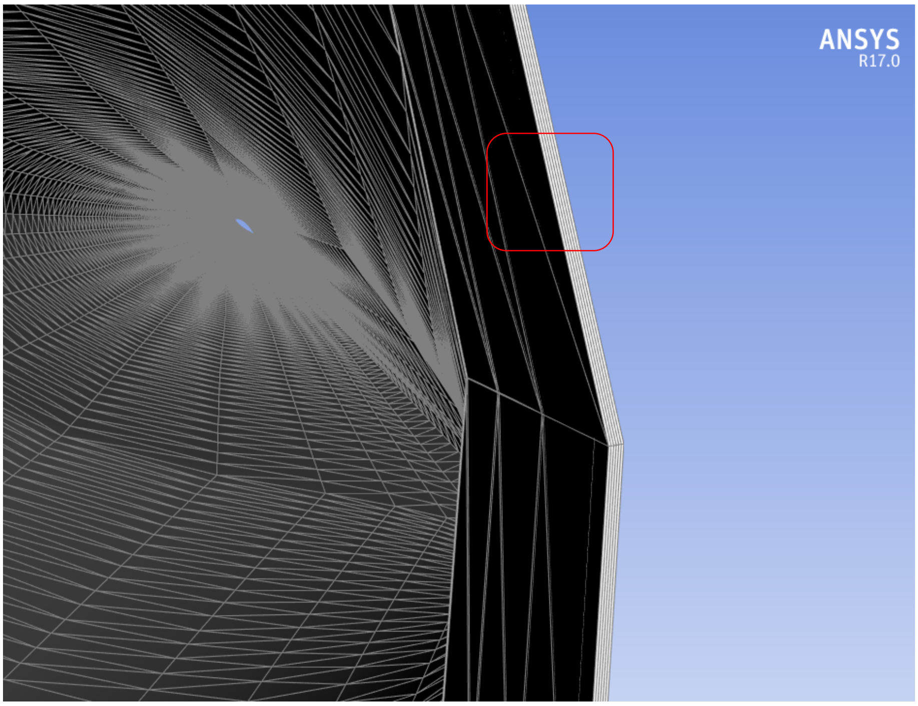


*Figure 161: Extruded model*

- The final but most essential step involves setting up the parameters for the optimization process. As previously discussed, the number of layers for each of the default orientations in each section of the blade will be set as an input parameter. Therefore, right click on **Parameters → Create Parameter**...

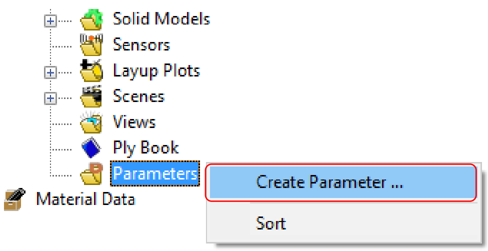


*Figure 162: Parameter definition*

- A **Parameter Properties** dialog box will appear where the object to be parametrized and the type of parameter can be set. The first parameter is named '*Base_zero*' of Property '*Number of layers*' which means that the number of layers (currently one layer) will be optimized for the glass fibre fabric of zero-degree orientation of the Base section. The object is the first modelling ply created named **'0'**. A description of the parameter can also be included.

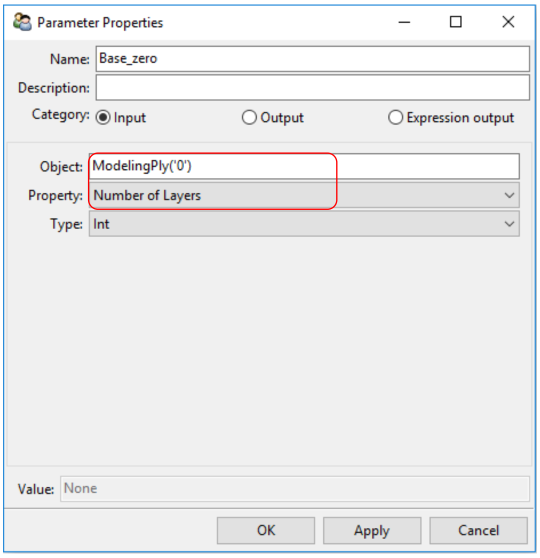


*Figure 163: Parameter definition*

- PARAMETERS 2 TO 49: Consequently, for the Base section of the blade, a total of four parameters have been created (for the $0, 90, \pm 30, \pm 45$ orientations)

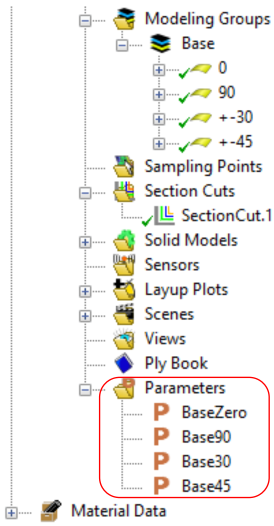


*Figure 164: Parameter of Base section*

○ Now that the composite layup configuration has been set for the initial section, the same procedure (starting from the **Element Orientation Sets** definition) is followed for the rest of the sections of the blade or **Element Sets**. At the end of this section of the tutorial, four parameters (of type number of layers) will be set for each of the Element sets, resulting in a total of **48 parameters** (12 blade sections) that will be implemented in the later optimization phase. Consequently, the final Model Tree with all the sections and parameters defined is illustrated in Figure 165.

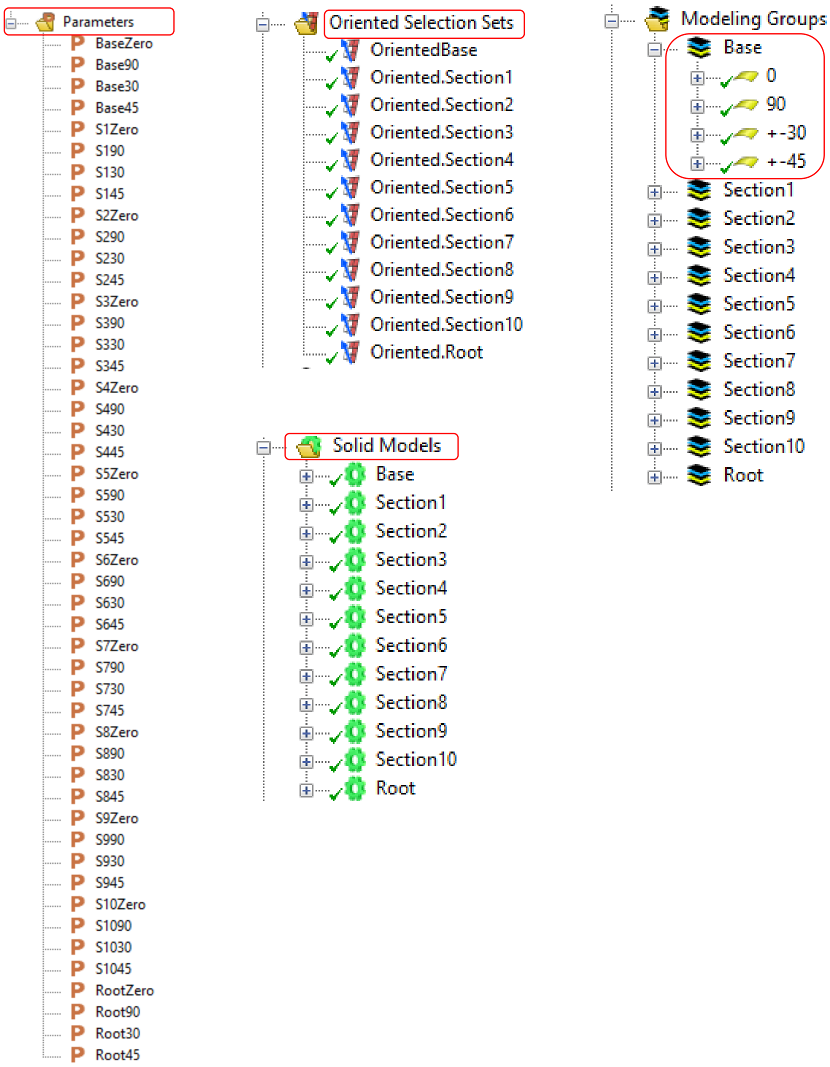


*Figure 165: Model parameters and components*

## III. CFD ANALYSIS

A Computational Fluid Dynamics (CFD) study is carried out in order to obtain a value for the Lift to Drag ratio of the turbine blade at the current pitch angle (zero degrees). Using the CFD results, a direct optimization process will follow in order to obtain a pitch angle that maximises the Lift to Drag ratio of the blade, increasing its efficiency. Additionally, the pressure distribution on the blade (obtained from the CFD analysis) will be used as one of the loads for the static structural study.

- As the air flow domain is the only body required for the CFD analysis, a **Boolean** operation is performed in order to subtract the blade shape from a circular extrusion. The circular shape is selected because this geometry will be arbitrarily rotated simulating a change in the pitch angle. The geometry is illustrated in Figure 166.

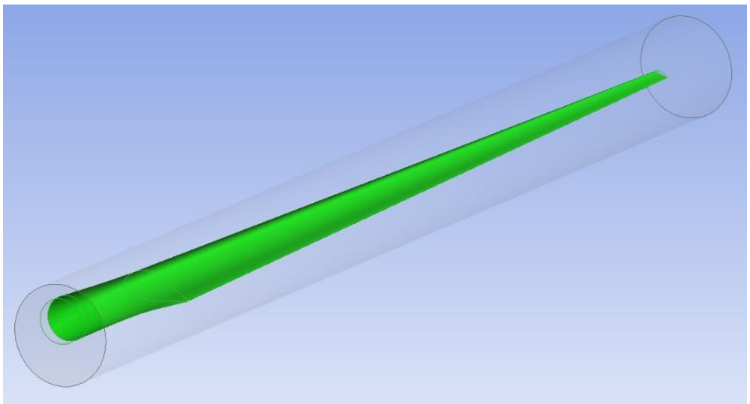

*Figure 166: Rotating geometry*

- Once the Boolean operation subtracts the blade geometry from the extruded cylinder, a **Rotation** type operation is implemented.

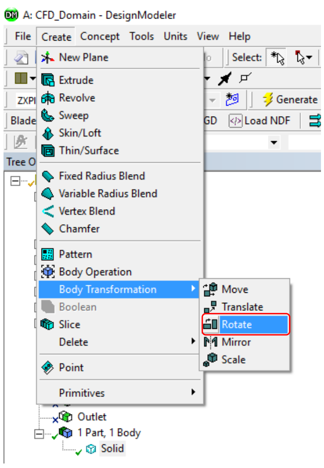


*Figure 167: Rotate feature*

- PARAMETER 50: The Rotation feature is then parametrised for the subsequent optimization process. The starting pitch angle is zero degrees.

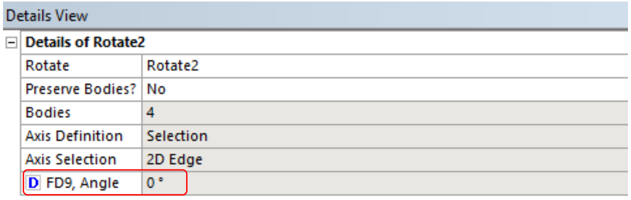


*Figure 168: Pitch angle parameter*

- The next step is to add an enclosure to the new geometry which also represents the air domain that will be studied. This new **enclosure** will have a rectangular shape so that the boundary conditions can be easily defined. A standard enclosure is setup on DesignModeler, Tools → Enclosure. The enclosure is automatically created around the existing bodies.

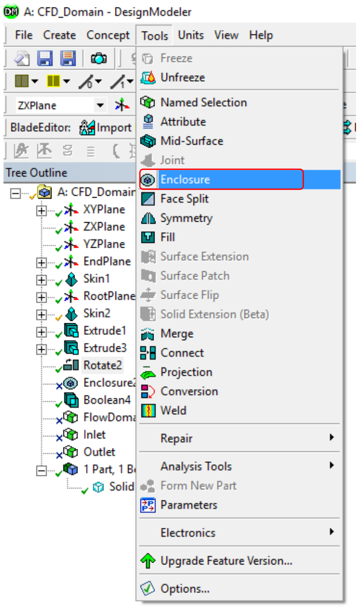


*Figure 169: Enclosure definition*

- The final fluid domain after the enclosure is implemented is illustrated in Figure 170.

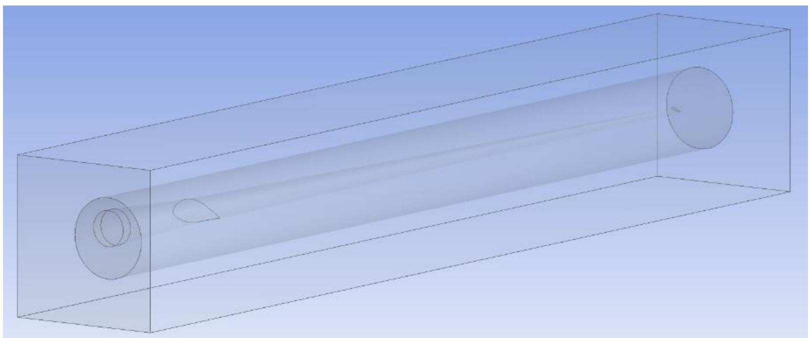

*Figure 170: Enclosed geometry*

- Subsequently, **Named Selections** are created for the boundary conditions (right click on desired face or body → Named Selection) The front side of the enclosure (leading edge side of the turbine) is set as the **inlet** while the remaining faces of the enclosure are set as **outlet**. The Named Selection illustrated in Figure 171 represents the flow domain's inlet.

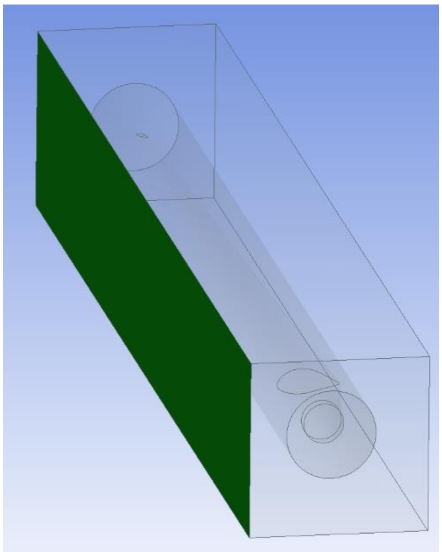

*Figure 171: Inlet of flow domain*

- As in previous studies, a **Mesh** needs to be generated for the new geometry. A **Curvature** size function is applied with a relatively coarse relevance centre (A sensitivity analysis was previously performed which suggested that a relatively coarse mesh does not have a major impact on the solution)

Details of "Mesh"

| | |
|---|---|
| **Display** | |
| Display Style | Body Color |
| **Defaults** | |
| Physics Preference | CFD |
| Solver Preference | Fluent |
| Relevance | 0 |
| Export Format | Standard |
| Shape Checking | CFD |
| Element Midside Nodes | Dropped |
| **Sizing** | |
| Size Function | Curvature |
| Relevance Center | Coarse |
| Initial Size Seed | Active Assembly |
| Smoothing | Medium |
| Transition | Fast |
| Span Angle Center | Medium |
| Curvature Normal A... | Default (45.0 °) |
| Min Size | 1.e-002 m |
| Max Face Size | 0.150 m |
| Max Tet Size | Default (2.70180 m) |
| Growth Rate | Default (1.850 ) |
| Automatic Mesh Base... | On |
| Defeaturing Tolera... | Default (5.e-003 m) |
| Minimum Edge Length | 0.596950 m |

*Figure 172: Mesh definition*

- The final **mesh** of what will become the air flow domain can be observed. As the model suggests, the blade body was extracted from the flow domain (performed by the Boolean operation) A finer mesh can be defined if higher accuracy is required.

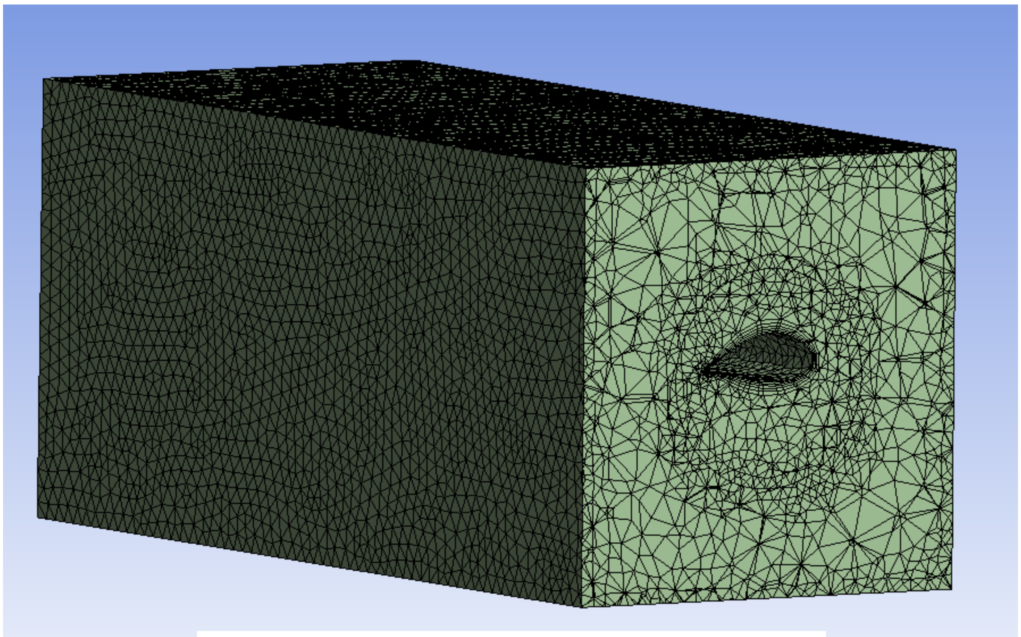

*Figure 173: Final mesh of the model*

- As with the Rocket Nozzle case, the **Setup** is now selected where the boundary conditions are set. Setup → Right click → Edit

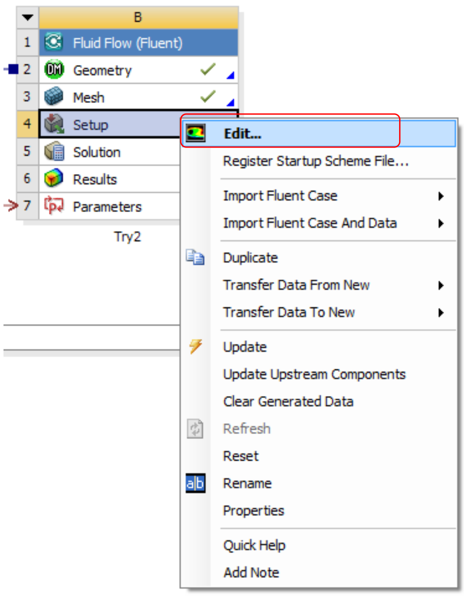


*Figure 174: Setup tab*

- A pressure based solver with an active **Energy equation** and a **k-epsilon viscous** method is implemented (a k-epsilon turbulent method is generally suitable for low speed turbulent studies)

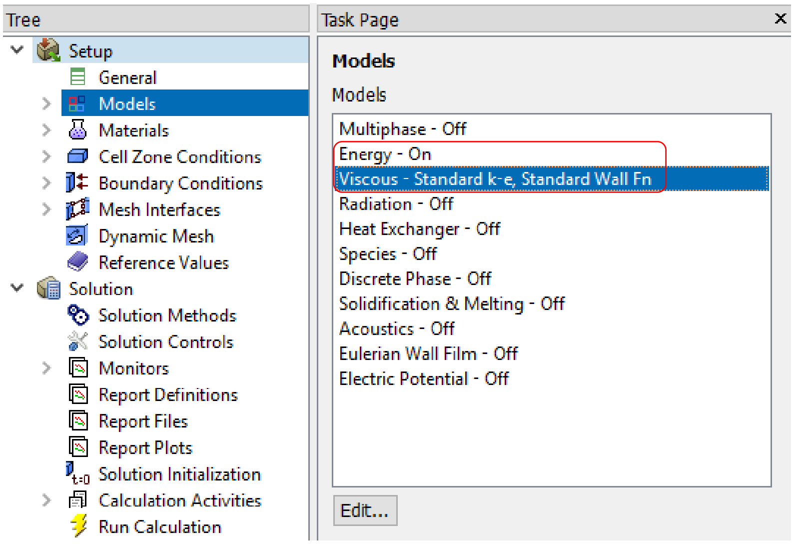


*Figure 175: Energy equation*

- Under **Boundary Conditions**, the default boundaries plus the previously defined Named Selections will appear. Most of the boundary conditions will have a default type defined by the solver, the only conditions that need modification are the Named Selections (**inlet** and **outlet**).

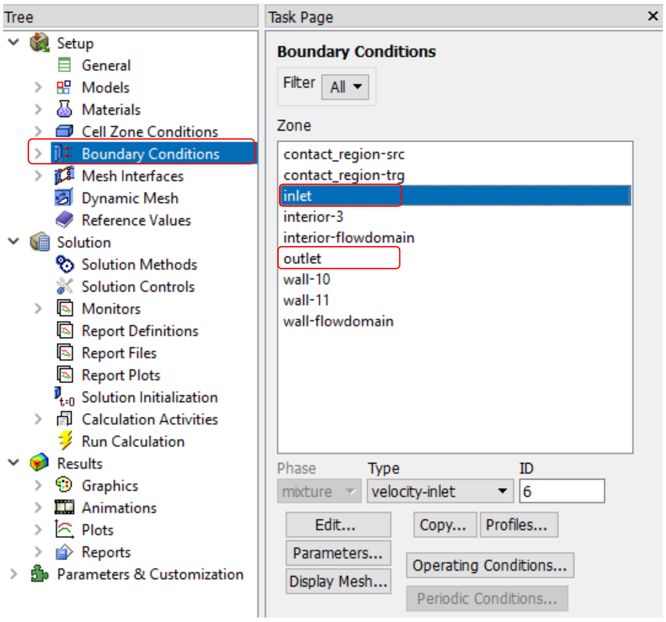


*Figure 176: Boundary conditions definition*

- Thus, the **inlet boundary condition** is set as a **velocity inlet type** with a velocity magnitude of 20 m/s (maximum wind speeds during operation of large wind turbines). While the outlet boundary condition is set as a pressure type outlet with a **Gauge Pressure** of 0 Pascals or standard atmospheric pressure (absolute pressure of 101325 Pa)

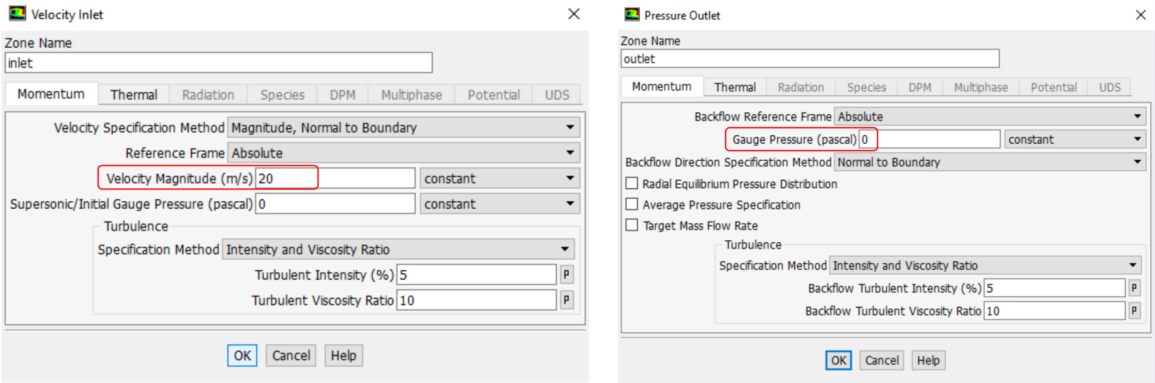


*Figure 177: Inlet and outlet conditions*

- Under **Reference Values**, the values are set to be computed from the inlet.

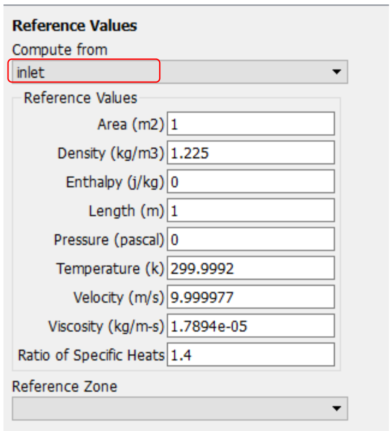


*Figure 178: Reference values*

- Under **Solution Methods**, Second Order Upwind methods are selected for the Momentum, Turbulent, and Energy solvers in order to achieve more accurate results.

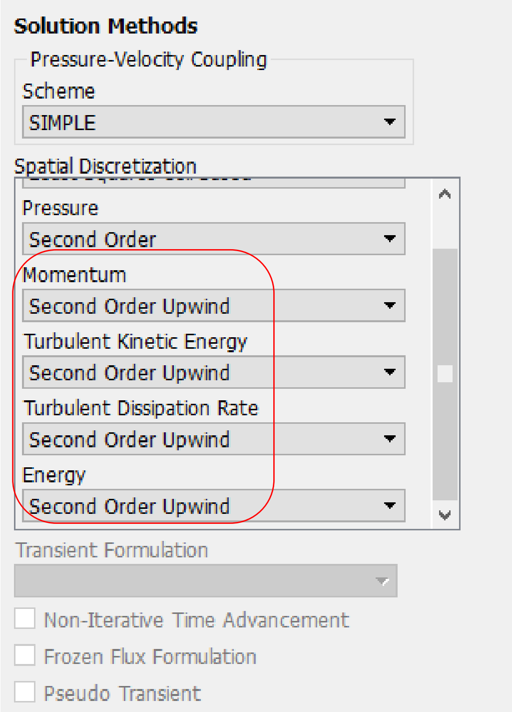


*Figure 179: Solution methods*

- The solution is then initialized (a **hybrid initialization** is recommended) and the model is solved. The number of iteration is set arbitrarily but a number should be selected for which convergence can be achieved. In this case 100 iterations were run.

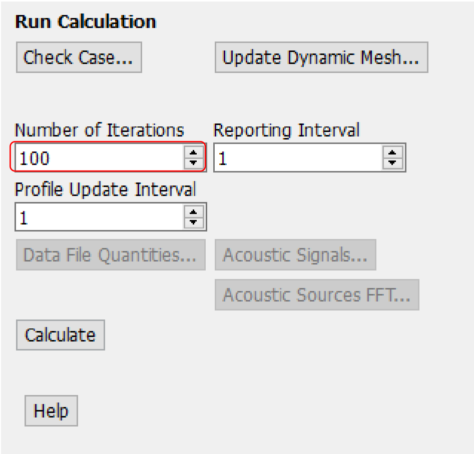


*Figure 180: Calculation run*

- The final step is to set the **Lift to Drag ratio** as an output parameter for the optimization process. Right click on the **Results** tab → Edit.

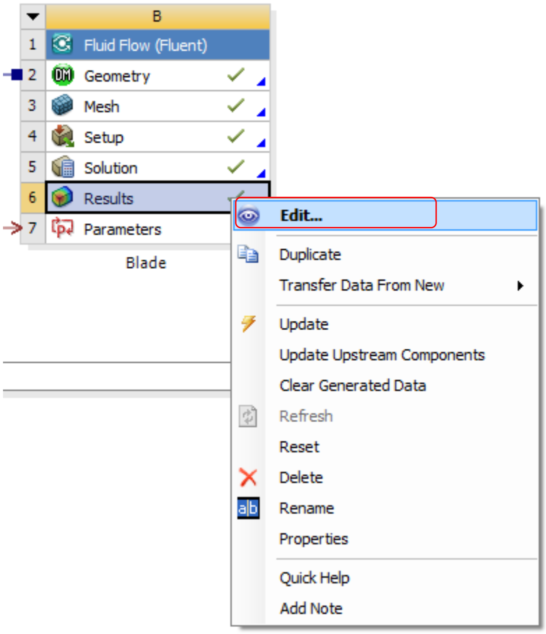


*Figure 181: Results tab CFD-Post*

- Once **CFD-Post** is open, click on the *Expressions* tab on the top let section of the screen. Right click → New.

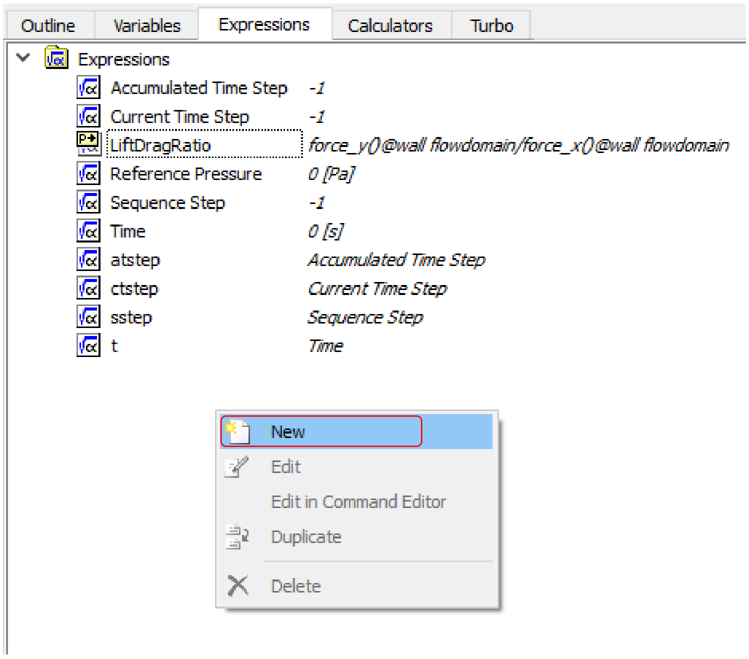


*Figure 182:Expression definition*

- In this case, the new expression will be called '*LiftDragRatio*'. A *Definition* screen will appear where the expression for the lift to drag ratio will be set. The desired expression will consist of the **y_force** (lift) divided by the **x_force** (drag) at the blade boundary. Thus, right click on the definition screen → functions → CFD Post → y_force.

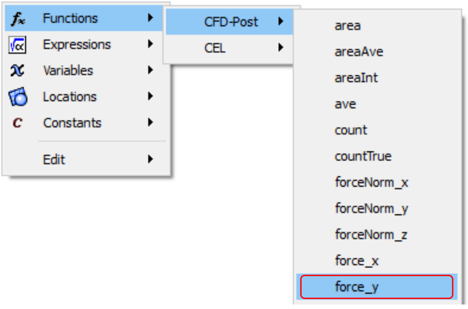


*Figure 183: Lift force definition*

- Subsequently, right click → Locations → Wall flow domain (blade domain)

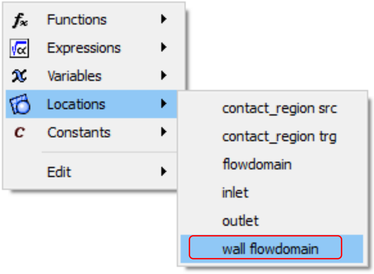


*Figure 184: Location definition*

Follow the same process for defining the **x_force** (drag) at the same location. The final expression will become the lift to drag ratio and the current value (1.6794) can be observed when clicking on **Apply**.

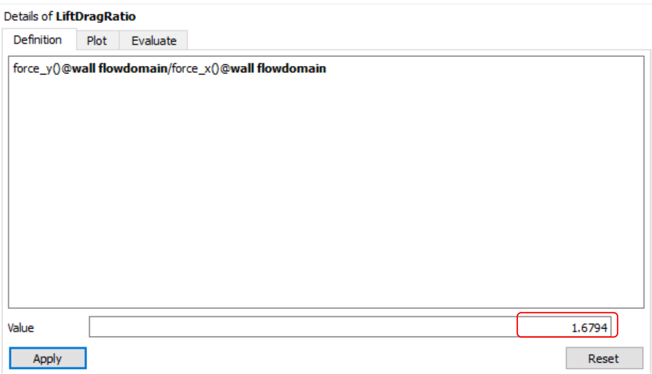


*Figure 185: Lift force value*

- OUTPUT PARAMETER 1: Once a value for the lift to drag ratio of the blade is obtained, this expression is set as an output parameter. Right click on the new expression → Use as Workbench Output Parameter.

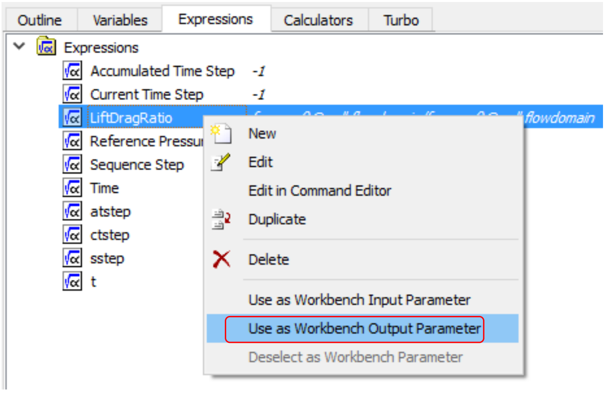


*Figure 186: Parameter definition*

## IV. Pitch angle Optimization

In this section, the pitch angle of the blade will be optimised in order to maximize the Lift to Drag ratio of the model under a constant wind speed of 20 meters per second (maximum wind speed operation) Subsequently, using the optimised model, the pressure distribution along the blade will be noted and imported as one of the loads acting on the blade for the following static structural analysis and later optimization process of the composite layers.

- A direct optimization method is implemented. Opening the **Parameters** tab, the input and output parameters set for the model can be observed. The input parameter being the Pitch angle of the blade (currently set a zero degrees) and the output parameter being the lift to drag ratio (estimated to be approximately 1.68)

Outline of All Parameters

| | A | B | C | D |
|---|---|---|---|---|
| 1 | ID | Parameter Name | Value | Unit |
| 2 | Input Parameters | | | |
| 3 | CFD_Domain (A1) | | | |
| 4 | P66 | PitchAngle | 0 | degree |
| * | New input parameter | New name | New expression | |
| 6 | Output Parameters | | | |
| 7 | Blade (B1) | | | |
| 8 | P67 | LiftDragRatio | 1.6794 | |
| * | New output parameter | | New expression | |
| 10 | Charts | | | |

*Figure 187: Model parameters*

- As previously stated, a direct optimization process is carried out. Therefore, drag the **Direct Optimization** module from the tool box and place it under the **Parameters** tab.

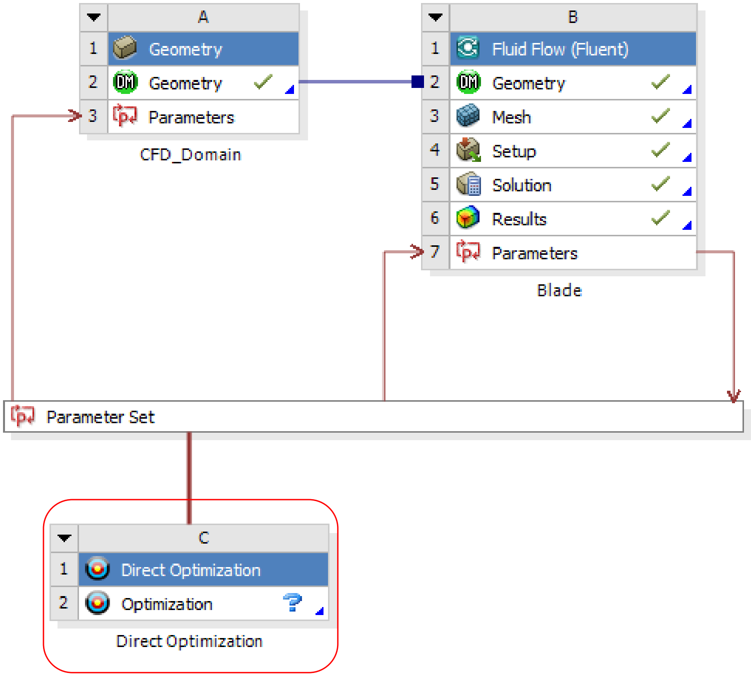


*Figure 188: Direct optimization module*

- Double click on **Optimization**. Click on **Objectives and Constraints**. To set the Objective of the optimization process, select the Lift to Drag ratio parameter and under Objective type select **Maximize**. No constraint is required for this case.

Table of Schematic C2: Optimization

| | A | B | C | D | E | F | G |
|---|---|---|---|---|---|---|---|
| 1 | Name | Parameter | Objective | | Constraint | | |
| 2 | | | Type | Target | Type | Lower Bound | Upper Bound |
| 3 | Maximize P67 | P67 - LiftDragRatio | Maximize | | No Constraint | | |
| * | | Select a Parameter | | | | | |

*Figure 189: Objectives definition*

- Then, click on the input parameter (Pitch angle) and select the desired **upper and lower bounds**. In this case the lower bound is set as zero degrees as it is known that a negative pitch angle would generally decrease the lift of a standard type of wing profile. The upper bound is set as 20 degrees.

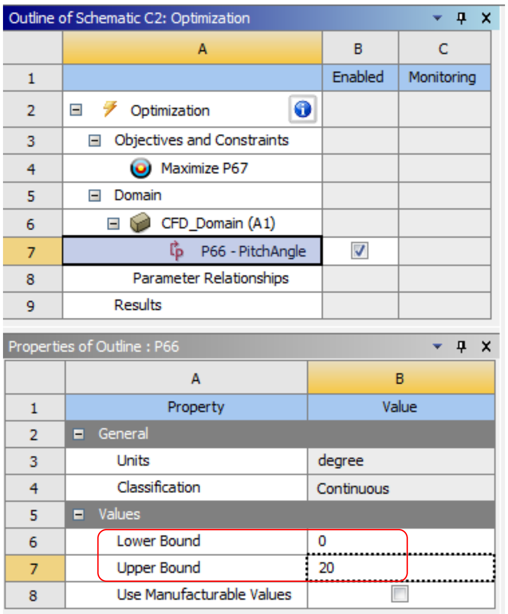


*Figure 190: Parameter bounds*

- Next, under Optimization, the optimization method is set as **Screening** (this method uses a simple approach based on sampling and sorting) with a number of 20 samples and 2 desired candidates.

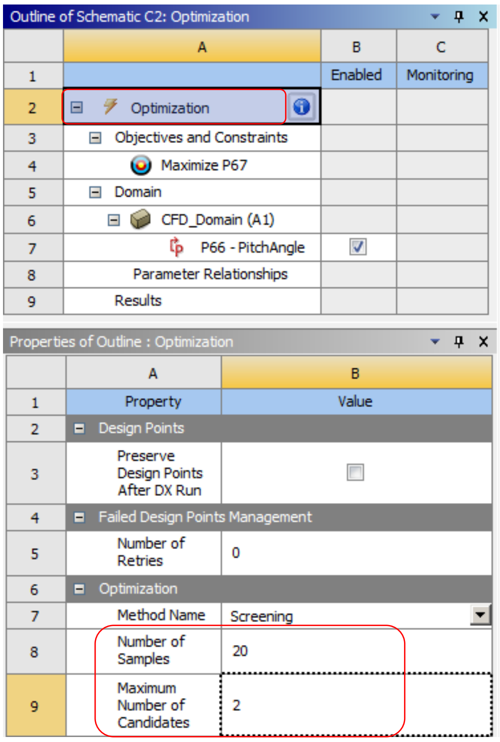


*Figure 191: Optimization parameters*

- Once the optimization setup is done, the process can be **run**. Right click on Optimization → Update.

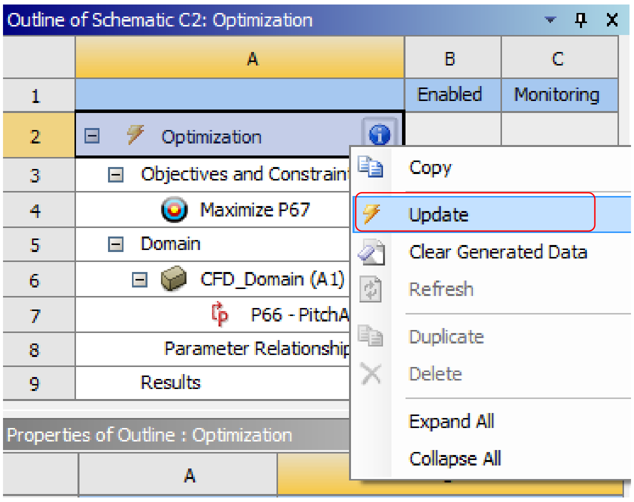


*Figure 192: Optimization process start*

- The computational time of the optimization process is directly proportional to the quality of the mesh. Once the process is done, the specified number of candidate points will appear (provided there are no errors during the optimization process) In this case, the 2 candidate points desired are suggested by the optimization module.

Table of Schematic C2: Optimization

| | A | B | C |
|---|---|---|---|
| 1 | ⊟ Optimization Study | | |
| 2 | Maximize P67 | Goal, Maximize P67 (Default importance) | |
| 3 | ⊟ Optimization Method | | |
| 4 | Screening | The Screening optimization method uses a simple approach based on sampling and sorting. It supports multiple objectives and constraints as well as all types of input parameters. Usually it is used for preliminary design, which may lead you to apply other methods for more refined optimization results. | |
| 5 | Configuration | Generate 30 samples and find 2 candidates. | |
| 6 | Status | Converged after 30 evaluations. | |
| 7 | ⊟ Candidate Points | | |
| 8 | | Candidate Point 1 | Candidate Point 2 |
| 9 | P66 - PitchAngle (degree) | 10.5 | 8.5 |
| 10 | P67 - LiftDragRatio | ★★★ 3.1829 | ★★ 3.0442 |

*Figure 193: Candidate points*

- The candidate points are illustrated with a **star** scheme where three stars suggest that the design meets all the specified objectives and constraints. Thus, the Lift to Drag ratio is maximized when the Pitch angle is 10.5 degrees. A plot of the Lift to Drag ratio versus the Pitch angle is also generated by the optimization module as per Figure 194 also validating the results.

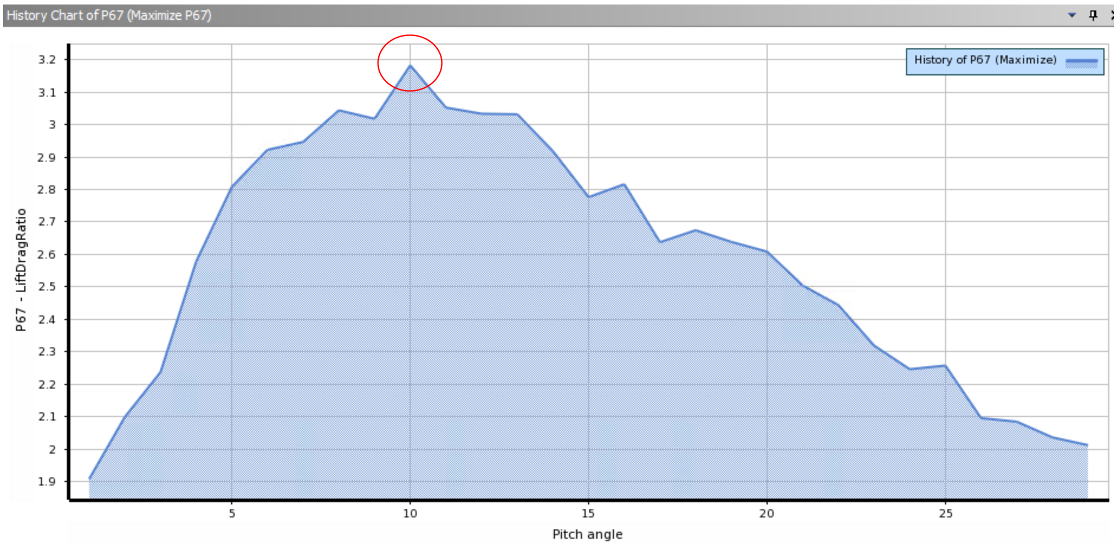


*Figure 194: Optimization chart*

## V. Structural Analysis

In order to achieve realistic results for the structural study and later optimization, the aerodynamic loads obtained from the previous CFD analysis will be implemented into the static structural study. Thus, the pressure loads along the blade were computed using the optimized Pitch angle (10.5 degrees)

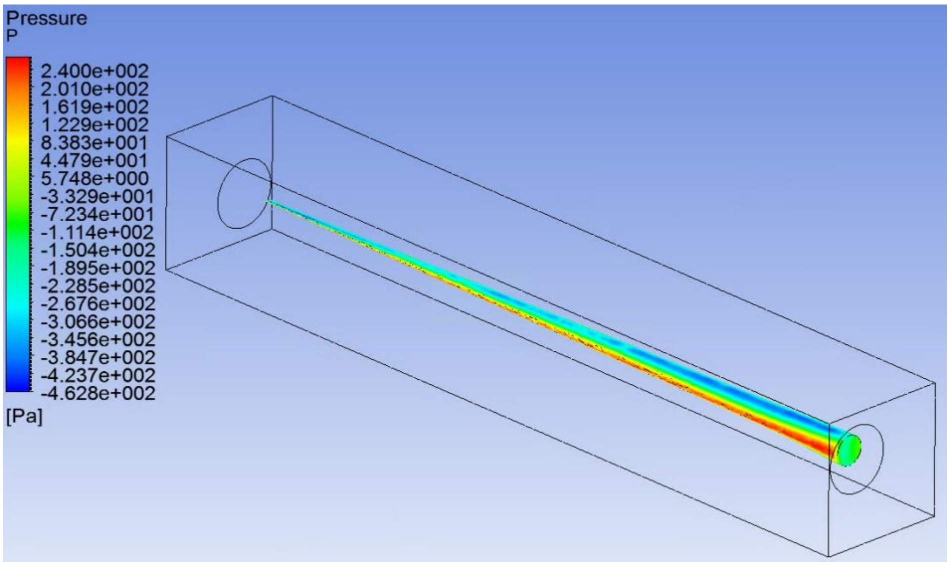


*Figure 195: CFD pressure results*

As it can be observed, the contours of **pressure** suggest that the aerodynamic effects on the blade are not negligible. For the structural analysis, and considering the pressure loads from the CFD study, an approximate value of 700 Pa (negative pressure on top surface plus positive pressure on bottom surface) will be applied to one third of the length of the blade (from the end point) that will simulate the lift force being generated under its maximum operational loads (wind speed of 20 m/s)

As discussed in the case description, the loads/constraints implemented for this model are the aerodynamic pressure load (from CFD), gravitational force, a constant rotational speed simulating real operation with the main constraint being the fixed base of the blade.

- The first step is to drag a **Static Structural** study module from the Workbench Toolbox and link the **Setup** tab from **ACP (Pre)** with the **Model** tab from the Static analysis module.

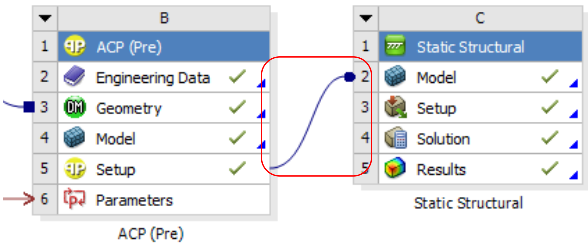


*Figure 196: Static Structural analysis*

- When linking the mentioned modules, a transfer toolbox will appear from which the **Transfer Solid Composite Data** option is selected.

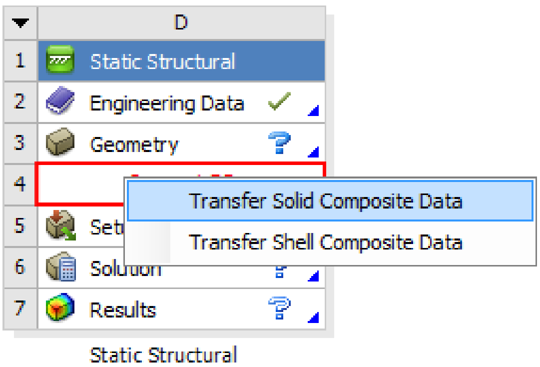


*Figure 197: Solid composite data transfer*

- Consequently, right click on **Setup → Edit**. Once the module is open, the composite plies will be automatically imported and applied to the model.

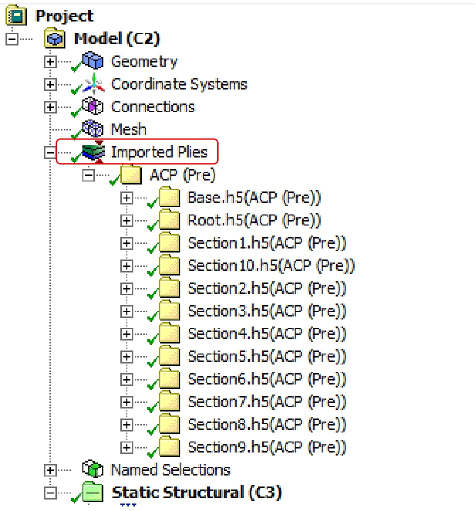


*Figure 198: Imported composite plies*

- The next step involves setting up the loads and constraints of the model. The maximum possible loads during operation are considered for the analysis. As illustrated by Figure 199, a fixed support is defined at the base of the blade, standard Earth gravity and a rotational velocity are also implemented. Additionally, aerodynamic pressure loads (obtained from the CFD analysis) are also applied to the section of the turbine blade where aerodynamic forces are more substantial. It is important to note that loads and constraints need to be defined via a **Named Selection Scoping method**, instead of the usual **Geometry selection** type to avoid optimization issues.

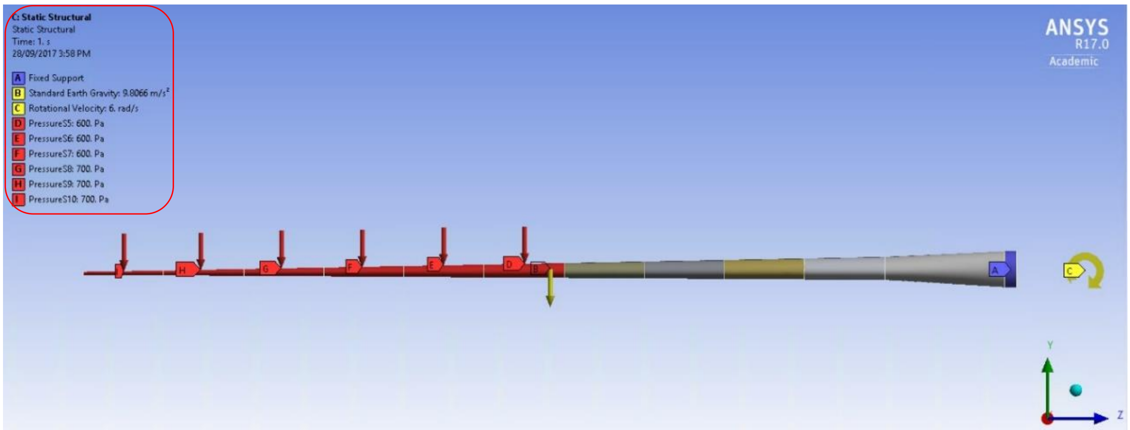


*Figure 199: Loads acting on the blade*

- Next, an **Equivalent Stress (von-Mises)** and **Total Deformation** solution types are incorporated to the solution process, from which the maximum deflection will be parametrised. The stress criteria will be utilized in ACP (Post) module where the layer failure will be parametrised so that the optimization process can minimize the probability of ply failure.

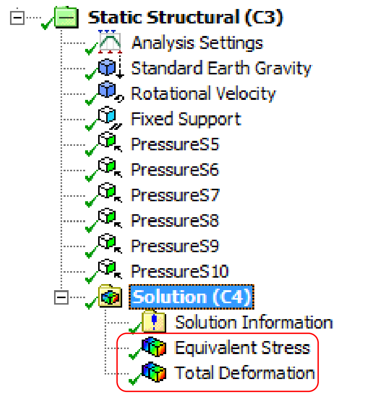


*Figure 200: Structural studies*

- Once the loads and constraints are properly set, the solution can be run. Right click on Solution → **Run**. The results can be observed below, where the maximum deflection occurs at the tip of the blade as expected and with a magnitude of approximately 4.8 meters (unfeasible). Furthermore, the equivalent stress shows a maximum value of approximately 255 MPa which goes beyond the Tensile and Compressive yield strengths of the material as suggested by the **Engineering Data** module. Therefore, stress failure will occur in some layers.

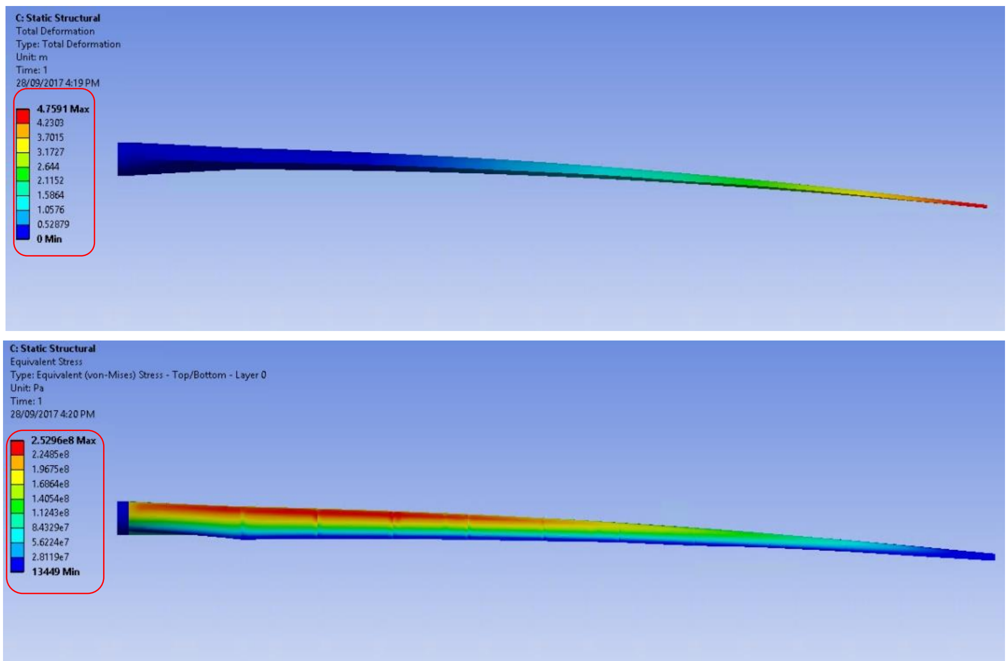


*Figure 201: Equivalent stress and deformation results*

- Output Parameter 2: After the solution is run, the **Total Deformation** can be parametrised.

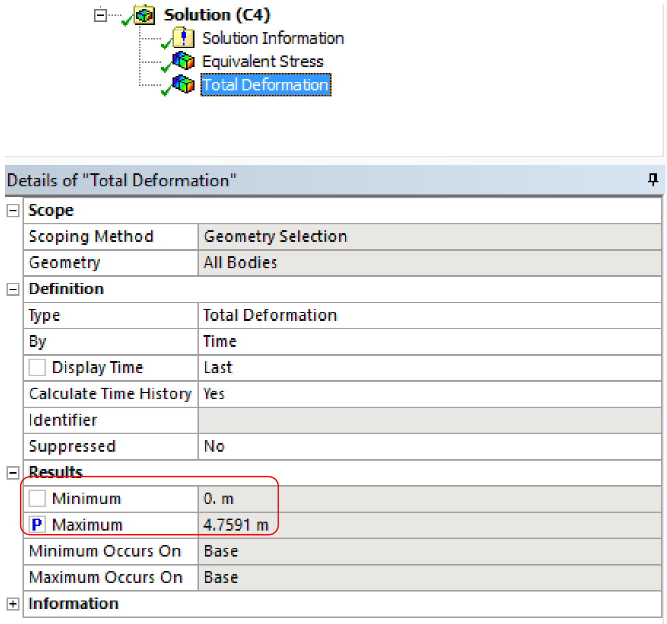


*Figure 202: Deflection parametrisation*

- The next step has to do with the inspection and parametrisation of ply stress failure for the subsequent optimisation. This step is done in the **ACP (Post)** module from the Toolbox in Workbench. Thus, select the ACP (Post) module from the Toolbox and link the **Engineering Data, Geometry** and **Model** from ACP (Pre) with ACP (Post). Then link the **Solution** tab from Static Structural with the **Results** tab from **ACP (Post)**. This will load the composite configuration data along with the loads/constraints and results from the structural analysis.

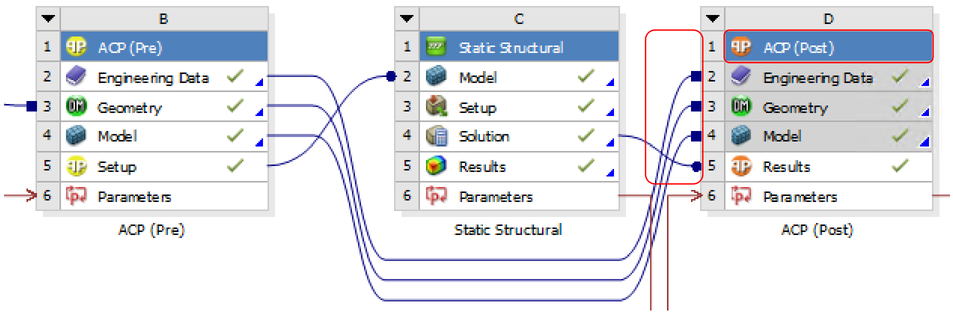


*Figure 203: Project schematic*

- Subsequently, open the **Results** tab from **ACP (Post)**. In this step, a failure criterion will be defined. The failure type considered in this case will be maximum stress failure as the deformation was already parametrised in the structural analysis. Accordingly, right click under **Definitions** *on* the Model Tree → Create Failure Criteria…

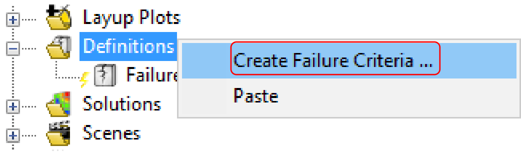


*Figure 204: Failure criteria definition*

- The Failure Criteria Definition box will appear. The available criteria include strain, stress, Tsai-Wu, Hoffman, Puck and other types of failures that can be implemented. In this study, the stress criterion is considered and thus, the **Max Stress** criteria is selected.

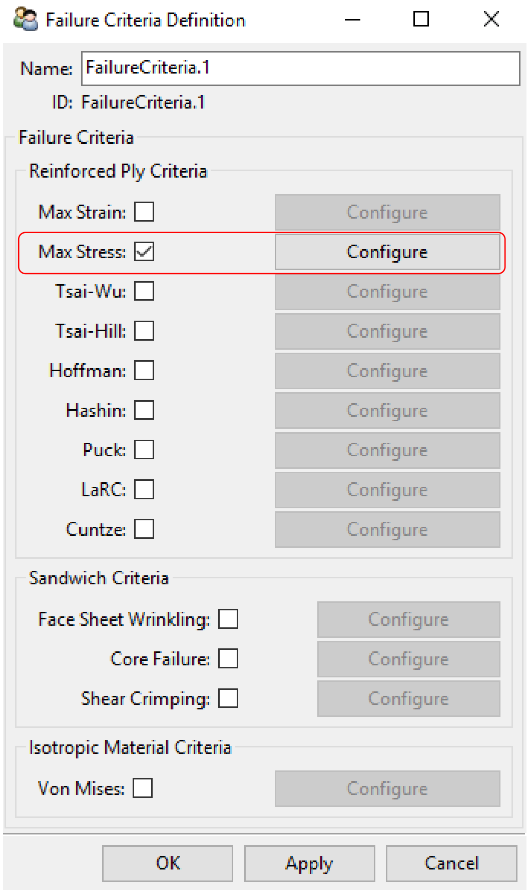


*Figure 205: Failure criteria*

- The **Max Stress** criterion can be configured to suit design purposes. The configuration box automatically considers fibre, matrix and in-plane shear failure types. Additionally, out-of-plane shear and delamination failure types can also be implemented. For this study case, only the default failure types selected are considered.

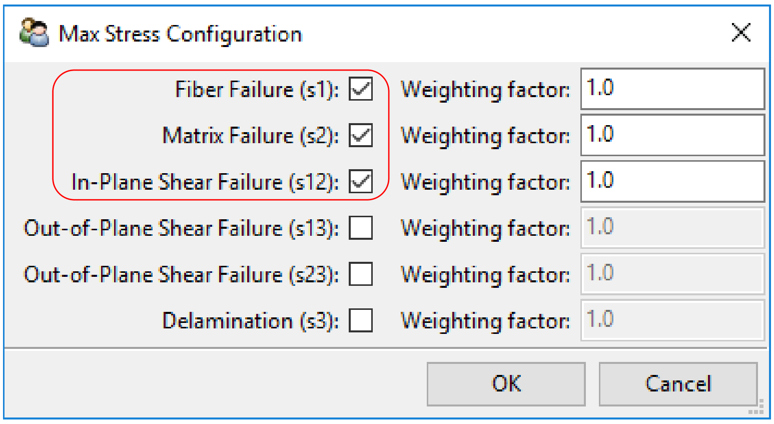


*Figure 206: Max stress configuration*

- Once the **Failure Criteria** is created, the results from the structural analysis will automatically appear under Solutions. Therefore, right click on Solution.1 (structural solution) → Create Failure…

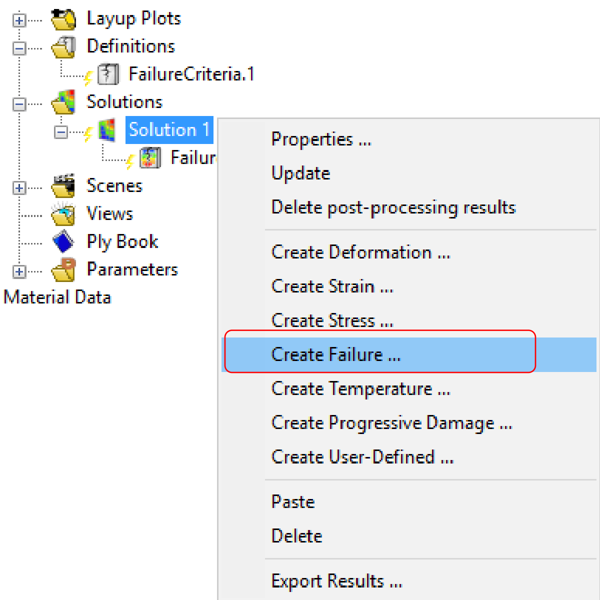


*Figure 207: Failure specification*

- The **Failure configuration** box will appear. The Data Scope is automatically set to '*All Elements*' as the objective is to avoid play failure in any layer of the entire model. Accordingly, the **Ply-Wise** option is selected with the rest of the configuration being left as default.

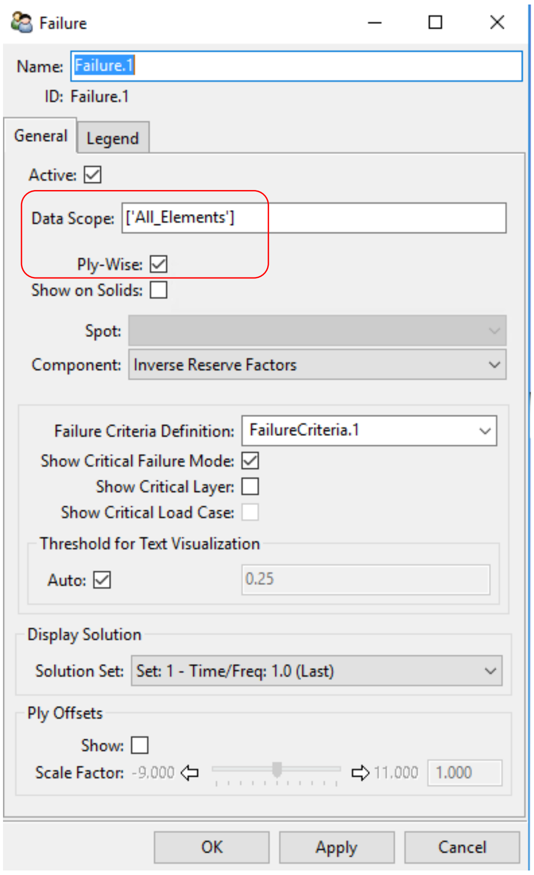


*Figure 208: Failure criterion definition*

- Once the failure model is created, the solution can be updated. Right click on Failure.1 → Update.

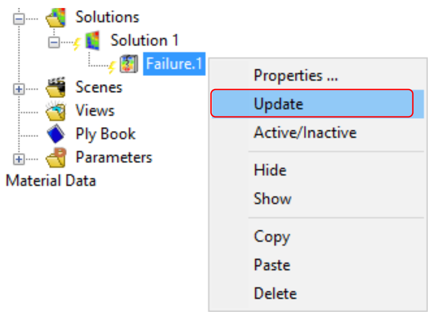


*Figure 209: Solution update*

- When the Failure Criteria is updated, by selecting an arbitrary layer of the model (under Modeling Groups) contours of failure will be displayed on the selected layer along with a reference failure number from zero to one (if this number is greater than one, the layer fails under stress) Additionally, on the selected section, a code is displayed which suggests the failure type. On the figure below, the **90-degree layer** of a section of the blade is displayed, as it can be seen, such layer fails under stress. Furthermore, the code displayed on the failing section is **'*s2t*'** which suggests that the layer fails in stress **(s)** on second direction of the material **(s2)** while in tension **(t).**

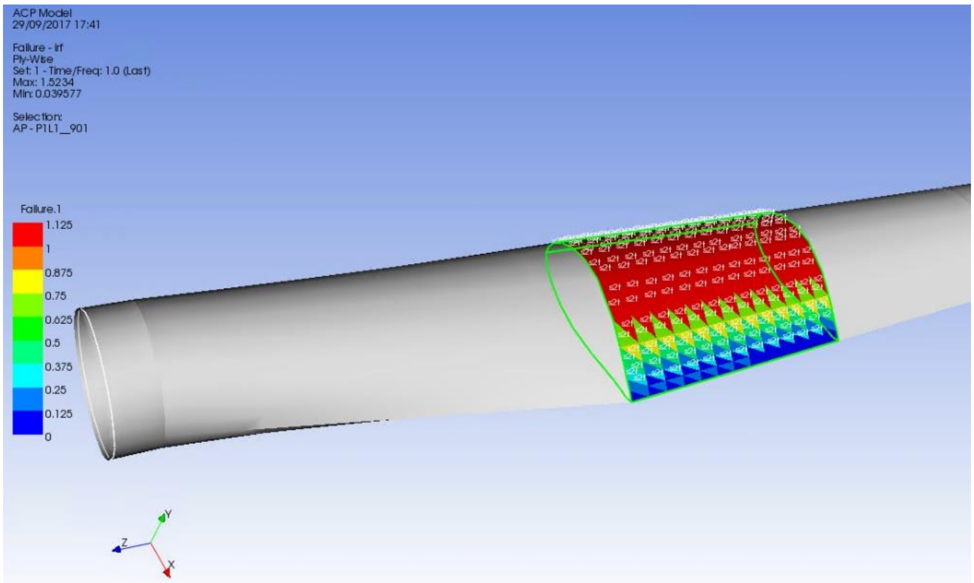


*Figure 210: Failure in 90-degree plies*

- By inspection, the layer that fails most frequently in most of the sections of the blade is the 90-degree ply with failure values of more than 1.5. However, the $\pm 45$ layer is also close to failure with values near 0.8 as seen below.

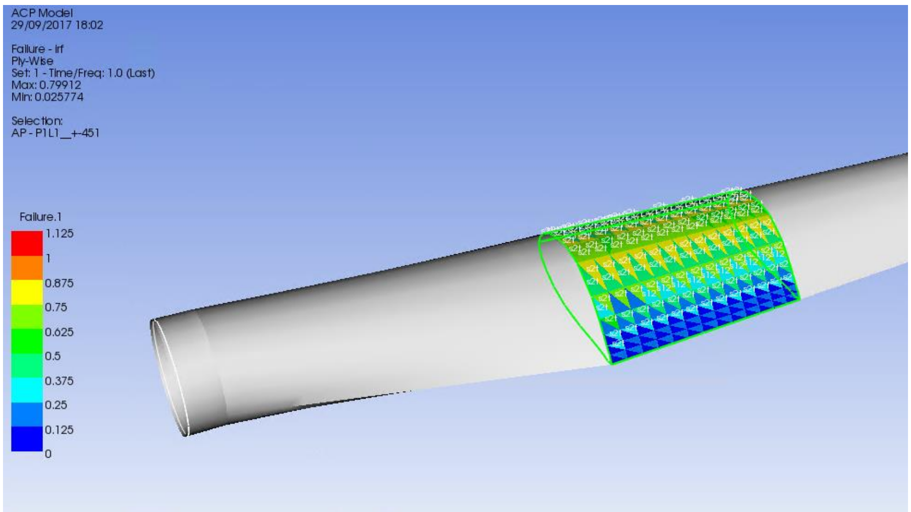


*Figure 211: Failure in 45-degree plies*

- The final step involves the parametrisation of the failure criteria. So, right click on Parameters → Create Parameter.

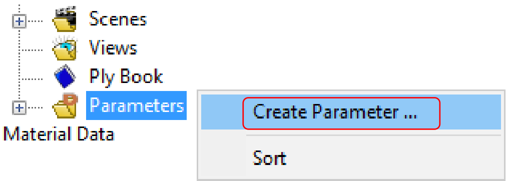


*Figure 212: Parameter definition*

- OUTPUT PARAMETER 3: The failure parameter needs to be created as an **Expression output** of type **Float**. Furthermore, as the baseline coding software for ACP is Python, its coding style has to be followed when typing expressions. In brief, the expression created considers the current model (**ACP Model**) and its specified solution (**Solution 1**) in order to output a maximum failure value from the failure criteria previously created (***Failure 1***) As it can be seen after updating the model, the maximum failure value is approximately 1.542 (well beyond 1)

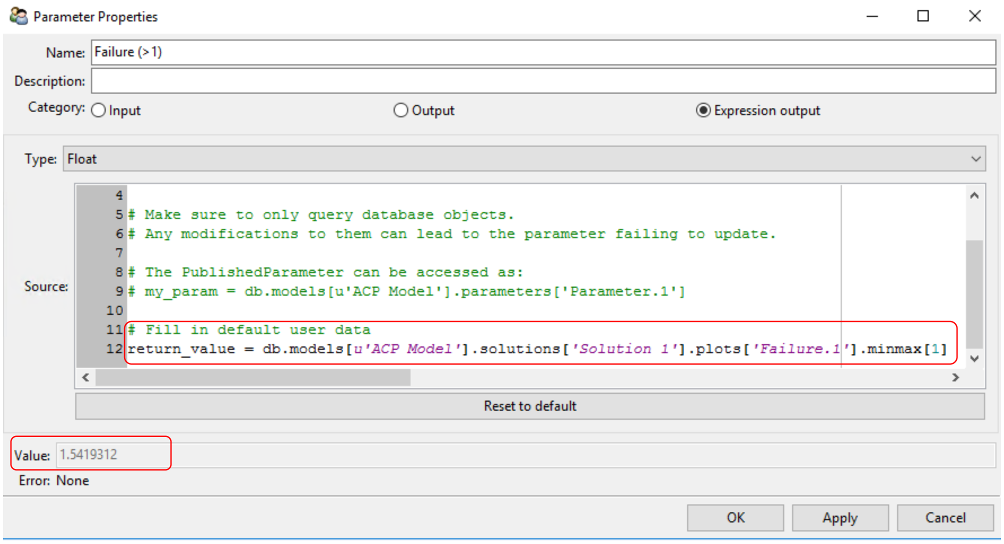


*Figure 213: Output parameter definition*

# VI. Optimization

This optimization process will attempt to minimize the tip deflection (between upper and lower limits) and avoid stress failure of any of the fibreglass layers. The input parameters include the length of the blade and the number of fibreglass layers for each of the 12 sections of the blade. A previously mentioned, the default composite configuration is $[0, 90, \pm 30, \pm 45]$ Thus, the number of layers for each of the orientations will be optimized.

*Note: As the optimization module in ANSYS 18 only supports 20 or less input parameters, a **parameter sensitivity** analysis was carried out where parameters that do not have a significant impact on the output values are identified and set as a constant value. These low impact parameters were found to be the zero degree and $\pm 30$ degree layers which were then set as sensible constant values according to the section location and the structural analysis results. The total number of input parameters considered where only the 90 and $\pm 45$ degree plies.*

- The first step involves the implementation of the **Direct Optimization** module to the Parameter set in Workbench.

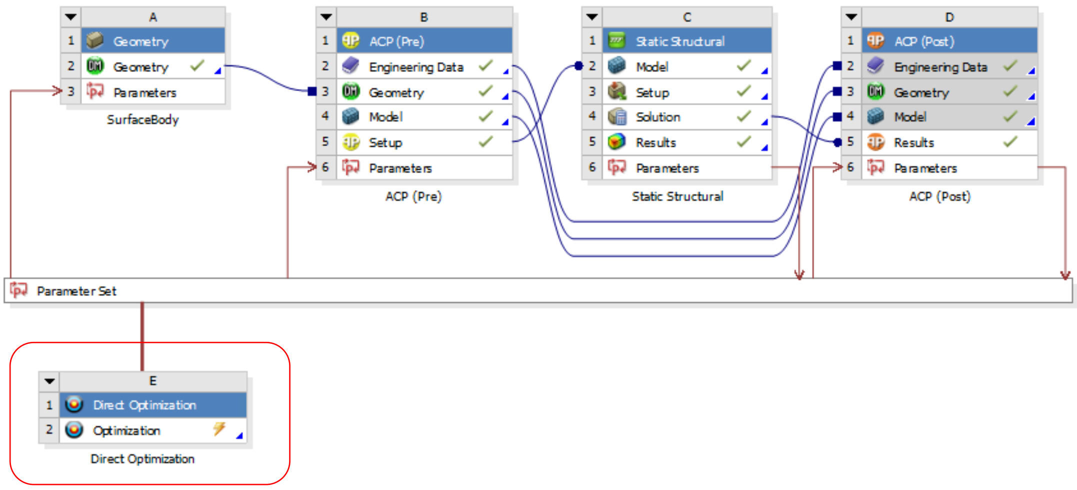


*Figure 214: Optimization module*

- Double click on the Optimization tab. Under **Objectives and Constraints**, the two objective functions of the optimization process are defined. Select the first output parameter (total deflection) and define the objective (**Minimize**) The constraint for this parameter is created for the target value to be between 1 and 1.5 meters (if no constraint is created, the optimization module will try to obtain a deflection of zero which is not practical) Then, the same process is followed for the second output parameter (Failure criterion) with a similar objective type (**Minimize**) with an Upper bound constraint of 0.66 (An upper bound of 1 would suggest that no failure occurs but a safety factor of 1.5 is applied)

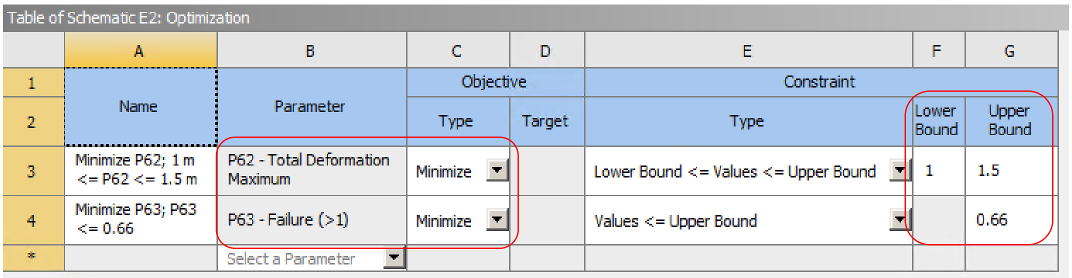

Table of Schematic E2: Optimization

| | A | B | C | D | E | F | G |
|---|---|---|---|---|---|---|---|
| 1 | Name | Parameter | Objective | | Constraint | | |
| 2 | | | Type | Target | Type | Lower Bound | Upper Bound |
| 3 | Minimize P62; 1 m <= P62 <= 1.5 m | P62 - Total Deformation Maximum | Minimize | | Lower Bound <= Values <= Upper Bound | 1 | 1.5 |
| 4 | Minimize P63; P63 <= 0.66 | P63 - Failure (>1) | Minimize | | Values <= Upper Bound | | 0.66 |
| * | | Select a Parameter | | | | | |

*Figure 215: Objectives and constraints definition*

- The objectives will now appear under the general Optimization schematic.

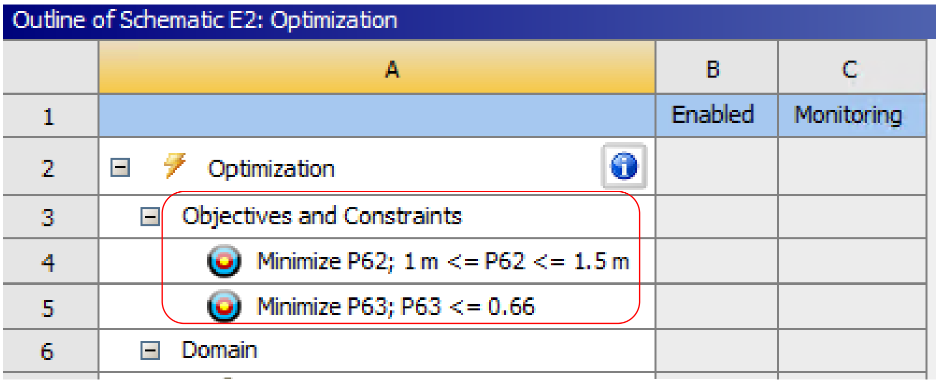

Outline of Schematic E2: Optimization

| | A | B | C |
|---|---|---|---|
| 1 | | Enabled | Monitoring |
| 2 | Optimization | | |
| 3 | Objectives and Constraints | | |
| 4 | Minimize P62; 1 m <= P62 <= 1.5 m | | |
| 5 | Minimize P63; P63 <= 0.66 | | |
| 6 | Domain | | |

*Figure 216: Objectives and Constraints*

- The next step involves the definition of upper and lower bounds of the input parameters. This is simply done by clicking on a parameter and typing the desired limit values. Figure 217 suggests that the length of the blade will be varied between 18 and 22 meters.

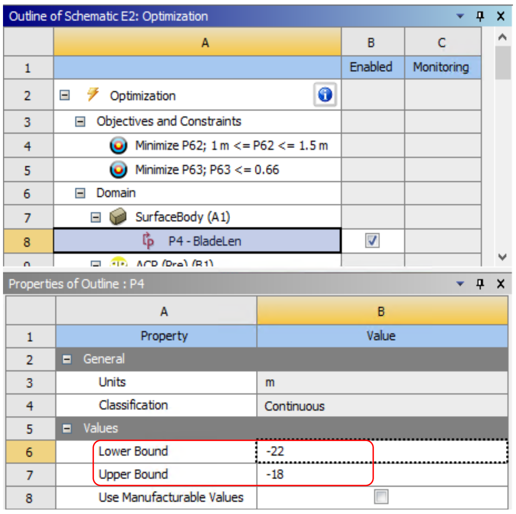


*Figure 217: Blade length bounds*

- For the **number of layers**, however, upper and lower values cannot be easily set because these parameters are of a discrete type, meaning that only a single integer value can be applied at a time. Therefore, for these discrete parameters, a range of individual values (levels) that represent the number of layers will be defined. The values selected for 90-degree layers are between 2 and 10 plies for all sections and the values for $\pm 45, \pm 30\ and\ 0$ degree oriented plies are between 2 and 6 layers in line with the failure analysis results.

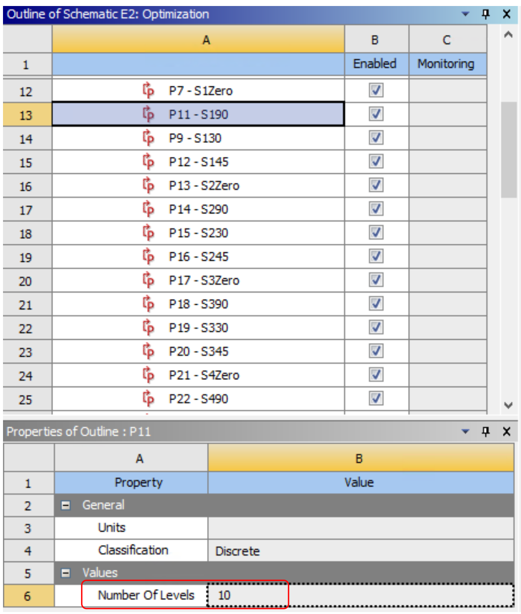


*Figure 218: Number of layers values*

- Once the Objectives, constraints and input parameter values have been set, the optimization method is configured. For this study case, a **MOGA** (Multi-Objective Genetic Algorithm) method is implemented. This method aims to find a global optimum of a function. Additionally, the number of samples is defined as **100** due to the relatively large number of input parameters.

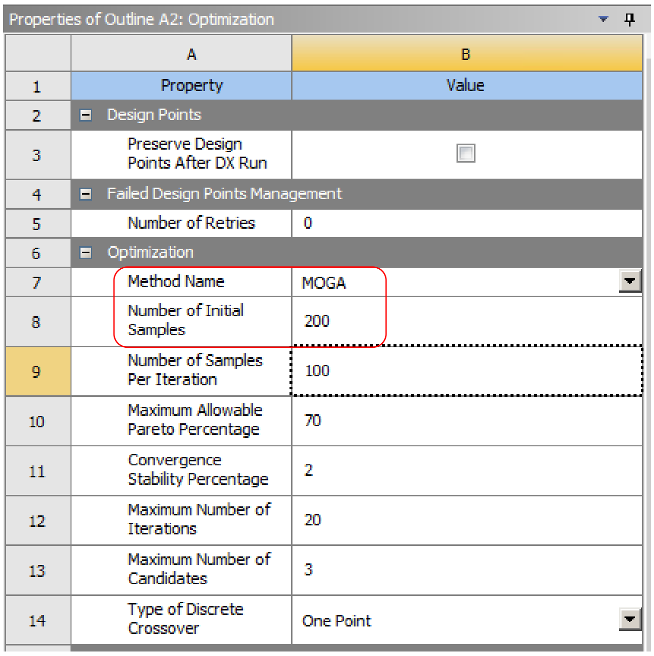


*Figure 219: Optimization method*

- Consequently, the optimization is run. Right click on Optimization → **Update**. The computational time is directly proportional to the number of samples, the mesh quality and the number of studies performed. Therefore, this process takes several hours to complete.

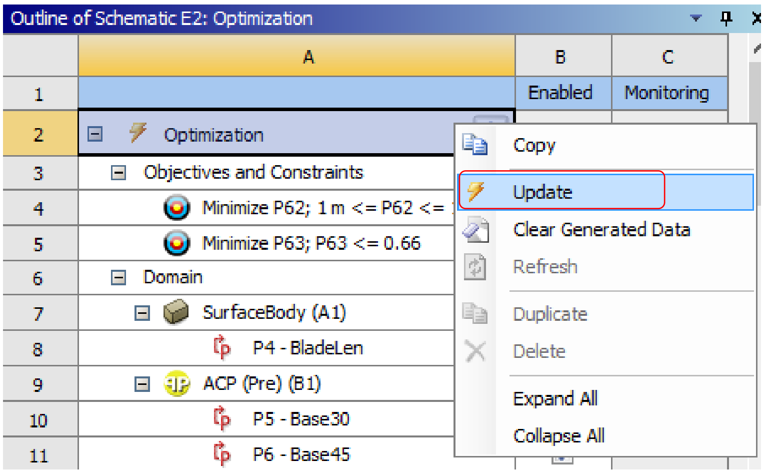


*Figure 220: Optimization run*

## VII. Results

- After the optimization process is completed, the optimum number of layers for the considered orientations are suggested by the solver. The overall thickness of each section of the optimized blade is illustrated in Figure 221.

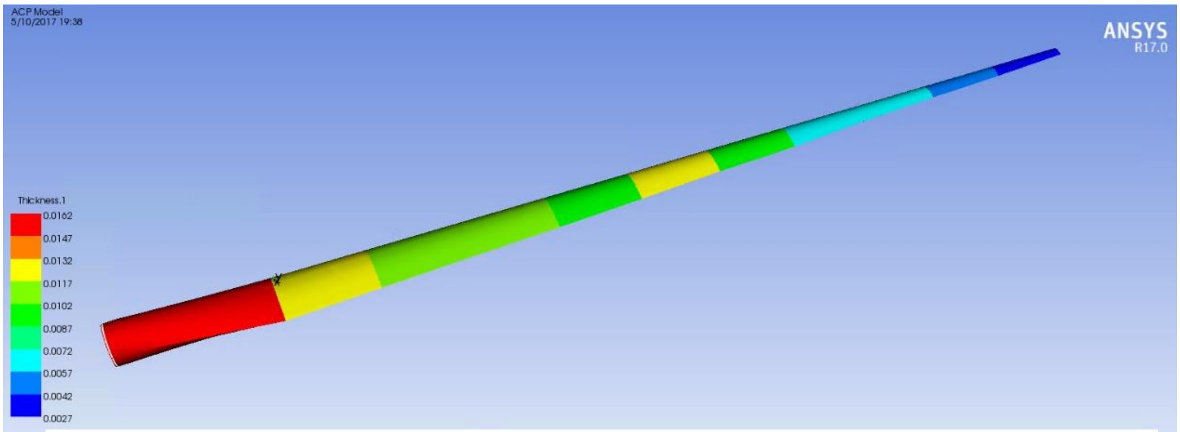


*Figure 221: Optimized blade section thickness*

- Table 13 describes the optimum number of layers for each section of the blade that should be implemented in order to successfully meet the case requirements. From Table 13, it can be inferred that more layers are required for sections closer to the base where the highest equivalent stress is acting. As the sections continue down the blade towards the tip, the number of layers required to meet the load specifications constantly decreases until the minimum possible number of layers is applied to the last section at the tip of the blade.

Table 13: Optimized number of layers

| **Optimum number of layers** | | | | | |
|---|---|---|---|---|---|
| **Blade section** | **0 Degrees** | **90 Degrees** | **±45 Degrees** | **±30 Degrees** | **Total** |
| Base | 8 | 8 | 6 | 4 | 26 |
| Root | 8 | 8 | 6 | 4 | 26 |
| Section 1 | 6 | 10 | 2 | 4 | 22 |
| Section 2 | 4 | 8 | 4 | 2 | 18 |
| Section 3 | 4 | 4 | 4 | 4 | 16 |
| Section 4 | 4 | 6 | 4 | 2 | 16 |
| Section 5 | 4 | 6 | 6 | 2 | 18 |
| Section 6 | 2 | 6 | 4 | 2 | 14 |
| Section 7 | 2 | 4 | 2 | 2 | 10 |
| Section 8 | 2 | 6 | 2 | 2 | 12 |
| Section 9 | 2 | 2 | 2 | 2 | 8 |
| Section 10 | 1 | 1 | 1 | 1 | 4 |

- A new **static structural** study was carried out with the optimized number of layers where the maximum total deformation is now less than 1.5 meters which is a sensible result following industry practices.

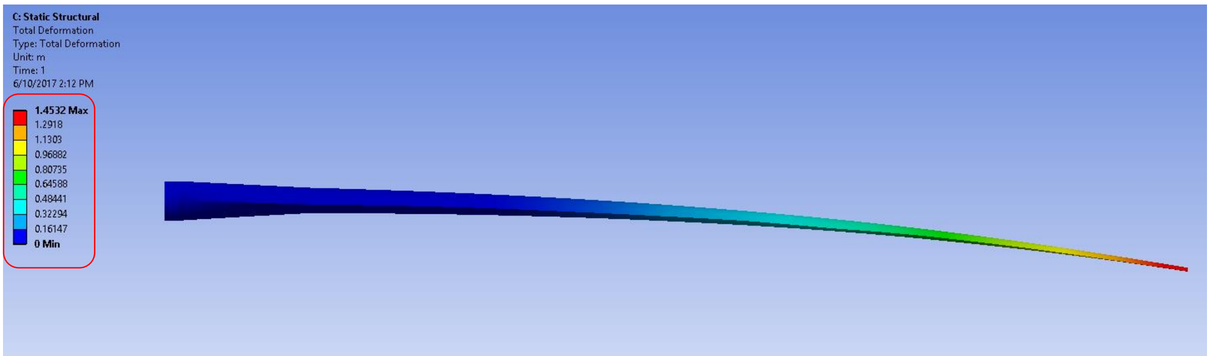


*Figure 222: Optimized blade deflection*

- The failure criterion now suggests that the maximum value is less than 0.36 in the same section of the blade where plies failed (values more than 1.5) before the optimization process took place. This results strongly suggest that the blade would now successfully sustain the maximum possible loads during operation.

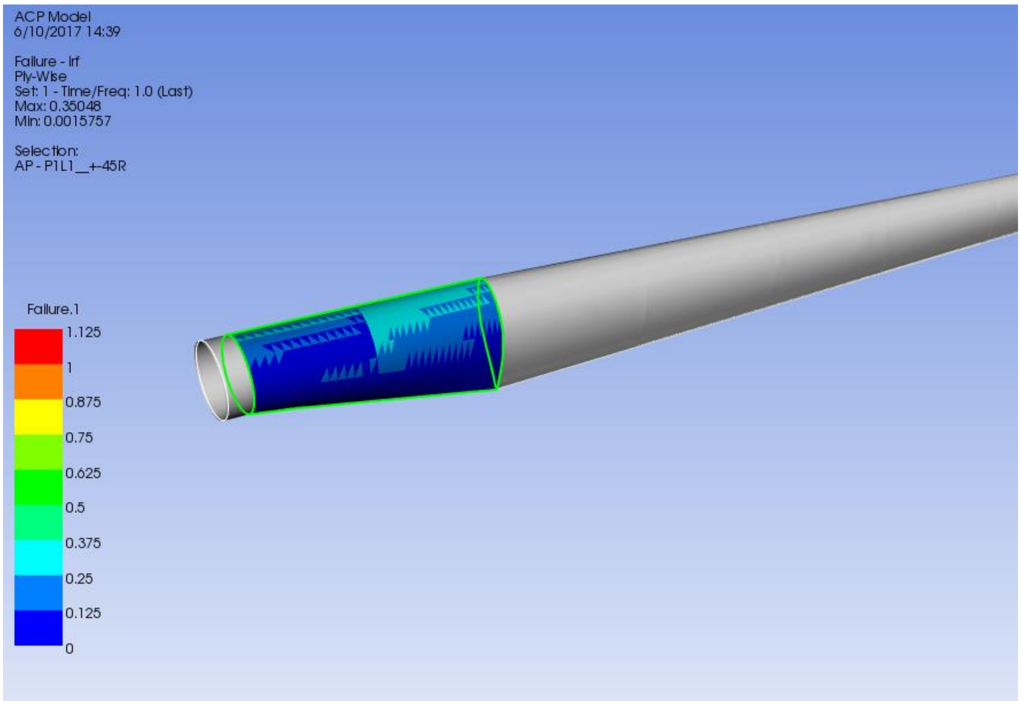


*Figure 223: Optimized blade failure criterion*

# 4 Conclusions

In brief, taking into consideration the methodology and by exploring the optimization results in each of the study cases, it can be concluded that:

- Four study cases comprising analyses relevant to the Mechanical and Aerospace fields were efficaciously selected and incorporated to the analysis.
- The optimization capabilities of modern FEA software and specifically ANSYS 18 were effectively tested and demonstrated though the mentioned study cases.
- Modern optimization software offers advanced optimization techniques and a user-friendly interface. The main factor hindering its broad implementation in high complexity and precise applications, at this stage, is the computational time required which increases exponentially with the quality of the desired outcomes.
- A tutorial-style methodology was successfully created for each of the considered study cases. It efficiently demonstrates the optimization process from the initial model generation to the results acquisition phase in an informative and illustrative manner.

# 5 Limitations and Recommendations

A number of limitations were encountered along the way. The main limitations with the topology and parametric optimization modules in ANSYS 18 are discussed.

## 5.1 Topology module limitations

The topology optimization module is relatively new to ANSYS Workbench and therefore, a few limitations exist in terms of the optimization outcomes.

- The outcomes of a topology optimization study are considerably sensitive to the constraints of the objective function. Defining a relatively low value for the constraint of type ‘mass to retain’ or ‘volume to retain’ can return unfeasible optimization results (too much material is removed, and model becomes ill-conditioned) without previous warning from the module. Thus, the optimization constraints need to be carefully selected and tested.
- The overall shape of topology optimization results may be too coarse, and the post processing phase can become complex. Additionally, surface smoothing features implemented can result in unanticipated sources of stress concentration.

## 5.2 Parametric module limitations

The parametric optimization modules present some important limitations that hinder the acquisition of effective optimization outcomes. Such limitations include:

- Direct and response surface optimization types work with a maximum of 20 input parameters. Above this number, various errors arise, and the process cannot continue.
- The design of experiments, response surface generation and parameter correlation analyses work well for a small number of input parameters (less than 10) Without the implementation of such features, a global optimum is not achievable and only a local optimum design can be obtained for a relatively large number of input parameters.
- Convergence plays a significant role when dealing with CFD studies, convergence criteria needs to be carefully set to avoid issues during the optimization process.
- The overall optimization process is relatively quick. However, the design points generation (generally 100 points) and solution can take considerable amounts of time as each point needs to be solved for the subsequent optimization process to function.

## 5.3 Recommendations

Regarding the optimization process and general work in ANSYS® 18, the following recommendations can be considered:

- The use of the academic version of the software is not advised when working with medium complexity problems as problem size limitations are substantial.
- A mesh of improved quality should be applied when the accuracy of results is a major factor. However, computational time will be penalized. A workaround for this issue can be the use of a remote solver if available.
- CFD analyses are highly sensitive to the type of solver and boundary conditions implemented. Thus, an in-depth investigation on suitable conditions for a specific model is recommended.
- If the number of input parameters for the optimization study is higher than the allowable number (20), a sensitivity analysis is recommended where parameters that do not have a significant impact on the solution can be identified and not considered in the optimization process.
- It is also recommended that before any study is carried out in ANSYS 18, the user is familiarised with the relevant user's manual available online.

# 6 Future work

The proposed subsequent work to be carried out includes:

- The implementation of both optimization methods (topological and parametric) in one study case. The Jib crane is a suitable candidate for the suggested study as a parametric optimization analysis would substantially increase its current capabilities achieved by the topology optimization method only.
- The development of relatively more advanced Multiphysics optimization studies with the combination of CFD, structural, heat transfer, and other analyses in one study case. E.g. Combustion can be incorporated into the rocket nozzle case.
- The implementation of other modern optimization programs so a suitable comparison of optimization capabilities can be performed.
- Manufacturing and mass productions considerations can be implemented as constraints for topological or parametric optimization studies. Additionally, ANSYS 18, offers manufacturing analyses coupled with the CFD module Polyflow for extrusion, forming, and moulding simulations.
- External optimization modules or add-ins considerations. A number of external modules that can be coupled with the standard optimization module in ANSYS can be explored. Such modules offer design robustness studies to further increase the performance of already optimized models.

# 7 References


A. Vaidya, S. Y. (2005). *Multiphysics CAD-Based Design Optimization.*

*Airfoil Tools*. (2017). Retrieved from NACA 63-412 AIRFOIL (n63412-il): http://airfoiltools.com/airfoil/details?airfoil=n63412-il

Alan Parkinson, R. B. (2013). *Optimization Methods for Engineering Design: Applications and Theory*. Brigham Young University.

ANSYS, I. (2004). *ANSYS, Inc. Theory Reference* . Canonsburg, PA.

ANSYS, I. (2013). *Design Exploration User's Guide.* Canonsburg.

Arora, J. S. (2012). *Introduction to Optimum Design.* Iowa: ELSEVIER.

Brownlee, J. (2011). *Clever Algorithms: Nature-inspired Programming Recipes.*

Bryce, H. (2015). *Finite Element Based Structural Otimization Techniques.* Brisbane Australia: The University of Queensland EAIT Faculty.

Chang, K.-H. (2015). *e-Design Computer Aided Engineering Design.* ELSEVIER.

J. C. Dai, Z. Q. (2017). Structural parameters multi-objective optimization and dynamic characteristics analysis of large-scale wind turbine towers. *Australian Journal of Mechanical Engineering*.

Javidinejad, A. (2012). Theory of Parametric Design Optimization Approach via Finite Element Analysis.

Jorge Nocedal, S. W. (1999). *Numerical Optimization.* New York: Springer.

Kitti, M. (2016). History of Optimization. Turku, Finland.

Li Xue-ping, Z. L.-y.-z. (2017). Topological Optimization of Continuum Structure based on ANSYS. *MATEC Web of Conferences*.

MENON, A. (2005). *Structural Optimization using Ansys and regulated Multiquadric Response Surface Model.* Arlington Texas: THE UNIVERSITY OF TEXAS AT ARLINGTON.

Mr. H.B.Ramani, M. N. (2013). Using Shape Optimization Tool In Ansys Software For Weight Reduction of Steel Connecting Rod. *International Journal of Engineering Research & Technology (IJERT).*

P. Meghashyam, S. G. (2013). Design and Analysis of Wheel Rim using CATIA & ANSYS. *International Journal of Application or Innovation in Engineering & Management*.

Panos Papalambros, D. J. (2017). Principles of Optimal Design Modeling and Computation. Cambridge University Press.

Ragheb, M. (2013). *Aerodynamics of Rotor Blades.*

Rao, S. (2009). *Engineering Optimization: Theory and Practice.* Wiley.

Razvan Cazacu, L. G. (2014). Overview of Structural Topology Optimization Methods for Plane and Solid Structures. *Annals of the University of Oradea*.

Staff, T. E. (2013). Spotlight on Turbomachinery. *ANSYS Advantage*.

Thieffry, P. (2010). Using ANSYS Workbench techniques with APDL delivers. *Best of Both Worlds: Combining APDL with ANSYS Workbench for Structural Simulations*.

Weck, O. L. (2004). *Multiobjective Optimization: History and Promise.* Msettsassac: Dept. of Aeronautics & Astronautics, Engineering Systems Division, Massachusetts Institute of Technology.

Wilhelm Forst, D. H. (2009). Optimization Theory and Practice. *Springer*.

Wook-han Choi, C.-g. H.-m.-J. (2015). Comparison of some commercial software systems for structural optimization. *11th World Congress on Structural and Multidisciplinary Optimisation*.

Yun, Y. (2004). Design of Structure Optimization with APDL. *Journal of East China Jiaotong University*.